

การพัฒนาศักย์ปฏิยานุภาคของเคออนกับนิวคลีออนบนพื้นฐานของ
สมมาตรโคแรลแบบ SU(3)



วิทยานิพนธ์นี้เป็นส่วนหนึ่งของการศึกษาตามหลักสูตรปริญญาวิทยาศาสตรมหาบัณฑิต
สาขาวิชาฟิสิกส์
มหาวิทยาลัยเทคโนโลยีสุรนารี
ปีการศึกษา 2553

**DEVELOPMENT OF $\bar{K}N$ POTENTIAL
BASED ON CHIRAL SU(3) SYMMETRY**



Rintarn Saengsai

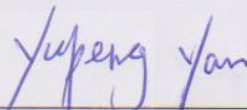
**A Thesis Submitted in Partial Fulfillment of the Requirements for the
Degree of Master of Science in Physics
Suranaree University of Technology**

Academic Year 2010

**DEVELOPMENT OF $\bar{K}N$ POTENTIAL
BASED ON CHIRAL SU(3) SYMMETRY**

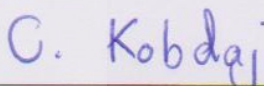
Suranaree University of Technology has approved this thesis submitted in partial fulfillment of the requirements for the Degree of Master of Science in Physics.

Thesis Examining Committee



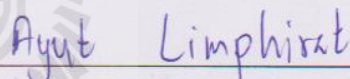
(Prof. Dr. Yupeng Yan)

Chairperson



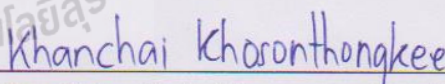
(Asst. Prof. Dr. Chinorat Kobdaj)

Member (Thesis Advisor)



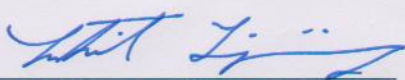
(Dr. Ayut Limphirat)

Member



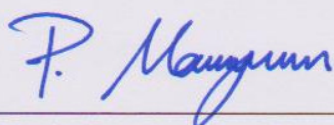
(Dr. Khanchai Khosonthongkee)

Member



(Prof. Dr. Sukit Limpijummong)

Vice Rector for Academic Affairs



(Assoc. Prof. Dr. Prapun Manyum)

Dean of Institute of Science

คุณธาร แสงไสย: การพัฒนาศักยภาพปฏิยานุภาคของเคออนกับนิวคลีออนบนพื้นฐานของ
สมมาตรไครลแบบ SU(3) (DEVELOPMENT OF $\bar{K}N$ POTENTIAL BASED
ON CHIRAL SU(3) SYMMETRY). อาจารย์ที่ปรึกษา :
ผู้ช่วยศาสตราจารย์ ดร.ชิโนรัตน์ กอบเดช, 97 หน้า.

วิทยานิพนธ์นี้มีวัตถุประสงค์เพื่อศึกษาศักยภาพปฏิยานุภาคเคออนกับนิวคลีออนบนพื้นฐานของ
 $\bar{K}N - \pi\Sigma - \pi\Lambda$ ซึ่งศักย์นี้คาดว่าจะสามารถทำซ้ำข้อมูลการกระเจิงที่พลังงานต่ำของอันตรกิริยา
 $K^-p \rightarrow K^-p \bar{K}^0n \pi^0\Sigma^0 \pi^+\Sigma^- \pi^-\Sigma^+$ และ $\pi^0\Lambda$ ซึ่งทำนายโดยใช้ทฤษฎีอื่นในการประมาณ
ในวิทยานิพนธ์นี้เราหาสมการพลวัตสำหรับระบบคู่ควบบปฏิยานุภาคเคออนนิวคลีออน แบบหลาย
ช่องและทำการคำนวณหาค่าภาคตัดขวางของอันตรกิริยา $K^-p \rightarrow K^-p \bar{K}^0n \pi^0\Sigma^0 \pi^+\Sigma^-$
 $\pi^-\Sigma^+$ และ $\pi^0\Lambda$ โดยใช้ศักย์ที่เกี่ยวข้องกับปรากฏการณ์ที่ตรวจวัดได้ของระบบคู่ควบบปฏิยานุภาค
เคออนนิวคลีออนแบบหลายช่อง



สาขาวิชาฟิสิกส์
ปีการศึกษา 2553

ลายมือชื่อนักศึกษา คุณธาร แสงไสย
ลายมือชื่ออาจารย์ที่ปรึกษา ชินรัตน์ กอบเดช
ลายมือชื่ออาจารย์ที่ปรึกษาร่วม Yupeng Yan

RINTARN SAENGSAI : DEVELOPMENT OF $\bar{K}N$ POTENTIAL
BASED ON CHIRAL SU(3) SYMMETRY. THESIS ADVISOR :
ASST. PROF. CHINORAT KOBDAJ, Ph.D. 97 PP.

$\bar{K}N$ POTENTIAL / CHIRAL SU(3) SYMMETRY

The work has investigated the potential proposed by Akaishi and Yamazaki in coordinate space for the coupled $\bar{K}N - \pi\Sigma - \pi\Lambda$ system. The potential is expected to reproduce the low-energy scattering data of the reactions $K^-p \rightarrow K^-p, \bar{K}^0n, \pi^0\Sigma^0, \pi^+\Sigma^-, \pi^-\Sigma^+$ and $\pi^0\Lambda$, predicted by other theoretical approaches. In this thesis we have derived the dynamical equations for the coupled-channel $\bar{K}N$ system and evaluate the cross sections of the reactions $K^-p \rightarrow K^-p, \bar{K}^0n, \pi^0\Sigma^0, \pi^+\Sigma^-, \pi^-\Sigma^+$ and $\pi^0\Lambda$, with a phenomenological potential for the coupled $\bar{K}N$ system.

School of Physics

Academic Year 2010

Student's Signature Rintarn Saengsai

Advisor's Signature C. Kobdaj

Co-Advisor's Signature Yupeng Yan

ACKNOWLEDGEMENTS

This thesis arose in part out of the research that has been done since I came to particle physics's group. By that time, I have worked with a great number of people whose contributions in assorted ways to the research and the making of this thesis deserved special mention. It is a pleasure to convey my gratitude to them all in my humble acknowledgment.

I am heartily thankful to my supervisor, Asst. Prof. Dr. Chinorat Kobdaj for his supervision in quantum physics and particle physics, advice in High-Performance Computing (HPC), for teaching me how to use Linux systems, TightVNC, SSH, Putty program to connect with SUT-HPCC, and guidance from the very early stage enabled to develop an understanding of the subject of this research as well as giving extraordinary experiences through out the work. Above all and the most needed, he provided me a place to learn, unflinching encouragement and support in various ways. His true scientist intuition has made him as exceptionally inspired and enriched my growth as a student, a researcher and a scientist want to be. I am indebted to him more than he knows.

I gratefully acknowledge Prof. Dr. Yupeng Yan for his advice in group theory and collision theory discussion, supervision in FORTRAN program and furthermore, for using his precious times to look my results and give his comments about them, his crucial contributions have made him a backbone of this research and so to this thesis. His involvement with his originality has triggered and nourished my intellectual maturity that I will benefit from, for a long time to come.

I gratefully thank Dr. Khanchai Khosonthongkee for being my first advisor when I arrived at the university. He is the first person who taught me how to study at SUT. I am proud to record that I had several opportunities to study with an experienced teacher like him.

Many thanks go to Mr. Wanchaleom Poonsawat. I also benefited by outstanding works from his help with his particular skill in computer programming, for teaching how to use NAG library on SUT-HPCC and how to login to Linux by using line mode. Many thanks go in particular to Dr. Nopmanee Suphanam and Dr. Ayut Limphirat for helping me solving the problems in my work. I would like to thank Mr. Daris Samart and Mr. Xuyang Liu for their suggestions in physics. I would like to thank Ms. Jittima Chaodamrongsakul for teaching how to use Qsub running programs on the cluster. My special thanks go to Dr. Suppiya Siranan for science discussion, for lending me physics books, and for his suggestions in LaTeX. I definitely could not pass the first year of my study without his support.

Furthermore, I would like to acknowledge Suranaree University of Technology for the research grant, the Commission on Higher Education, CHE-RG Theoretical Physics and Thailand Center of Excellence in Physics (ThEP) for the financial support throughout the entire length of my stay in the Nakhon Ratchasima.

I thank Mr. Pakorn Thaipituk for being a wonderful source of inspiration for me. He helped me to regain confidence and a positive attitude in handling the obstacles and challenges in my life.

I would like to thank my family for being the first people who put the foundation of my learning character, when I was a child.

Lastly, I offer my regards and blessings to all of those who have supported my work in any aspect during the completion of the project.

Rintarn Saengsai

CONTENTS

	Page
ABSTRACT IN THAI	I
ABSTRACT IN ENGLISH	II
ACKNOWLEDGEMENTS	III
CONTENTS	V
LIST OF FIGURES	IX
CHAPTER	
I INTRODUCTION	1
II DYNAMICAL EQUATIONS FOR COUPLED ANTIKAON- NUCLEON SYSTEMS	4
2.1 Dynamical equations for coupled $\bar{K}N$ systems	4
2.2 The initial free wave	7
2.3 The Green's function	9
2.4 Radial Lippmann-Schwinger Equation	11
III THE METHOD OF SOLVING THE LIPPMANN- SCHWINGER EQUATION	12
3.1 The matrix representation of radial part of Lippmann-Schwinger equation	12
3.2 Required parameters	14
3.3 Cross Sections of $\bar{K}N$ Collision	17
3.3.1 Direct Process ($\alpha \rightarrow \alpha$)	17
3.3.2 Cross Process ($\alpha_0 \rightarrow \alpha$)	18

CONTENTS (Continued)

	Page
IV RESULTS AND CONCLUSIONS	20
4.1 Numerical Results	20
4.2 Conclusions	27
4.3 The final goal of the research	27
 APPENDICES	
APPENDIX A LIST OF SYMBOLS	34
APPENDIX B USE SUT-HPCC MACHINES	36
B.1 Connecting to SUT-HPCC machines via SSH Secure Shell	36
B.1.1 Logging into SUT-HPCC machines	36
B.1.2 Using SSH Secure Shell	36
B.1.3 Using SSH Secure File Transfer	38
B.2 Using the NAG FORTRAN libraries at SUT-HPCC	39
B.2.1 FORTRAN Source Codes	39
B.2.2 Compiling Multiple Source Files	40
B.3 Using NAG FORTRAN Libraries	43
B.4 Job submission by the qsub command	45
APPENDIX C SCRIPT FILES FOR SUT-HPCC	49
C.1 Script for NAG FORTRAN Libraries	49
C.2 qsub script for submitting jobs to the SUT-HPCC cluster	50
APPENDIX D CONFIGURATION PARAMETERS	53
D.1 Bounds of integrations	53
D.2 Integration points	53
D.3 Selection of basis, isospin and the number of channel	54
D.4 Input the potential into the program	55

CONTENTS (Continued)

	Page
D.5 Relativistic and Non-Relativistic calculation (IREV)	55
D.6 Highest angular momentum in question (LMAX)	56
APPENDIX E FORTRAN SOURCE CODE	57
E.1 MAINS.F source code	57
E.1.1 FORTRAN code in MAINPROGRAM	58
E.1.2 READ and PRINT parameters	59
E.1.3 Open a files for writing the calculation results	61
E.1.4 Starting numerical calculation	62
E.2 Source code for numerical functions	66
E.2.1 Function CK1(X,S,L)	66
E.2.2 Function CK2(X,S,L)	66
E.2.3 Function FJ(X,L)	67
E.2.4 Function FN(X,L)	67
E.2.5 Function FJD(X,L)	68
E.2.6 Function FND(X,L)	69
E.3 List of Subroutines	70
E.3.1 Subroutine in MAINS file	70
E.3.2 Subroutine in KAONIC file	70
E.3.3 Subroutine in KP file	70
E.3.4 External Subroutine	71
E.4 Subroutine for calculate cross section	71
E.4.1 Subroutine RMASS(IREV)	71
E.4.2 Subroutine CALLLINEAREQ(A,B,MM,LX)	72
E.4.3 Subroutine POINTOUT(MM,AA,BB)	74

CONTENTS (Continued)

	Page
E.4.4 Subroutine POTGUIDE(MM,LL)	74
E.4.5 Subroutine XXINS1(MM,LX)	75
E.4.6 Subroutine PHINT(B,MM,LX)	77
APPENDIX F GLE (Graphics Layout Engine)	80
F.1 The example GLE source code for drawing graphs	80
F.2 The GLE graph plots six channels in one product page	84
APPENDIX G USING TightVNC ON THE SUT-HPCC	85
G.1 The installation of TightVNC Client	85
G.2 Getting started with TightVNC Client	85
G.3 How to stop the vncserver process	89
APPENDIX H PUBLICATIONS	90
H.1 Conference proceeding	90
H.2 Presentation in conference	90
CURRICULUM VITAE	97

LIST OF FIGURES

Figure	Page	
4.1	Theoretical cross section of the reaction $K^-p \rightarrow K^-p$ compared with the experimental data from Mast et al., Humphrey et al. and Sakit et al. (Mast et al., 1976; Humphrey and Ross, 1962; Sakit et al., 1965).	21
4.2	Theoretical cross section of the reaction $K^-p \rightarrow \bar{K}^0n$ compared with the experimental data from Mast et al., Evans et al., Humphrey et al., Kittel et al. and Abrams et al. (Mast et al., 1976; Evans et al., 1983; Humphrey and Ross, 1962; Kittel et al., 1966; Abrams and Sechi-Zorn, 1965).	22
4.3	Theoretical cross section of the reaction $K^-p \rightarrow \pi^0\Sigma^0$ compared with the experimental data from Mast et al. and Kim et al. (Mast et al., 1975; Kim, 1966).	23
4.4	Theoretical cross section of the reaction $K^-p \rightarrow \pi^-\Sigma^+$ compared with the experimental data from Bangerter et al., Ciborowski et al., Humphrey et al. and Sakit et al. (Bangerter et al., 1981; Ciborowski et al., 1982; Humphrey and Ross, 1962; Sakit et al., 1965).	24

LIST OF FIGURES (Continued)

Figure		Page
4.5	Theoretical cross section of the reaction $K^-p \rightarrow \pi^+\Sigma^-$ compared with the experimental data from Bangerter et al., Ciborowski et al., Humphrey et al. and Sakit et al. (Bangerter et al., 1981; Ciborowski et al., 1982; Humphrey and Ross, 1962; Sakit et al., 1965).	25
4.6	Theoretical cross section of the reaction $K^-p \rightarrow \pi^0\Lambda$ compared with the experimental data from Mast et al. and Kim et al. (Mast et al., 1975; Kim, 1966).	26
B.1	Connect to SSH Secure Shell.	37
B.2	Connect to Remote Host.	37
B.3	Enter Password screen.	38
B.4	SSH Secure File Transfer icon.	38
B.5	SSH Secure File Transfer in a window with two panels.	39
B.6	Making a directory to contain source codes.	40
B.7	Showing a script file and source code files for NAG FORTRAN Libraries.	41
B.8	Using Emacs editor to make a script file for compiling our programs.	41
B.9	Showing the script file in Emacs.	42
B.10	Showing the outputs when we use the compile.sh script.	42
B.11	Showing the executable files “myprog” after compiling.	43
B.12	Creating nag.sh in Emacs.	44
B.13	Showing the nag.sh script in Emacs.	44
B.14	Showing the qsub command for submitting job on SUT-HPCC.	45

LIST OF FIGURES (Continued)

Figure		Page
B.15	Checking the status of the job using “qstat” command.	46
B.16	Qdel is a command to delete the job from the cluster.	47
B.17	The list of our results.	47
F.1	The example of GLE plots (theoretical cross section of the reaction $K^-p \rightarrow K^-p, \bar{K}^0n, \pi^0\Sigma^0, \pi^+\Sigma^-, \pi^-\Sigma^+$ and $\pi^0\Lambda$, compared with the experimental data).	84
G.1	Connecting to the SUT-HPCC using the SSH Secure Shell and showing how to start vncserver.	86
G.2	Inserting server name or IP address and the display number.	86
G.3	Entering the TightVNC password at the password box.	87
G.4	Showing how to run Mathematica 7.0 via TightVNC.	88
G.5	Showing the Mathematica window on TightVNC screen.	88
G.6	Showing how to stop the vncserver process in SSH secure shell.	89
H.1	Proceeding in Thai Physics Journal series 6 page 1.	91
H.2	Proceeding in Thai Physics Journal series 6 page 2.	92
H.3	Proceeding in Thai Physics Journal series 6 page 3.	93
H.4	Proceeding in Thai Physics Journal series 6 page 4.	94
H.5	Abstract in English for The 3 rd SUT Grad Conference 2010.	95
H.6	Abstract in Thai for The 3 rd SUT Grad Conference 2010.	96

CHAPTER I

INTRODUCTION

The \bar{K} -nuclear systems have drawn considerable attentions. Experimentally, the K^-p collisions provides information of interactions of the coupled $\bar{K}N - \pi\Sigma - \pi\Lambda$ system above the $\bar{K}N$ threshold. However, the interaction below the $\bar{K}N$ threshold, which is dominated by the $\Lambda(1405)$ resonance, is not well understood. It is, therefore, essential to study the extrapolation of the $\bar{K}N$ interaction below the threshold, by properly treating the $\Lambda(1405)$ (Doté et al., 2009a; Hyodo and Weise, 2008b). Historically, the $\Lambda(1405)$ which is the lowest-energy negative-parity baryon with nonzero strangeness, has been studied for some time. In the following works (Akaishi and Yamazaki, 2002; Kaiser et al., 1995b; Takeuchi and Shimizu, 2009; Yamazaki and Akaishi, 2002), the $\Lambda(1405)$ has been reexamined as a baryon-meson resonance. It is found that the $\Lambda(1405)$ may not be an elementary particle, but the bound state of $\bar{K}N$ that becomes a resonance when there is a coupling between the $\bar{K}N$ and $\pi\Sigma$ (Nacher et al., 2000; Hyodo et al., 2008).

The $\bar{K}N$ interaction has been studied in the vector-meson exchange model. The basic ingredient of this method is the single meson exchange, which provides the driving force (potential). The scattering equation is usually the relativistic form of the Lippmann-Schwinger (LS) equation or the Blankenbecler-Sugar (BbS) equation. The original idea was that, in the absence of any well-defined low-mass scalar mesons, the potential should be due to the exchange of vector mesons. In Durso, Siegel et al. and Landau (Durso, 1998; Siegel and Weise, 1988; Landau, 1983), the $\Lambda(1405)$ has been successfully described in the coupled channel approach

with vector-meson exchange potential (Hyodo and Weise, 2008b).

A large number of works on $\bar{K}N$ interactions has been done in the chiral coupled channel approach (Nacher et al., 2000; Hyodo and Weise, 2008a; Kaiser et al., 1995a; Doté et al., 2009b; Entem et al., 2000; Bianco, 1998; Waas and Weise, 1997), where the interaction Lagrangian is determined by chiral $SU(3) \times SU(3)$ symmetry of Quantum chromodynamics (QCD). The idea of chiral perturbation theory is to realize that at low energies the dynamics should be controlled by the symmetry of QCD and the lightest particles such as pions or nucleon.

The $\bar{K}N$ interactions derived in the above approaches are in momentum space and energy dependent. It is inconvenient to apply such interactions to multi-particle systems, for example, the \bar{K} -nuclear states. There have been attempts to construct $\bar{K}N$ potentials in r-space phenomenologically (Akaishi and Yamazaki, 2002) by reproducing transition amplitudes derived in the chiral coupled channel approach (Hyodo and Weise, 2008b). However, these potentials are capable of understanding only some parts of experimental data. We have been constructing a potential in coordinate space for the coupled $\bar{K}N - \pi\Sigma - \pi\Lambda$ system, which is expected to reproduce the low-energy scattering data of the reactions $K^-p \rightarrow K^-p$, \bar{K}^0n , $\pi^0\Sigma^0$, $\pi^+\Sigma^-$, $\pi^-\Sigma^+$ and $\pi^0\Lambda$, the properties of the $\Lambda(1405)$ resonance, kaonic hydrogen atom data, and transition amplitudes predicted by other theoretical approaches. In this work we derive the dynamical equations for the coupled-channel $\bar{K}N$ system and evaluate the cross sections of the reactions $K^-p \rightarrow K^-p$, \bar{K}^0n , $\pi^0\Sigma^0$, $\pi^+\Sigma^-$, $\pi^-\Sigma^+$ and $\pi^0\Lambda$ with the phenomenological potential for the coupled $\bar{K}N$ system introduced in the work (Akaishi and Yamazaki, 2002).

This thesis is organized into four chapters. Chapter I is a brief introduction to the $\bar{K}N$ interaction and related work. In Chapter II, we also rewrite the Lippmann-Schwinger equation in terms of radial part of the outgoing scat-

tered wave function. In Chapter III, we transform the radial part of Lippmann-Schwinger equation into the matrix representation and construct the FORTRAN codes. Some parameters and inputs are obtained from the chiral symmetry and isospin basis. At the end of Chapter III we show how to compute cross section of the scattering process in general case. Finally, in Chapter IV we present our calculation of the $K^-p \rightarrow K^-p$, \bar{K}^0n , $\pi^0\Sigma^0$, $\pi^+\Sigma^-$, $\pi^-\Sigma^+$ and $\pi^0\Lambda$ cross section compared with experimental data.



CHAPTER II

DYNAMICAL EQUATIONS FOR COUPLED ANTIKAON-NUCLEON SYSTEMS

In scattering theory we convert the Schrödinger equation (SE) into an equation of amplitudes rather than wave functions. An integral form of the Schrödinger equation dealing with the amplitudes is the Lippmann-Schwinger equation. In this chapter we show how to convert from Schrödinger equation into Lippmann-Schwinger equation using Green's functions and partial wave expansions. Eventually, we manage to rewrite the Lippmann-Schwinger in term of radial part only as shown in section 2.4.

2.1 Dynamical equations for coupled $\bar{K}N$ systems

We have studied the $\bar{K}N$ systems by using the scattering. This section we try to solve the Lippmann-Schwinger equation for outgoing scattered waves function. We start from the time-dependent Schrödinger equation

$$H|\psi\rangle = E|\psi\rangle, \quad (2.1)$$

for scattering process. The hamiltonian is given by

$$H = H_0 + V, \quad (2.2)$$

where $H_0 = \frac{\vec{P}^2}{2m}$ is the kinetic energy operator for free particles and V is the potential energy. In the absence of scattering, V would be zero. Here we let $|\phi\rangle$

be the energy eigenket of H_0 satisfied the homogeneous equation

$$H_0|\phi\rangle = E|\phi\rangle. \quad (2.3)$$

If scattering process is an elastic scattering process, there is no changing in energy, we can use full hamiltonian SE with the same energy eigenvalue E ,

$$(H_0 + V)|\psi\rangle = E|\psi\rangle. \quad (2.4)$$

Let α and β be the initial and final state, we have

$$(E - H_0)|\psi_\alpha\rangle = V_{\alpha\beta}|\psi_\beta\rangle \quad (2.5)$$

where $V_{\alpha\beta}$ is the interaction between the α and β channels (sum over repeated indices), ψ_α and ψ_β are the eigen functions of the initial and final states, and E is the energy eigen value of H_0 .

Because of the continuity of the energy eigenvalues, we can use $|\phi\rangle$ instead of $|\psi_\alpha\rangle$ when V is zero. But if there exists a potential, a general solution is

$$|\psi_\alpha\rangle = |\phi_\alpha\rangle + \frac{1}{E - H_0} V_{\alpha\beta} |\psi_\beta\rangle. \quad (2.6)$$

When $(E - H_0)$ is singular, the equation (2.6) has no meaning, so we can eliminate the singularity in distinct ways by adding the denominator with a small imaginary $i\epsilon$,

$$|\psi_\alpha\rangle = |\phi_\alpha\rangle + \frac{1}{E - H_0 + i\epsilon} V_{\alpha\beta} |\psi_\beta\rangle. \quad (2.7)$$

This equation (2.7) is known as the Lippmann-Schwinger equation. It is a ket equation independent of particular representations. If we confine ourselves to the position basis by multiplying $\langle \vec{r}, s |$ from the left, thus equation (2.7) become

$$\langle \vec{r}, s | \psi_\alpha \rangle = \langle \vec{r}, s | \phi_\alpha \rangle + \langle \vec{r}, s | \frac{1}{E - H_0 + i\epsilon} V_{\alpha\beta} |\psi_\beta\rangle. \quad (2.8)$$

Inserting the completeness relation, $\int d^3\vec{r}' |\vec{r}', s'\rangle \langle \vec{r}', s'| = 1$, into the above equation, we have

$$\psi_\alpha(\vec{r}, s) = \phi_\alpha(\vec{r}, s) + \int d^3\vec{r}' \langle \vec{r}, s | \frac{1}{E - H_0 + i\epsilon} | \vec{r}', s' \rangle \langle \vec{r}', s' | V_{\alpha\beta} | \psi_\beta \rangle. \quad (2.9)$$

Consider term $\langle \vec{r}', s' | V_{\alpha\beta} | \psi_\beta \rangle$ by inserting completeness relation again,

$$\langle \vec{r}', s' | V_{\alpha\beta} | \psi_\beta \rangle = \int d^3\vec{r}'' \langle \vec{r}', s' | V_{\alpha\beta} | \vec{r}'', s'' \rangle \langle \vec{r}'', s'' | \psi_\beta \rangle, \quad (2.10)$$

the matrix element in position basis can be written as

$$\langle \vec{r}', s' | V_{\alpha\beta} | \vec{r}'', s'' \rangle = V_{\alpha\beta}(\vec{r}', s') \langle \vec{r}', s' | \vec{r}'', s'' \rangle = V_{\alpha\beta}(\vec{r}', s') \delta(\vec{r}' - \vec{r}''). \quad (2.11)$$

So, we get

$$\begin{aligned} \langle \vec{r}', s' | V_{\alpha\beta} | \psi_\beta \rangle &= \int d^3\vec{r}'' V_{\alpha\beta}(\vec{r}', s') \langle \vec{r}', s' | \vec{r}'', s'' \rangle \langle \vec{r}'', s'' | \psi_\beta \rangle \\ &= V_{\alpha\beta}(\vec{r}', s') \psi_\beta(\vec{r}', s'), \end{aligned} \quad (2.12)$$

and,

$$\begin{aligned} \psi_\alpha(\vec{r}, s) &= \phi_\alpha(\vec{r}, s) + \int d^3\vec{r}' \langle \vec{r}, s | \frac{1}{E - H_0 + i\epsilon} | \vec{r}', s' \rangle V_{\alpha\beta}(\vec{r}', s') \psi_\beta(\vec{r}', s') \\ &= \phi_\alpha(\vec{r}) + \int d^3\vec{r}' \langle \vec{r} | \frac{1}{E - H_0 + i\epsilon} | \vec{r}' \rangle V_{\alpha\beta}(\vec{r}') \psi_\beta(\vec{r}'). \end{aligned} \quad (2.13)$$

Next, we write an operator $\frac{1}{E - H_0 + i\epsilon}$ of the bra-ket notation in term of inverted Green's function,

$$G(\vec{r}, \vec{r}') = \frac{\hbar^2}{2m} \langle \vec{r} | \frac{1}{E - H_0 + i\epsilon} | \vec{r}' \rangle, \quad (2.14)$$

satisfying the equation,

$$(\nabla^2 + k^2)G(\vec{r}, \vec{r}') = \delta^{(3)}(\vec{r} - \vec{r}'). \quad (2.15)$$

Thus, the formal solution of the Lippmann-Schwinger equation for outgoing scattered waves take the form

$$\psi_\alpha(\vec{r}) = \phi_\alpha(\vec{r}) + \frac{2m}{\hbar^2} \int d^3\vec{r}' G(\vec{r}, \vec{r}') V_{\alpha\beta}(\vec{r}') \psi_\beta(\vec{r}'). \quad (2.16)$$

The outgoing scattered wave consists of the initial free wave $\phi_\alpha(\vec{r})$, Green's function $G(\vec{r}, \vec{r}')$, and the wave function for the final state $\psi_\beta(\vec{r}')$. In next section, we shown how to obtain each term in details.

2.2 The initial free wave

In this section we use the partial wave expansion and spherical harmonics properties to write down the initial free wave function. Firstly, we decompose the initial free wave function by writing

$$\phi_\alpha(\vec{r}) = \langle r, s | \vec{k}_\alpha \rangle = (2\pi)^{-\frac{3}{2}} \exp(i\vec{k}_\alpha \cdot \vec{r}) \chi_{s, m_s} \quad (2.17)$$

where $\exp(i\vec{k}_\alpha \cdot \vec{r})$ comes from plane wave. It is an eigenfunction common to the free hamiltonian $H_0 = -\frac{\hbar^2}{2m} \nabla_r^2$, χ_{s, m_s} is the spin eigen vector of a particle. Since we can construct the plane wave $\exp(i\vec{k}_\alpha \cdot \vec{r})$ in a series of the product between spherical Bessel ($j_l(kr)$) and spherical harmonics ($Y_{lm}(\theta, \phi)$). By choosing the z-axis along the direction of \vec{k}_α so that

$$\exp(i\vec{k}_\alpha \cdot \vec{r}) = \exp(ik_\alpha r \cos\theta) \quad (2.18)$$

is independent of the azimuthal angle ϕ . Then, we obtain

$$\exp(i\vec{k}_\alpha \cdot \vec{r}) \chi_{s, m_s} \equiv \exp(ik_\alpha z) \chi_{s, m_s} = \sum_{l=0}^{\infty} (2l+1) i^l j_l(k_\alpha r) P_l(\cos\theta) \chi_{s, m_s} \quad (2.19)$$

which is the partial wave expansion. Here the functions $P_l(\cos\theta)$ are the legendre polynomials

$$P_l(\cos\theta) = \left(\frac{4\pi}{2l+1} \right)^{\frac{1}{2}} Y_{l,0}(\theta). \quad (2.20)$$

Using the addition theorem of the spherical harmonics, namely

$$P_l(\cos\theta) = \left(\frac{4\pi}{2l+1} \right) \sum_{m=-l}^{+l} Y_{lm}^*(\hat{k}) Y_{lm}(\hat{r}), \quad (2.21)$$

we can rewrite (2.19) as

$$\exp(i\vec{k}_\alpha \cdot \vec{r})\chi_{s,m_s} = 4\pi \sum_{l=0}^{\infty} \sum_{m=-l}^{+l} i^l j_l(k_\alpha r) Y_{lm}^*(\hat{k}) Y_{lm}(\hat{r}) \chi_{s,m_s}, \quad (2.22)$$

and the decoreponding development of the incident plane wave is simply

$$\begin{aligned} \phi_\alpha(\vec{r}) &= \frac{1}{(2\pi)^{3/2}} (4\pi) \sum_{l=0}^{\infty} \sum_{m=-l}^{+l} i^l j_l(k_\alpha r) Y_{lm}^*(\hat{k}) Y_{lm}(\hat{r}) \chi_{s,m_s}, \\ &= \left(\frac{2}{\pi}\right)^{\frac{1}{2}} \sum_{l=0}^{\infty} \sum_{m=-l}^{+l} i^l j_l(k_\alpha r) Y_{lm}^*(\hat{k}) Y_{lm}(\hat{r}) \chi_{s,m_s}. \end{aligned} \quad (2.23)$$

In the $\bar{K}N$ system, we include the spin eigenvector χ_{s,m_s} so, we can write the above equation as

$$\phi_\alpha(\vec{k}, s, m_s, \vec{r}) = \left(\frac{2}{\pi}\right)^{\frac{1}{2}} \sum_{l=0}^{\infty} \sum_{m=-l}^{+l} i^l j_l(k_\alpha r) Y_{lm}^*(\hat{k}) Y_{lm}(\hat{r}) \chi_{s,m_s}. \quad (2.24)$$

Using

$$Y_{lm}(\hat{r}) \chi_{s,m_s} = \sum_{J=|l-s|}^{l+s} \sum_M C(lm, sm_s, JM) Y_{l_s}^{JM}(\hat{r}), \quad (2.25)$$

and, then substituting into equation (2.24), we get

$$\begin{aligned} \phi_\alpha(\vec{k}, s, m_s, \vec{r}) &= \left(\frac{2}{\pi}\right)^{\frac{1}{2}} \sum_{l=0}^{\infty} \sum_{m=-l}^{+l} i^l j_l(k_\alpha r) Y_{lm}^*(\hat{k}) \\ &\quad \times \sum_{J=|l-s|}^{l+s} \sum_M C(lm, sm_s, JM) Y_{l_s}^{JM}(\hat{r}). \end{aligned} \quad (2.26)$$

Now we define

$$Z_{l_s}^{JM}(\hat{k}) = \sum_{m=-l}^{+l} C(lm, sm_s, JM) Y_{lm}(\hat{k}), \quad (2.27)$$

and

$$Z_{l_s}^{JM*}(\hat{k}) = \sum_{m=-l}^{+l} C(lm, sm_s, JM) Y_{lm}^*(\hat{k}). \quad (2.28)$$

Then, combining all these equations together

$$\begin{aligned} \phi_\alpha(\vec{k}, s, m_s, \vec{r}) &= \left(\frac{2}{\pi}\right)^{\frac{1}{2}} \sum_{l=0}^{\infty} \sum_{JM} i^l j_l(k_\alpha r) Z_{l_s}^{JM*}(\hat{k}) Y_{l_s}^{JM}(\hat{r}) \\ &= \left(\frac{2}{\pi}\right)^{\frac{1}{2}} \sum_{l_s} \sum_{JM} i^l j_l(k_\alpha r) Z_{l_s}^{JM*}(\hat{k}) Y_{l_s}^{JM}(\hat{r}) \\ &= \left(\frac{2}{\pi}\right)^{\frac{1}{2}} \sum_{l's's'} \sum_{JM} i^{l'} j_{l'}(k_\alpha r) Z_{l_s}^{JM*}(\hat{k}) Y_{l's'}^{JM}(\hat{r}) \delta_{l'l} \delta_{s's'}, \end{aligned} \quad (2.29)$$

finally, we get the initial free wave function as shown below

$$\phi_\alpha(\vec{k}, \vec{r}) = \left(\frac{2}{\pi}\right)^{\frac{1}{2}} \sum_{l's's'JM} j_l(k_\alpha, r) Z_{ls}^{JM*}(\hat{k}) Y_{l's'}^{JM}(\hat{r}) i^{l'} \delta_{ll'} \delta_{ss'}. \quad (2.30)$$

2.3 The Green's function

This section we write the Green's function in equation (2.16) in terms of spherical harmonics as

$$\begin{aligned} G(\vec{r}, \vec{r}') &= \sum_{l=0}^{\infty} \sum_{m=-l}^{+l} g_l(k, \vec{r}, \vec{r}') Y_{lm}^*(\hat{r}') Y_{lm}(\hat{r}) \\ &= \sum_{l=0}^{\infty} \sum_{m=-l}^{+l} g_l(k, \vec{r}, \vec{r}') Y_{lm}^*(\hat{r}') Y_{lm}(\hat{r}) \chi_{s,m_s}^\dagger \chi_{s,m_s} \\ &= \sum_{l=0}^{\infty} \sum_{m=-l}^{+l} g_l(k, \vec{r}, \vec{r}') Y_{lm}^*(\hat{r}') \chi_{s,m_s}^\dagger \sum_{J=|l-s|}^{l+s} \sum_M C(lm, sm_s, JM) Y_{ls}^{JM}(\hat{r}) \\ &= \sum_{l=0}^{\infty} \sum_{JM} g_l(k, \vec{r}, \vec{r}') Y_{ls}^{JM*}(\hat{r}') Y_{ls}^{JM}(\hat{r}) \\ &= \sum_{JMs} g_l(k, \vec{r}, \vec{r}') Y_{ls}^{JM*}(\hat{r}') Y_{ls}^{JM}(\hat{r}), \end{aligned} \quad (2.31)$$

then we determine the radial part of Green's function $g_l(k, \vec{r}, \vec{r}')$ in momentum space by using

$$G(\vec{r}, \vec{r}') = -\frac{1}{(2\pi)^3} \lim_{\varepsilon \rightarrow 0^+} \int \frac{\exp i\vec{k}' \cdot (\vec{r} - \vec{r}')}{k'^2 - k^2 - i\varepsilon} d\vec{k}'.$$

According equation (2.22) we expand the plane wave in spherical harmonics, we find that

$$\begin{aligned} G(\vec{r}, \vec{r}') &= -\frac{1}{(2\pi)^3} \lim_{\varepsilon \rightarrow 0^+} \int \frac{d\vec{k}'}{k'^2 - k^2 - i\varepsilon} \left[4\pi \sum_{l=0}^{\infty} \sum_{m=-l}^{+l} i^l j_l(k'r) Y_{lm}^*(\hat{k}') Y_{lm}(\hat{r}) \right] \\ &\quad \times \left[4\pi \sum_{l'=0}^{\infty} \sum_{m'=-l'}^{+l'} i^{-l'} j_{l'}(k'r') Y_{l'm'}(\hat{k}'_i) Y_{l'm'}^*(\hat{r}') \right]. \end{aligned} \quad (2.32)$$

After carrying out the integrations over $\theta_{k'}$ and $\phi_{k'}$, one obtains

$$G(\vec{r}, \vec{r}') = -\frac{2}{\pi} Y_{l'm'}^*(\hat{r}') Y_{lm}(\hat{r}) \int_0^\infty \frac{j_l(k'r) j_l(k'r')}{k'^2 - k^2 - i\varepsilon} k'^2 dk', \quad (2.33)$$

and hence

$$g_l(k, \vec{r}, \vec{r}') = -\frac{2}{\pi} \int_0^\infty \frac{j_l(k'r)j_l(k'r')}{k'^2 - k^2 - i\varepsilon} k'^2 dk'. \quad (2.34)$$

Since $j_l(-z) = (-1)^l j_l(z)$ we may write equation (2.34) as

$$\begin{aligned} g_l(k, \vec{r}, \vec{r}') &= -\frac{1}{\pi} \int_0^\infty \frac{j_l(k'r)j_l(k'r')}{k'^2 - k^2 - i\varepsilon} k'^2 dk' - \frac{1}{\pi} \int_0^\infty \frac{j_l(k'r)j_l(k'r')}{k'^2 - k^2 - i\varepsilon} k'^2 dk' \\ &= -\frac{1}{\pi} \int_0^\infty \frac{j_l(k'r)j_l(k'r')}{k'^2 - k^2 - i\varepsilon} k'^2 dk' - \frac{1}{\pi} \int_{-\infty}^0 \frac{j_l(-k'r)j_l(-k'r')}{k'^2 - k^2 - i\varepsilon} k'^2 dk' \\ &= -\frac{1}{\pi} \int_0^\infty \frac{j_l(k'r)j_l(k'r')}{k'^2 - k^2 - i\varepsilon} k'^2 dk' - \frac{1}{\pi} \int_{-\infty}^0 \frac{(-1)^l j_l(k'r)(-1)^l j_l(k'r')}{k'^2 - k^2 - i\varepsilon} k'^2 dk' \\ &= -\frac{1}{\pi} \int_0^\infty \frac{j_l(k'r)j_l(k'r')}{k'^2 - k^2 - i\varepsilon} k'^2 dk' - \frac{1}{\pi} (-1)^{2l} \int_{-\infty}^0 \frac{j_l(k'r)j_l(k'r')}{k'^2 - k^2 - i\varepsilon} k'^2 dk' \\ &= -\frac{1}{\pi} \int_0^\infty \frac{j_l(k'r)j_l(k'r')}{k'^2 - k^2 - i\varepsilon} k'^2 dk' - \frac{1}{\pi} \int_{-\infty}^0 \frac{j_l(k'r)j_l(k'r')}{k'^2 - k^2 - i\varepsilon} k'^2 dk' \\ &= -\frac{1}{\pi} \int_{-\infty}^\infty \frac{j_l(k'r)j_l(k'r')}{k'^2 - k^2 - i\varepsilon} k'^2 dk'. \end{aligned} \quad (2.35)$$

Applying the properties

$$\begin{aligned} j_l &= \frac{1}{2}(h_l^{(1)} + h_l^{(2)}), \\ j_l(-z) &= (-1)^l j_l(z), \\ h_l^{(2)}(-z) &= (-1)^l h_l^{(1)}(z) \end{aligned} \quad (2.36)$$

and Cauchy's theorem to the integration above, we get

$$g_l(k, \vec{r}, \vec{r}') = -ik j_l(kr) h_l^{(1)}(kr') \quad (2.37)$$

for $r < r'$, and

$$g_l(k, \vec{r}, \vec{r}') = -ik j_l(kr') h_l^{(1)}(kr) \quad (2.38)$$

for $r > r'$, where j_l is the spherical Bessel function, $h_l^{(1)}$ and $h_l^{(2)}$ are respectively the first and second class spherical Hankel functions.

2.4 Radial Lippmann-Schwinger Equation

In analogy to the initial state wave function, the scattered state can be rewritten in the general form,

$$\psi_\alpha(\vec{r}) = \left(\frac{2}{\pi}\right)^{\frac{1}{2}} \sum_{l's's'JM} R_{l's',ls}^{\alpha,J}(k_\alpha, r) Z_{ls}^{JM*}(\hat{k}) Y_{l's'}^{JM}(\hat{r}) i^{l'}, \quad (2.39)$$

where α stands for channels, and $R_{l's',ls}^{\alpha,J}(k, r)$ are the radial parts of the scattered wave functions. The radial wave functions $R_{l's',ls}^{\alpha,J}(k, r)$ depend on the total orbital angular momenta l, l' and spins s, s' of the initial and final states, considering that only the total angular momentum J is conserved for a general interaction.

Finally, by substituting equations (2.30), (2.31) and (2.39) into equation (2.16), we obtain a set of coupled integral equations for the radial parts of the outgoing waves $\psi_\alpha(\vec{r})$ in the $|JMs\rangle$ basis,

$$R_{l's',ls}^{\alpha,J}(k_\alpha, r) = j_l(k_\alpha r) \delta_{\alpha\alpha_0} \delta_{l'l'} \delta_{ss'} + \sum_{l''s''} \int_0^\infty r'^2 dr' g_l(k_\alpha, r, r') V_{l's',l''s''}^{\alpha\beta,J}(r') R_{l''s'',ls}^{\beta,J}(k_\beta, r') \quad (2.40)$$

where α_0 stands for the initial state, k_α and k_β are the momenta of channels α and β , respectively. g_l is the radial component of the Green's function $G(\vec{r}, \vec{r}')$ and $V_{l's',l''s''}^{\alpha\beta,J}$ is the radial part of the interaction from the channel β to α (Landau and Páez, 1997).

In this chapter we have written down the Lippmann-Schwinger equation in term of generalized radial function which is the integral equation and very difficult to solve. Next step, we transform this equation into the matrix form and solve numerically. The details will be shown in Chapter III.

CHAPTER III

THE METHOD OF SOLVING THE LIPPMANN-SCHWINGER EQUATION

In this chapter we divide into three sections. Section 3.1 shows how to transform integral equation to matrix equation. All required parameters are given in section 3.2 with the framework of chiral symmetry. We also show how to compute the analytical cross section for both direct process and cross process in section 3.3.

3.1 The matrix representation of radial part of Lippmann-Schwinger equation

This section we solve dynamical equations in case of s-wave of Meson-Baryon interaction for the radial part of out scattered wave equation (2.40). Let $kr' = x'$, we get

$$R_\alpha(x) = j_0(x)\delta_{\alpha\alpha_0} + \int_0^\infty \frac{x'^2}{k^3} dx' g(x, x') V_{\alpha\beta}(x') R_\beta(x'). \quad (3.1)$$

We use the numerical Gaussian-Legendre with the weight function $\omega(x)$ corresponding to the size of each interval of integration. We changing variables

$$V_{\alpha\beta}(x') \rightarrow \frac{2m}{\hbar^2} V_{\alpha\beta}(x') \quad (3.2)$$

and substituting $x'^2 g(x, x') = f(x')$, the integral term of equation (3.1) will be written as

$$R_\alpha(x) = j_0(x)\delta_{\alpha\alpha_0} + \frac{2m}{\hbar^2 k^3} \int_0^\infty dx' V_{\alpha\beta}(x') f(x') R_\beta(x'). \quad (3.3)$$

Let $x' = x_j$ and $x = x_i$, where the indices i and j represent the final and initial state, respectively. So, we can approximate the value of integration by using the summation, and write into the matrix form as

$$[R]_{j \times 1} = [A]_{i \times j}^{-1} [J]_{i \times 1}. \quad (3.4)$$

Where

$$\sum_{j=1}^N [R_\beta(x_j)] = [R_{j1}], \quad (3.5)$$

$[A]_{i \times j}^{-1}$ is the inverse matrix of

$$\sum_{j=1}^N [(\delta_{ij} \delta_{\alpha\beta} - F_{ij}^{\alpha\beta}(x_j))] = [A_{ij}], \quad (3.6)$$

in which we define

$$\sum_{j=1}^N F_{ij}^{\alpha\beta}(x_j) = \frac{2m}{\hbar^2 k^3} \left[\sum_{j=1}^N f(x_j) \omega(x_j) V_{\alpha\beta}(x_j) \right],$$

and

$$j_0(x_i) \delta_{\alpha\alpha_0} = [J_{i1} \delta_{\alpha\beta}]. \quad (3.7)$$

In order to calculate equation (2.40) we consider the Green's function for two cases, first, for $r > r'$, ($x_i > x_j$), and second, for $r < r'$, ($x_i < x_j$). The radial Green's function for both cases can be written as

$$g_0(x_i, x_j) = k j_0(x_i) n_0(x_j), \quad (3.8)$$

and

$$g_0(x_i, x_j) = k j_0(x_j) n_0(x_i), \quad (3.9)$$

where j_0 and n_0 are the spherical Bessel function of the 1st and 2nd kind for rank $l = 0$, respectively.

3.2 Required parameters

This section we would like to get input parameter for $\bar{K}N$ channel by considering the chiral symmetry framework. The s-wave resonance in $\bar{K}N$ coupled-channel system tells us that the strong interaction is invariant under the unitary transformation of u , d and s quarks and the interactions among the channels $\bar{K}N$, $\pi\Sigma$ and $\pi\Lambda$ are related to each others. We then use the Weinberg-Tomozawa Lagrangian with the lowest order momentum

$$\mathcal{L}_{WT} = Tr \left(\bar{B} i \gamma^\mu \frac{1}{4f^2} [(\Phi \partial_\mu \Phi - \partial_\mu \Phi \Phi) B - B(\Phi \partial_\mu \Phi - \partial_\mu \Phi \Phi)] \right), \quad (3.10)$$

where f is the meson decay constant, ∂_μ is the covariant derivative, Φ is the matrices of the octet pseudoscalar meson and B is the matrices of the octet baryon.

For $\bar{K}N$ sector, the Lagrangian in the particle basis takes the form

$$\begin{aligned} \mathcal{L}_{WT_{particle}} &= \sum_{i,j} C_{ij} \bar{B}_i \Phi_i K p \Phi_j B_j \\ &= 2\bar{p} K^- K p K^+ p + 2\bar{n} \bar{K}^0 K p \bar{K}^0 n \\ &\quad + \bar{n} \bar{K}^0 K p K^- p + \bar{p} K^- K p \bar{K}^0 n + \dots, \end{aligned} \quad (3.11)$$

where Kp is the interaction kernel in the particles basis and the coefficient between the various channels, C_{ij} , are the relative coupling strength. Because the strong interaction is isospin conserved, so we can express C_{ij} in the form of isospin basis by writing the physical states of $\bar{K}N$ system as linear combinations of the $I = 0, 1, 2$ states and using the rules for adding angular momentum in quantum mechanics and Clebsch-Gordan coefficients,

$$|I, I_z\rangle = \sum_{I_{z1}+I_{z2}=I_z} C_{I_{z1}I_{z2}I_z}^{II} |I_1, I_{z1}\rangle |I_2, I_{z2}\rangle. \quad (3.12)$$

The particle basis can be written in term of isospin basis related for $\bar{K}N$, $\pi\Sigma$ and $\pi\Lambda$ as

$$|K^- p\rangle = \frac{1}{\sqrt{2}} |\bar{K}N(1) - \bar{K}N(0)\rangle, \quad (3.13)$$

$$|\bar{K}^0 n\rangle = \frac{1}{\sqrt{2}}|\bar{K}N(1) + \bar{K}N(0)\rangle, \quad (3.14)$$

$$|\pi^0 \Sigma^0\rangle = \sqrt{\frac{2}{3}}|\pi\Sigma(2)\rangle - \frac{1}{\sqrt{3}}|\pi\Sigma(0)\rangle, \quad (3.15)$$

$$|\pi^- \Sigma^+\rangle = \frac{1}{\sqrt{6}}|\pi\Sigma(2)\rangle - \frac{1}{\sqrt{2}}|\pi\Sigma(1)\rangle + \frac{1}{\sqrt{3}}|\pi\Sigma(0)\rangle, \quad (3.16)$$

$$|\pi^+ \Sigma^-\rangle = \frac{1}{\sqrt{6}}|\pi\Sigma(2)\rangle + \frac{1}{\sqrt{2}}|\pi\Sigma(1)\rangle + \frac{1}{\sqrt{3}}|\pi\Sigma(0)\rangle, \quad (3.17)$$

$$|\pi^0 \Lambda\rangle = |\pi\Lambda(1)\rangle. \quad (3.18)$$

Then substituting these physical states into the Lagrangian (3.11), we get

$$\mathcal{L}_{WT_{isospin}} = 3\bar{K}N(0)K_I\bar{K}N(0) + 1\bar{K}N(1)K_I\bar{K}N(1) + \dots, \quad (3.19)$$

where K_I is the interaction kernel in isospin basis. The coupled interactions must be related to the coupling strength coefficient, so we can write C_{ij} for $I = 0$ and $I = 1$ states with the following matrices,

$$\mathbf{C}_{ij}^{I=0} = \begin{pmatrix} 3 & -\sqrt{\frac{3}{2}} \\ -\sqrt{\frac{3}{2}} & 4 \end{pmatrix}, \text{ for isospin } \mathbf{I} = 0 \quad (3.20)$$

where i and $j = 1, 2$ refer to the $\bar{K}N$ and $\pi\Sigma$ channels, and

$$\mathbf{C}_{ij}^{I=1} = \begin{pmatrix} 1 & -1 & -\sqrt{\frac{3}{2}} \\ -1 & 2 & 0 \\ -\sqrt{\frac{3}{2}} & 0 & 0 \end{pmatrix}, \text{ for isospin } \mathbf{I} = 1 \quad (3.21)$$

where i and $j = 1, 2, 3$ refer to the $\bar{K}N$, $\pi\Sigma$ and $\pi\Lambda$ channels, respectively.

The interactions in the particle basis can be expressed in terms of interactions in the isospin space similar to the physical states. The isospin basis interaction terms are given as follows, for the processes $K^- p \rightarrow K^- p$, $\bar{K}^0 n$, $\pi^- \Sigma^+$, $\pi^+ \Sigma^-$, $\pi^0 \Sigma^0$ and $\pi^0 \Lambda$

$$\langle K^- p | V | K^- p \rangle = \frac{1}{2}C_{11}^{I=0}V^0(r) + \frac{1}{2}C_{11}^{I=1}V^1(r) \quad (3.22)$$

$$\langle K^- p | V | \bar{K}^0 n \rangle = -\frac{1}{2} C_{11}^{I=0} V^0(r) + \frac{1}{2} C_{11}^{I=1} V^1(r) \quad (3.23)$$

$$\langle K^- p | V | \pi^- \Sigma^+ \rangle = -\frac{1}{\sqrt{6}} C_{12}^{I=0} V^0(r) - \frac{1}{2} C_{12}^{I=1} V^1(r) \quad (3.24)$$

$$\langle K^- p | V | \pi^+ \Sigma^- \rangle = -\frac{1}{\sqrt{6}} C_{12}^{I=0} V^0(r) + \frac{1}{2} C_{12}^{I=1} V^1(r) \quad (3.25)$$

$$\langle K^- p | V | \pi^0 \Sigma^0 \rangle = \frac{1}{\sqrt{6}} C_{12}^{I=0} V^0(r) \quad (3.26)$$

$$\langle K^- p | V | \pi^0 \Lambda \rangle = \frac{1}{\sqrt{2}} C_{13}^{I=1} V^1(r) \quad (3.27)$$

$\bar{K}^0 n \rightarrow \bar{K}^0 n, \pi^- \Sigma^+, \pi^+ \Sigma^-$ and $\pi^0 \Sigma^0$

$$\langle \bar{K}^0 n | V | \bar{K}^0 n \rangle = \frac{1}{2} C_{11}^{I=0} V^0(r) + \frac{1}{2} C_{11}^{I=1} V^1(r) \quad (3.28)$$

$$\langle \bar{K}^0 n | V | \pi^- \Sigma^+ \rangle = \frac{1}{\sqrt{6}} C_{12}^{I=0} V^0(r) - \frac{1}{2} C_{12}^{I=1} V^1(r) \quad (3.29)$$

$$\langle \bar{K}^0 n | V | \pi^+ \Sigma^- \rangle = \frac{1}{\sqrt{6}} C_{12}^{I=0} V^0(r) + \frac{1}{2} C_{12}^{I=1} V^1(r) \quad (3.30)$$

$$\langle \bar{K}^0 n | V | \pi^0 \Sigma^0 \rangle = -\frac{1}{\sqrt{6}} C_{12}^{I=0} V^0(r) \quad (3.31)$$

$\pi^- \Sigma^+ \rightarrow \pi^- \Sigma^+, \pi^+ \Sigma^-$ and $\pi^0 \Sigma^0$

$$\langle \pi^- \Sigma^+ | V | \pi^- \Sigma^+ \rangle = \frac{1}{3} C_{22}^{I=0} V^0(r) + \frac{1}{2} C_{22}^{I=1} V^1(r) \quad (3.32)$$

$$\langle \pi^- \Sigma^+ | V | \pi^+ \Sigma^- \rangle = \frac{1}{3} C_{22}^{I=0} V^0(r) - \frac{1}{2} C_{22}^{I=1} V^1(r) \quad (3.33)$$

$$\langle \pi^- \Sigma^+ | V | \pi^0 \Sigma^0 \rangle = \frac{1}{3} C_{22}^{I=0} V^0(r) + \frac{1}{3} C_{22}^{I=1} V^1(r) \quad (3.34)$$

$\pi^+ \Sigma^- \rightarrow \pi^+ \Sigma^-$ and $\pi^0 \Sigma^0$

$$\langle \pi^+ \Sigma^- | V | \pi^+ \Sigma^- \rangle = \frac{1}{3} C_{22}^{I=0} V^0(r) + \frac{1}{2} C_{22}^{I=1} V^1(r) \quad (3.35)$$

$$\langle \pi^+ \Sigma^- | V | \pi^0 \Sigma^0 \rangle = -\frac{1}{3} C_{22}^{I=0} V^0(r) + \frac{1}{3} C_{22}^{I=1} V^1(r) \quad (3.36)$$

$\pi^0 \Sigma^0 \rightarrow \pi^0 \Sigma^0$

$$\langle \pi^0 \Sigma^0 | V | \pi^0 \Sigma^0 \rangle = \frac{1}{3} C_{22}^{I=0} V^0(r) \quad (3.37)$$

where $V^0(r)$ and $V^1(r)$ are the isospin-based $I = 0$ and 1 potentials, respectively. We expect that the potentials reproduce the low-energy scattering data of the reactions $K^- p \rightarrow K^- p, \bar{K}^0 n, \pi^0 \Sigma^0, \pi^+ \Sigma^-, \pi^- \Sigma^+$ and $\pi^0 \Lambda$, predicted by other theoretical approaches.

3.3 Cross Sections of $\bar{K}N$ Collision

The cross section is an effective area measured around the colliding particles. It is one of the most important properties of the scattering process. We can calculate cross sections by considering the out scattered wave in equation (2.40). In case of s-wave with the total orbital angular momentum $l = l' = 0$, and $s = s' = 0$, the coupling state of the radial part can be solved by treating as a hard sphere scattering. Assuming that $V(r) \rightarrow 0$ at $r \geq R$, so equation (2.40) becomes

$$R_\alpha(k_\alpha, r) = j_0(k_\alpha r)\delta_{\alpha\alpha_0} + \int r'^2 dr' g(k_\alpha, r, r') V_{\alpha\beta}(r') R_\beta(k_\beta, r'). \quad (3.38)$$

In Chapter II we use the results from the radial part of the out scattered wave function to calculate cross section and compare them with the experimental data (Mast et al., 1975; Mast et al., 1976; Armenteros et al., 1970; Humphrey and Ross, 1962; Sakit et al., 1965; Evans et al., 1983; Kittel et al., 1966; Abrams and Sechi-Zorn, 1965; Kim, 1966; Siegel and Weise, 1988; Bangerter et al., 1981; Ciborowski et al., 1982).

In general, there are two cases for analytical solution, a direct process and an indirect process. Next we will give a brief details of both processes.

3.3.1 Direct Process ($\alpha \rightarrow \alpha$)

From the Schrödinger equation in the spherical coordinates, in the far-field solution where the distance $r > R$ and $V(r) \approx 0$, we have

$$\left[\frac{1}{r^2} \frac{\partial}{\partial r} r^2 \frac{\partial}{\partial r} - \frac{l(l+1)}{r^2} \right] R_l(r) = -k^2 R_l(r). \quad (3.39)$$

The general solution and the asymptotically general solution can be written as

$$R_l(r) = a_l j_l(kr) - b_l n_l(kr), \quad (3.40)$$

$$R_l(r) = A_l j_l(kr) \cos \delta_l - A_l n_l(kr) \sin \delta_l, \quad (3.41)$$

where a_l and b_l are constant coefficients, A_l is the amplitude of the asymptotic solution and δ_l is a phase shift due to the scattering potential. At the boundary, $r = R$, (R being the range of the potential), the wave function and its derivative should be continuous, so we have

$$\frac{r}{R_l(r)} \frac{dR_l(r)}{dr} \Big|_{r=R^-} = kR \frac{j_l'(kR) \cos \delta_l - n_l'(kR) \sin \delta_l}{j_l(kR) \cos \delta_l - n_l(kR) \sin \delta_l} = \beta_l. \quad (3.42)$$

Then the phase shift becomes

$$\delta_l = \arctan \left(\frac{\beta_l j_l(kR) - kR j_l'(kR)}{\beta_l n_l(kR) - kR n_l'(kR)} \right). \quad (3.43)$$

According to the optical theorem, the phase shift depends on the energy of the incoming particle and the total orbital angular momentum l . The total cross section are given in term of phase shift in case of direct process

$$\sigma_{tot} = \frac{4\pi}{k^2} \sum_{l=0}^{l=kR} (2l+1) \sin^2 \delta_l. \quad (3.44)$$

3.3.2 Cross Process ($\alpha_0 \rightarrow \alpha$)

When the potential is zero the radial part of the out scattering wave becomes

$$R_l^\alpha(r) = \int r'^2 dr' g_l(r, r') V^{\alpha\beta}(r') R_l^\beta(r'), \quad (3.45)$$

where $\alpha \neq \alpha_0$. The wave functions with the scatterer at large-distance are given by

$$\langle \vec{x} | \varphi^{(+)} \rangle = \frac{1}{(2\pi)^{3/2}} \left[f(\theta) \frac{e^{ikr}}{r} \right], \quad (3.46)$$

where $f(\theta)$ is the scattering amplitude. Using the partial wave expansion, we get the wave functions in terms of spherical as

$$\langle \vec{x} | \varphi^{(+)} \rangle = \frac{1}{(2\pi)^{3/2}} \sum_l (2l+1) f_l(k) P_l(\cos\theta) \frac{e^{ikr}}{r}, \quad (3.47)$$

where $f_l(k)$ is the partial-wave amplitude, and P_l is Legendre function of rank l .

For $r > R$ can be written as

$$\langle \vec{x} | \varphi^{(+)} \rangle = \frac{1}{(2\pi)^{3/2}} \sum_l i^l (2l+1) R_l(r) P_l(\cos\theta). \quad (3.48)$$

From the equation (3.47) and (3.48) the definition of the partial-wave amplitude is given by

$$f_l(k) = i^l e^{-ikR} R_l(R) R. \quad (3.49)$$

Therefore, the total cross section is

$$\sigma_{tot} = 4\pi \sum_{l=0}^{l=kR} (2l+1) |f_l(k)|^2. \quad (3.50)$$

In next chapter, we compare our the numerical results with experimental data of all six channels of $\bar{K}N$ interactions.

CHAPTER IV

RESULTS AND CONCLUSIONS

In this chapter we present our results generated by FORTRAN program, using parameters from Chapter III and the specific potential proposed by Akaishi and Yamazaki (see equation (4.2)).

4.1 Numerical Results

We apply the Lippmann-Schwinger equation (2.40) to evaluate the cross sections of the reactions $K^-p \rightarrow K^-p$, \bar{K}^0n , $\pi^0\Sigma^0$, $\pi^-\Sigma^+$, $\pi^+\Sigma^-$ and $\pi^0\Lambda$ with the potential constructed phenomenologically in the works (Akaishi and Yamazaki, 2002; Yamazaki and Akaishi, 2002). The employed potential takes the form

$$V_{\alpha\beta}^I(r) = V_{\alpha,\beta}^I \exp \left[- \left(\frac{r}{b} \right)^2 \right], \quad (4.1)$$

where the range parameter $b = 0.66$ fm and $V_{\alpha,\beta}^I$ are as follows:

$$\begin{aligned} V_{\bar{K}N,\bar{K}N}^{I=0} &= -436 \text{ MeV}, V_{\bar{K}N,\bar{K}N}^{I=1} = -62 \text{ MeV}, \\ V_{\bar{K}N,\pi\Sigma}^{I=0} &= -412 \text{ MeV}, V_{\bar{K}N,\pi\Sigma}^{I=1} = -285 \text{ MeV}, \\ V_{\bar{K}N,\pi\Lambda}^{I=0} &= 0 \text{ MeV}, V_{\bar{K}N,\pi\Lambda}^{I=1} = -285 \text{ MeV}. \end{aligned} \quad (4.2)$$

Shown in Figures 4.1, 4.2, 4.3, 4.4, 4.5 and 4.6 are our results on the cross section of the reactions $K^-p \rightarrow K^-p$, $K^-p \rightarrow \bar{K}^0n$, $K^-p \rightarrow \pi^0\Sigma^0$, $K^-p \rightarrow \pi^-\Sigma^+$, $K^-p \rightarrow \pi^+\Sigma^-$ and $K^-p \rightarrow \pi^0\Lambda$, respectively compared with the experimental data (Mast et al., 1975; Mast et al., 1976; Armenteros et al., 1970; Humphrey and Ross, 1962; Sakit et al., 1965; Evans et al., 1983; Kittel et al., 1966; Abrams

and Sechi-Zorn, 1965; Kim, 1966; Siegel and Weise, 1988; Bangerter et al., 1981; Ciborowski et al., 1982).

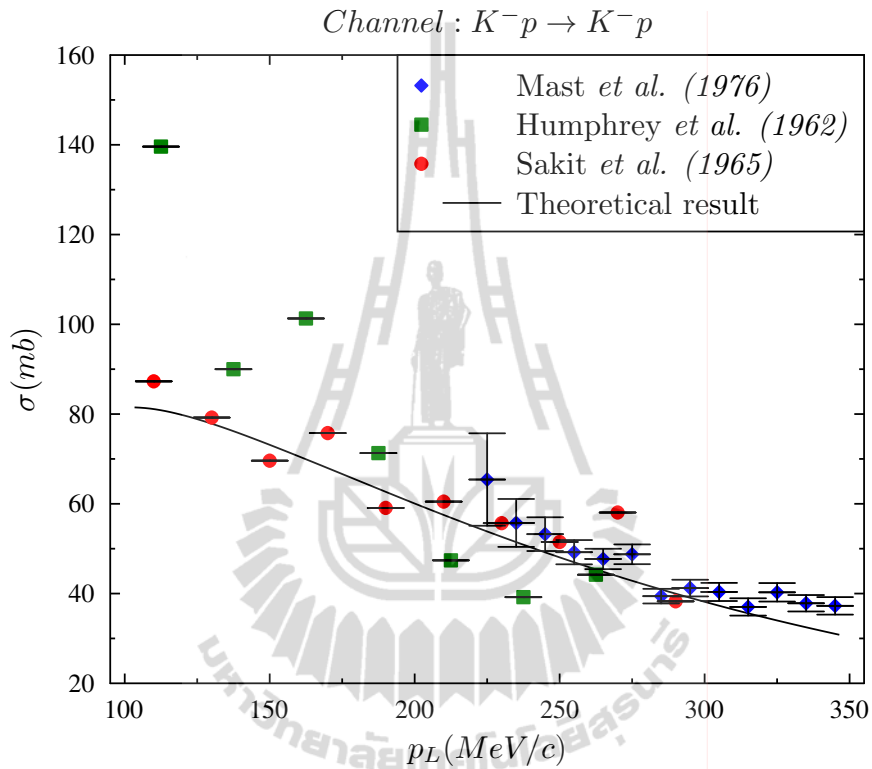


Figure 4.1 Theoretical cross section of the reaction $K^-p \rightarrow K^-p$ compared with the experimental data from Mast et al., Humphrey et al. and Sakit et al. (Mast et al., 1976; Humphrey and Ross, 1962; Sakit et al., 1965).

We plot our results of the elastic cross section of the reaction $K^-p \rightarrow K^-p$ compared to experimental data from Mast et al., Humphrey et al. and Sakit et al. (Mast et al., 1976; Humphrey and Ross, 1962; Sakit et al., 1965). The solid line in Figure 4.1 is our results. The diamonds represent data from Mast et al. The squares and the circles are data from Humphrey et al. and Sakit et al. respectively. It can be seen clearly that our results agree well with those of Sakit et al. at the

laboratory momentum between 100-250 MeV/c, and those of Mast et al. at the laboratory momentum between 225-350 MeV/c. However below 200 MeV/c we do not have good agreement with Humphrey et al.

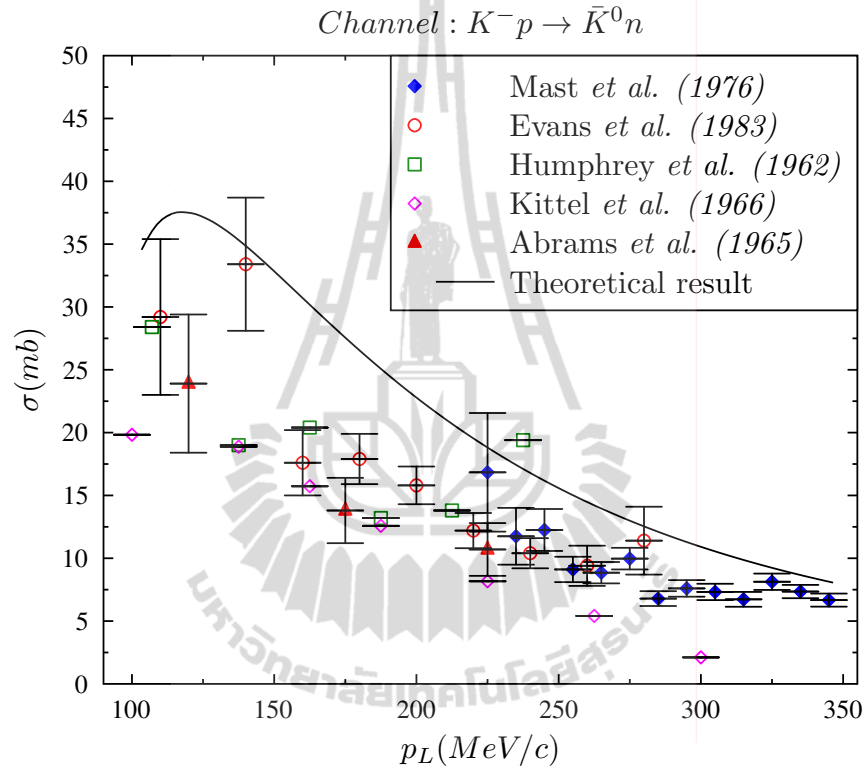


Figure 4.2 Theoretical cross section of the reaction $K^-p \rightarrow \bar{K}^0n$ compared with the experimental data from Mast et al., Evans et al., Humphrey et al., Kittel et al. and Abrams et al. (Mast et al., 1976; Evans et al., 1983; Humphrey and Ross, 1962; Kittel et al., 1966; Abrams and Sechi-Zorn, 1965).

The inelastic cross section of the reaction $K^-p \rightarrow \bar{K}^0n$ are shown in Figure 4.2. The data of Mast et al., Evans et al., Humphrey et al., Kittel et al. and Abrams et al. (Mast et al., 1976; Evans et al., 1983; Humphrey and Ross, 1962; Kittel et al., 1966; Abrams and Sechi-Zorn, 1965) are also given for comparison.

The solid line is our results. The diamonds represent data from Mast et al. and the open circles are data from Evans et al. Data from Humphrey et al., Kittel et al. and Abrams et al. are represented by the open squares, the open diamonds and the triangles respectively. We have found good agreement within error bars with Evan et al. at the laboratory momentum 140 MeV/c and 280 MeV/c and Mast et al. at the laboratory momentum 225 MeV/c. However at different laboratory momentums we can not find good agreement with Evan et al. and Mast et al. For the other experiments (Humphrey and Ross, 1962; Kittel et al., 1966; Abrams and Sechi-Zorn, 1965) we cannot fit our results with their data at all.

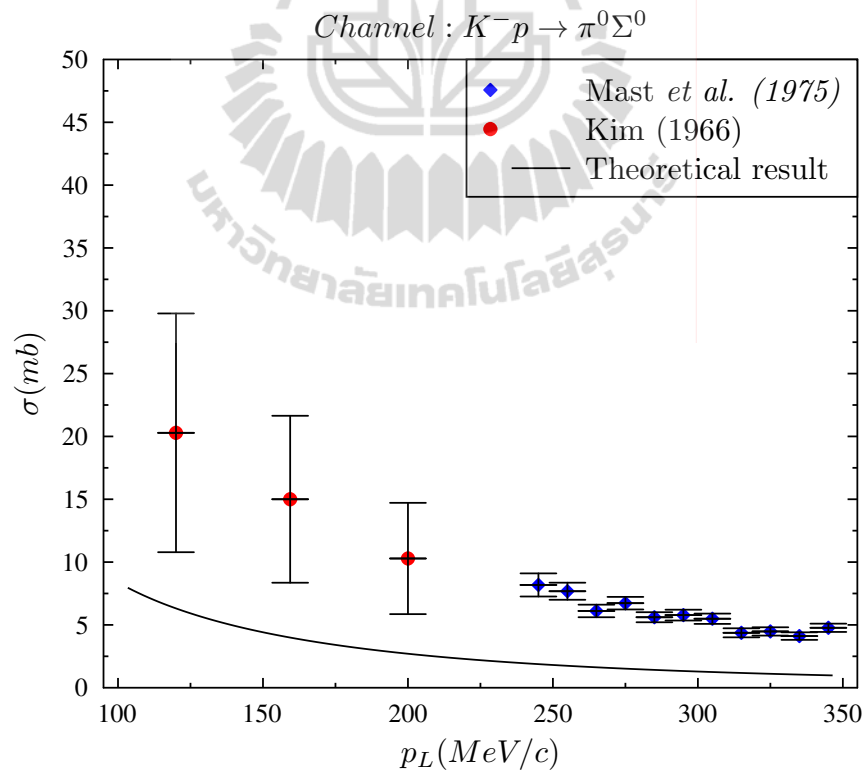


Figure 4.3 Theoretical cross section of the reaction $K^-p \rightarrow \pi^0\Sigma^0$ compared with the experimental data from Mast et al. and Kim et al. (Mast et al., 1975; Kim, 1966).

We cannot fit our results with the data for the inelastic cross section of the reaction $K^-p \rightarrow \pi^0\Sigma^0$ as shown in Figure 4.3. However we can see the same decreasing pattern as experimental data at every laboratory momentums. If we manage to find some shifting factor to move our results up it could fit both experimental data from Mast et al. and Kim et al.

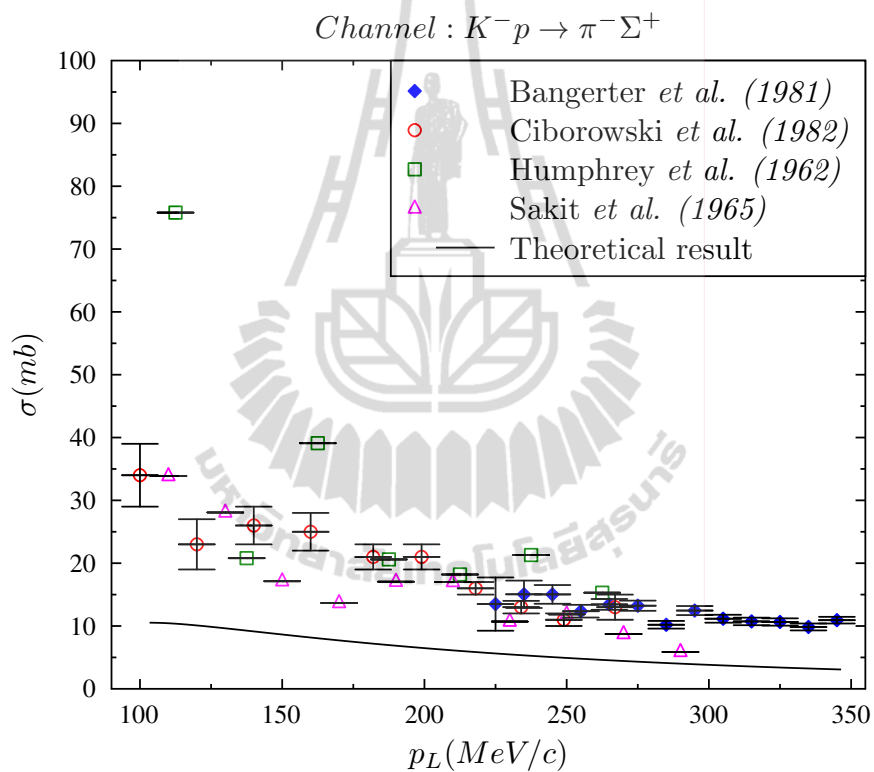


Figure 4.4 Theoretical cross section of the reaction $K^-p \rightarrow \pi^-\Sigma^+$ compared with the experimental data from Bangerter et al., Ciborowski et al., Humphrey et al. and Sakit et al. (Bangerter et al., 1981; Ciborowski et al., 1982; Humphrey and Ross, 1962; Sakit et al., 1965).

This figure (Figure 4.4) show our results of the inelastic cross section of the reaction $K^-p \rightarrow \pi^-\Sigma^+$. The data from Bangerter et al., Ciborowski et al.,

Humphrey et al. and Sakit et al. (Bangerter et al., 1981; Ciborowski et al., 1982; Humphrey and Ross, 1962; Sakit et al., 1965) cannot be fitted by our theoretical calculation. As we have seen already in previous figure (Figure 4.4) our numerical results have the same decreasing pattern as the experimental data except those from Humphrey et al. at the laboratory momentum between 100-250 MeV/c.

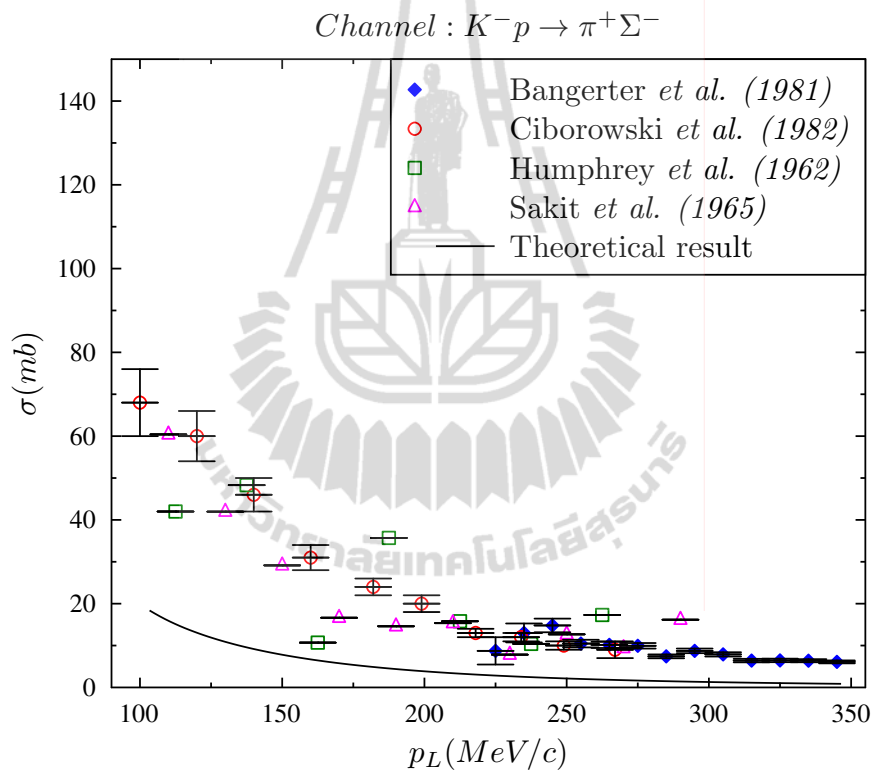


Figure 4.5 Theoretical cross section of the reaction $K^- p \rightarrow \pi^+ \Sigma^-$ compared with the experimental data from Bangerter et al., Ciborowski et al., Humphrey et al. and Sakit et al. (Bangerter et al., 1981; Ciborowski et al., 1982; Humphrey and Ross, 1962; Sakit et al., 1965).

The inelastic cross section of the reaction $K^- p \rightarrow \pi^+ \Sigma^-$ are shown in Figure 4.5 we have the same decreasing pattern as experimental data at the laboratory

momentum between 225-350 MeV/c with some shifting factor. For the laboratory momentum lower than 225 MeV/c our slope does not decrease as fast as that found in experimental data.

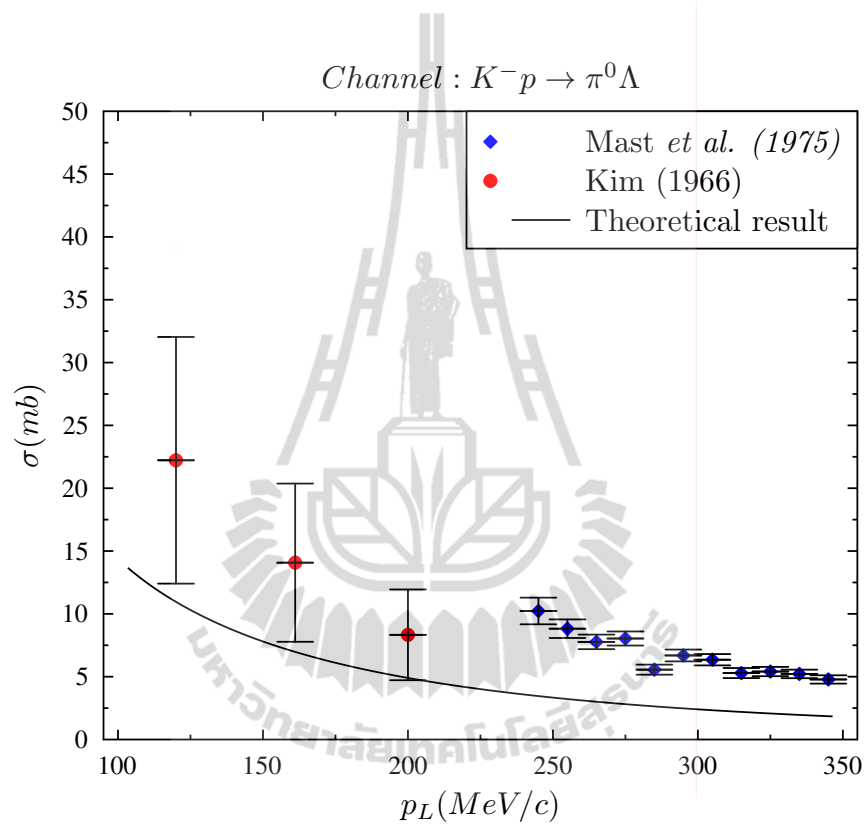


Figure 4.6 Theoretical cross section of the reaction $K^-p \rightarrow \pi^0 \Lambda$ compared with the experimental data from Mast et al. and Kim et al. (Mast et al., 1975; Kim, 1966).

In the last channel, the inelastic cross sections from our calculation still have the same decreasing behavior as the experimental data as shown in Figure 4.6 particularly at the laboratory momentum between 100-200 MeV/c. But at the higher laboratory momentum our results produce a smooth curve unlike the experimental data from Mast et al. they tend to move up and down.

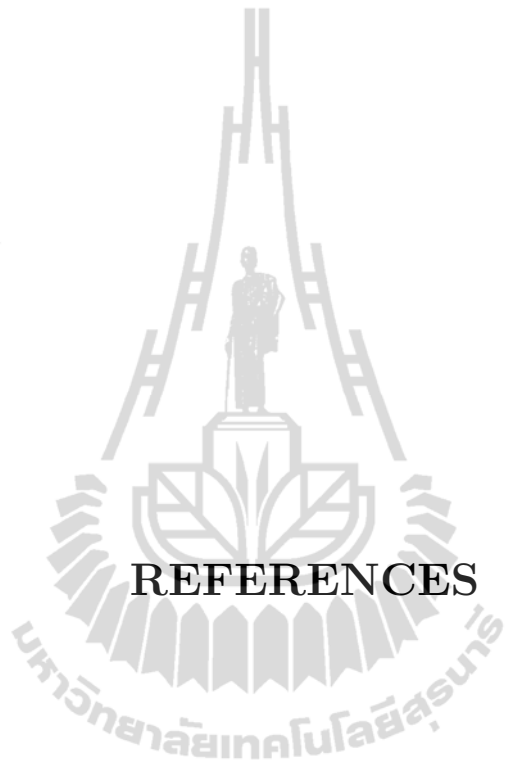
4.2 Conclusions

In our thesis, we have worked out the Lippmann-Schwinger equation for the coupled $\bar{K}N$ system and the relations for interactions among various channels for the coupled $\bar{K}N$ channels in the framework of the flavor SU(3) symmetry. The cross sections of the reactions $K^-p \rightarrow K^-p$, $K^-p \rightarrow \bar{K}^0n$, $K^-p \rightarrow \pi^0\Sigma^0$, $K^-p \rightarrow \pi^-\Sigma^+$, $K^-p \rightarrow \pi^+\Sigma^-$ and $K^-p \rightarrow \pi^0\Lambda$ are evaluated with the phenomenological potentials (Akaishi and Yamazaki, 2002; Yamazaki and Akaishi, 2002).

The results shown in section 4.1 tell us that the theoretical cross sections can reproduce the experimental data well for channel $K^-p \rightarrow K^-p$ only. But for the other channels the theoretical results and the experimental data are difference with some shifting factors.

4.3 The final goal of the research

In our research, we have tried to develop a better version of potential for the coupled $\bar{K}N$ in coordinate space. This potential is expected to reproduce the low-energy $\bar{K}N$ scattering data better. Apart from that, we can also improve our results by adding the coulomb interactions into the FORTRAN programs. This will help us to get the theoretical cross section in range of the laboratory momentum lower than 100 MeV/c. We can also consider to expand our calculation to include d-wave, p-wave and so on. In this way, it could help us to get the theoretical cross section in range of the laboratory momentum higher than 350 MeV/c.



REFERENCES

REFERENCES

- Abrams, G. S. and Sechi-Zorn, B. (1965). Charge-exchange scattering of low-energy interactions of K^- meson in hydrogen*. **Phys. Rev.** 139: B454.
- Akaishi, Y. and Yamazaki, T. (2002). Nuclear \bar{K} bound states in light nuclei. **Phys. Rev. C** 65: 044005.
- Armenteros, R., Baillon, P., Bricman, C., Ferro-Luzzi, M., Pagiola, E., Petersen, J., Plane, D. E., and Schmitz, N. (1970). K^-p cross sections from 440 to 800 MeV/c. **Nucl. Phys. B** 21: 13.
- Bangerter, R. O., Alston-Garnjost, M., Mast, T. S., Solmitz, F. T., and Tripp, R. D. (1981). Reactions $K^-p \rightarrow \Sigma^- \pi^+$ and $K^-p \rightarrow \Sigma^+ \pi^-$ in the momentum range from 220 to 470 MeV/c. **Phys. Rev. D** 23: 1484.
- Bianco, S. (1998). Kaon-Nucleon interaction studied by the kaonic X ray with deuterium at DAΦNE*. **Acta. Phys. Pol. B** 20: 9.
- Ciborowski, J., Gwizdz, J., Kielczewska, D., Nowak, R. J., Rondio, E., Zakrzewski, J. A., Goossens, M., Wilquet, G., Bedford, N. H., Evans, D., Fleming, G. P., Hamam, Y. A., Major, J. V., Bartley, J. H., Davis, D. H., Miller, D. J., Tovee, D. N., and Tymieniecka, T. (1982). Kaon scattering and charged sigma hyperon production in K^-p interactions below 300 MeV/c. **J. Phys. G** 18: 13.
- Doté, A., Hyodo, T., and Weise, W. (2009a). Variational calculation of K^-pp with chiral SU(3)-based $\bar{K}N$ interaction. **Nucl. Phys. A** 827: 315c–317c.

- Doté, A., Hyodo, T., and Weise, W. (2009b). Variational calculation of the ppK^- system base on chiral SU(3) dynamics. **Phys. Rev. C** 79: 014003.
- Durso, J. W. (1998). Origin of resonances in the chiral unitary approachChiral unitary approach to the $\pi N^* N^*$, $\eta N^* N^*$ couplings for the $N^*(1535)$ resonance. **Acta. Phys. Pol. B** 29: 9.
- Entem, D. R., Fernández, F., and Valcarce, A. (2000). Chiral quark model of the NN system within a Lippmann-Schwinger resonating group method. **Phys. Rev. C** 62: 034002.
- Evans, D., Major, J. V., Rondio, E., Zakrzewski, J. A., Conboy, J. E., Miller, D. J., and Tymieniecka, T. (1983). Charge-exchange scattering in K^-p interactions below 300 MeV/c. **J. Phys. G** 9: 885.
- Humphrey, W. E. and Ross, R. R. (1962). Low-energy interactions of K^- meson in hydrogen. **Phys. Rev.** 127: 1305.
- Hyodo, T., Jido, D., and Hosaka, A. (2008). Origin of resonances in the chiral unitary approach. **Phys. Rev. C** 78: 025203.
- Hyodo, T. and Weise, W. (2008a). Effective $\bar{K}N$ interaction and role of chiral symmetry. **Phys. Rev. C** 77: 035204.
- Hyodo, T. and Weise, W. (2008b). Effective $\bar{K}N$ interaction based on chiral SU(3) dynamics. **Phys. Rev. C** 77: 035204.
- Kaiser, N., Siegel, P. B., and Weise, W. (1995a). Chiral dynamics and the low-energy kaon-nucleon interaction. **Nucl. Phys. A** 594: 325–345.
- Kaiser, N., Siegel, P. B., and Weise, W. (1995b). Chiral dynamics and the $S_{11}(1535)$ nucleon resonance*. **Phys. Lett. B** 362: 23–28.

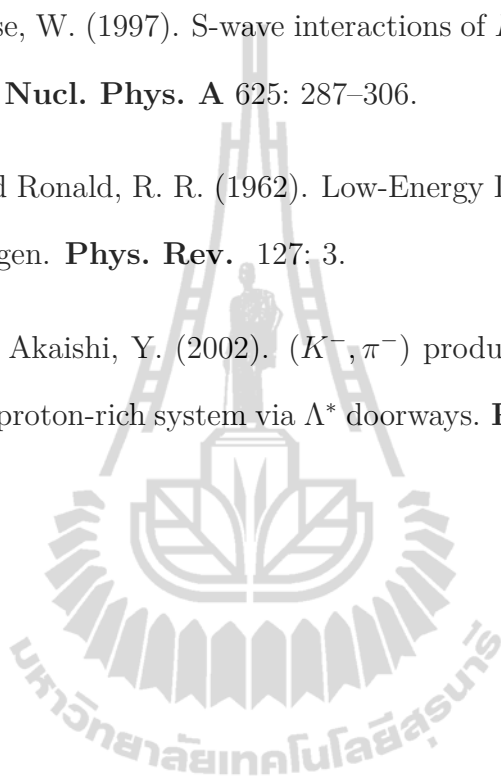
- Kim, J. K. (1966). *Columbia University Report, USA, No Nevis 149*.
- Kittel, W., Otter, G., and Wacek, I. (1966). The K^- proton charge exchange interactions at low energies and scattering lengths determination. **Phys. Lett.** 21: 349.
- Landau, R. H. (1983). K^-p bound states with coupling to hyperon channels. **Phys. Rev. C** 28: 3.
- Landau, R. H. and Páez, M. J. (1997). Computational Physics Problem Solving with Computers. *John Wiley and Sons Lnc, USA*.
- Mast, T. S., Alston-Garnjost, M., Bangerter, R. O., Barbaro-Galtieri, A. S., Solmitz, F. T., and Tripp, R. D. (1975). Reactions $K^-p \rightarrow \Sigma^0\pi^0$ and $K^-p \rightarrow \Lambda\pi^0$ in the momentum range 240 to 450 MeV/c*. **Phys. Rev. D** 11: 3078.
- Mast, T. S., Alston-Garnjost, M., Bangerter, R. O., Barbaro-Galtieri, A. S., Solmitz, F. T., and Tripp, R. D. (1976). Elastic, charge-exchange, and total K^-p cross sections in the momentum range 220 to 470 MeV/c*. **Phys. Rev. D** 14: 13.
- Nacher, J. C., Parreno, A., Oset, E., Ramos, A., Hosaka, A., and Oka, M. (2000). Chiral unitary approach to the πN^*N^* , ηN^*N^* couplings for the $N^*(1535)$ resonance. **Nucl. Phys. A** 678: 187–211.
- Sakit, M., Day, T. B., Glasser, R. G., and Seeman, N. (1965). Low-energy K^- -meson interactions in hydrogen*. **Phys. Rev.** 139: B719.
- Siegel, P. B. and Weise, W. (1988). Low-energy K^- -nucleon potentials and the nature of the $\Lambda(1405)$. **Phys. Rev. C** 38: 5.

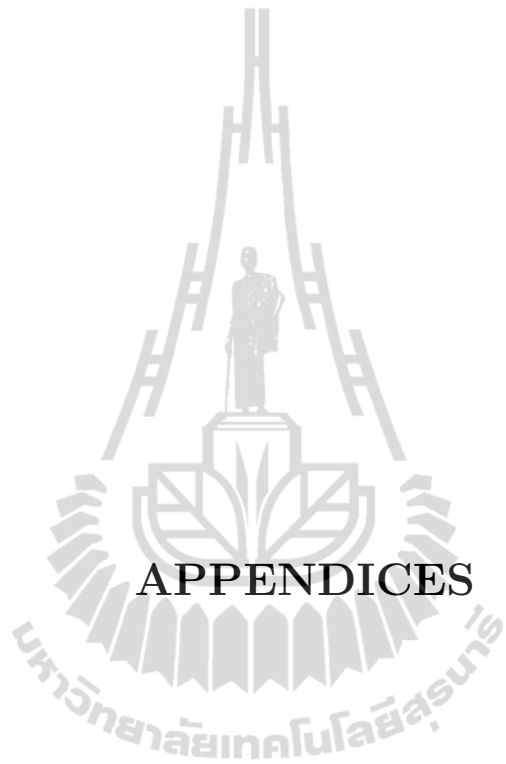
Takeuchi, S. and Shimizu, K. (2009). $\Lambda(1405)$ resonance in baryon-meson scattering with a bound state embedded in the continuum. **Phys. Rev. C** 79: 045204.

Waas, T. and Weise, W. (1997). S-wave interactions of \bar{K} and η mesons in nuclear matter*. **Nucl. Phys. A** 625: 287–306.

William, E. H. and Ronald, R. R. (1962). Low-Energy Interactions of K^- Mesons in Hydrogen. **Phys. Rev.** 127: 3.

Yamazaki, T. and Akaishi, Y. (2002). (K^-, π^-) production of nuclear \bar{K} bound states in proton-rich system via Λ^* doorways. **Phys. Lett. B** 535: 70–76.

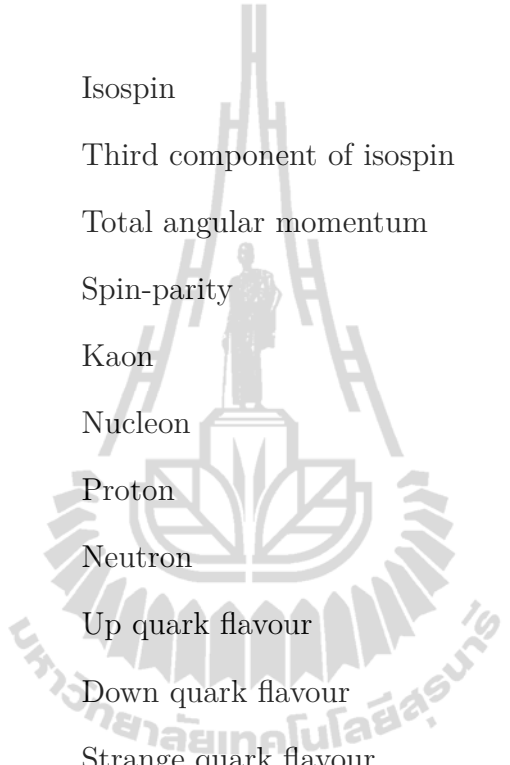




APPENDICES

APPENDIX A

LIST OF SYMBOLS



I	Isospin
I_3	Third component of isospin
J	Total angular momentum
J^p	Spin-parity
K	Kaon
N	Nucleon
p	Proton
n	Neutron
u	Up quark flavour
d	Down quark flavour
s	Strange quark flavour
π	Pion
Σ	Sigma baryons
Λ	Lambda baryons
$SU(3)$	Special unitary groups of transformation of order 3
CPT	Charged conjugation parity and time reversal
H_0	Kinetic energy operator for free particles ($H_0 = \frac{\vec{p}^2}{2m}$)
$ \phi\rangle$	Eigenket of H_0
E	Energy eigen value of H_0
$V_{\alpha\beta}$	Interaction between the α and β channels
ψ_α	Eigen functions of the initial states

ψ_β	Eigen functions of the final states
ϕ_α	Initial free wave
$G(\vec{r}, \vec{r}')$	Green's function
$g_l(k, \vec{r}, \vec{r}')$	Radial component of the Green's function
χ_{s,m_s}	Spin eigen vector of a particle
Y_{lm}	Spherical harmonics function
ϕ	Azimuthal angle
P_l	Legendre polynomials
j_l	Spherical Bessel functions of the 1 st kind
n_l	Spherical Bessel function of the 2 nd kind
h_l	Hankel functions
C_{lm}	Normalized coefficients
R_{lm}	Radial function
S	Spin
k	Momenta
$\omega(x)$	Weight function
f	Form factor
∂_μ	Covariant derivative
Φ	Matrices of the octet pseudoscalar meson
B	Matrices of the octet baryon
C_{ij}	Relative coupling strength
K_I	Interaction kernel in isospin basis
A_l	Amplitude of the asymptotic solution
δ_l	Phase shift due to the potential scattering
$f(\theta)$	Scattering amplitude
$f_l(k)$	Partial-wave amplitude

APPENDIX B

USE SUT-HPCC MACHINES

B.1 Connecting to SUT-HPCC machines via SSH Secure Shell

B.1.1 Logging into SUT-HPCC machines

To get an access to the SUT-HPCC, a user must first fill an application form (the identification card or student ID card are needed). The application form may be obtained in one of two ways:

1. at the Computer Center, second floor, research building,
2. online application forms via WWW at “<http://web.sut.ac.th/ccs/unc/>”.

After registration, you will receive a User name and a Password for the SUT-HPCC system (Linux system). To access this system, it's necessary to download and install programs PuTTY and WinSCP or SSH Secure Shell. You can download PuTTY from “<http://www.chiark.greenend.org.uk/~sgtatham/putty/download.html>”, WinSCP from “<http://winscp.net/eng/download.php>”, and SSH Secure Shell from “<http://www.cm.edu/webhosting/download/SSHSecureShellClient-3.2.9.exe>”.

B.1.2 Using SSH Secure Shell

In this thesis, we use SSH Secure Shell program to connect to SUT-HPCC. After installed SSH Secure Shell for Windows, we can click on the SSH Secure Shell Client icon on our desktop or click on the Start button then go to the Programs

menu and select SSH Secure Shell Client. The SSH Secure Shell window will pop up. Next we click on the “Quick Connect” tab (shown in Figure B.1),



Figure B.1 Connect to SSH Secure Shell.

and then in the “Connect to Remote Host” (Figure B.2) dialog, type in the Host Name : `suthpcc.sut.ac.th`, User Name : `m5110186`, Port Number : 22, and finally click on “Connect”.

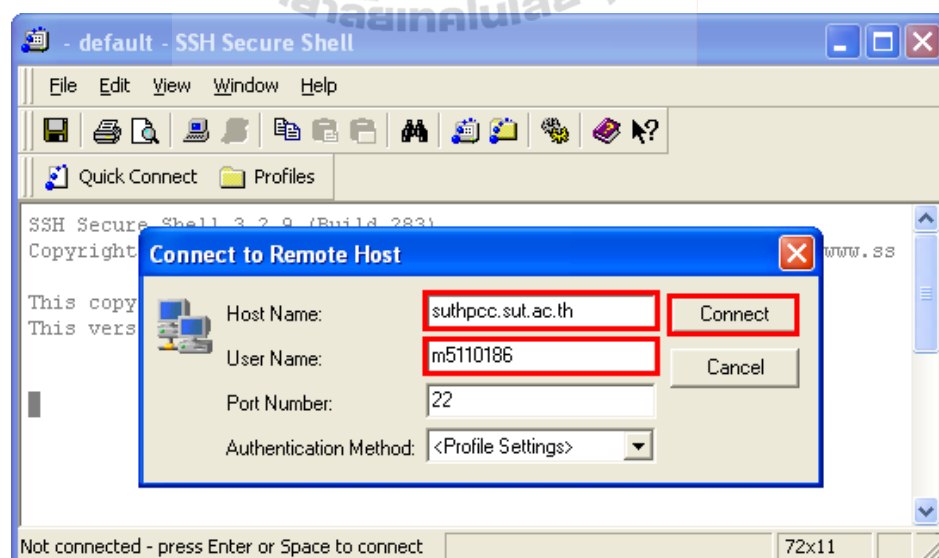


Figure B.2 Connect to Remote Host.

The program will ask for your password (Figure B.3).

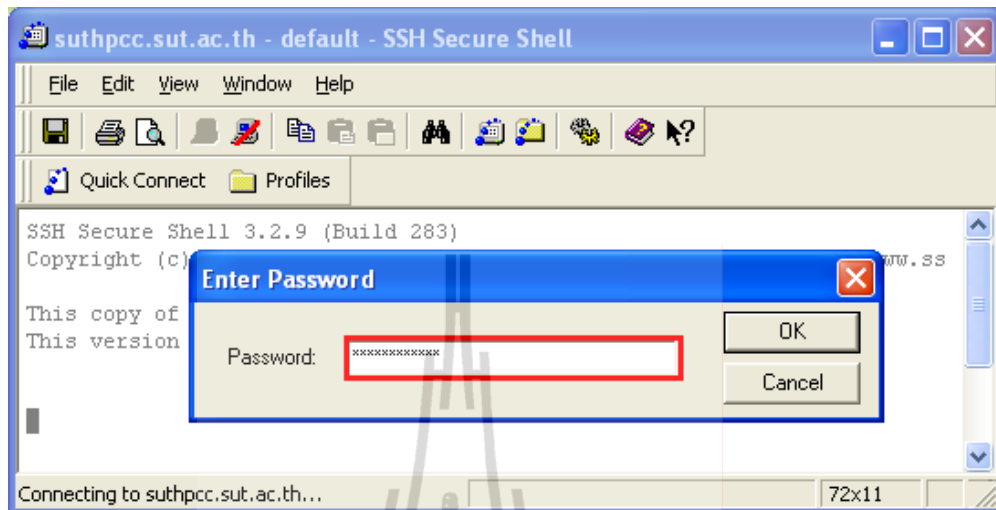


Figure B.3 Enter Password screen.

B.1.3 Using SSH Secure File Transfer

The SSH Secure Shell client can also be used to copy files back and forth between the server and our computer. In order to do that an user has to click on the file transfer icon (shown in Figure B.4).

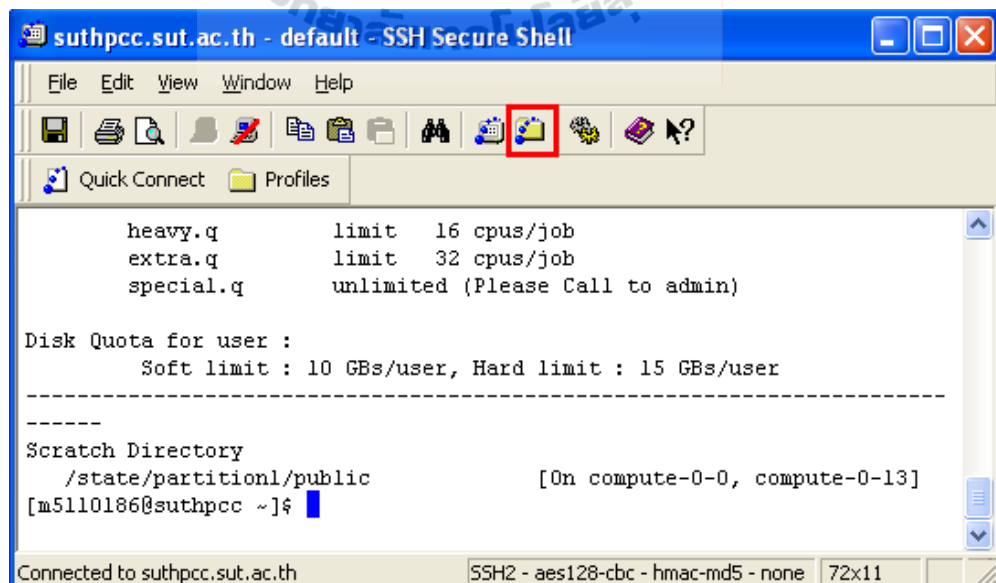


Figure B.4 SSH Secure File Transfer icon.

This will bring up a window with two panels (Figure B.5), the left side is

local file system of the client machine and the right side is files and folders in the server. We can then just drag and drop the files from one side to the other.

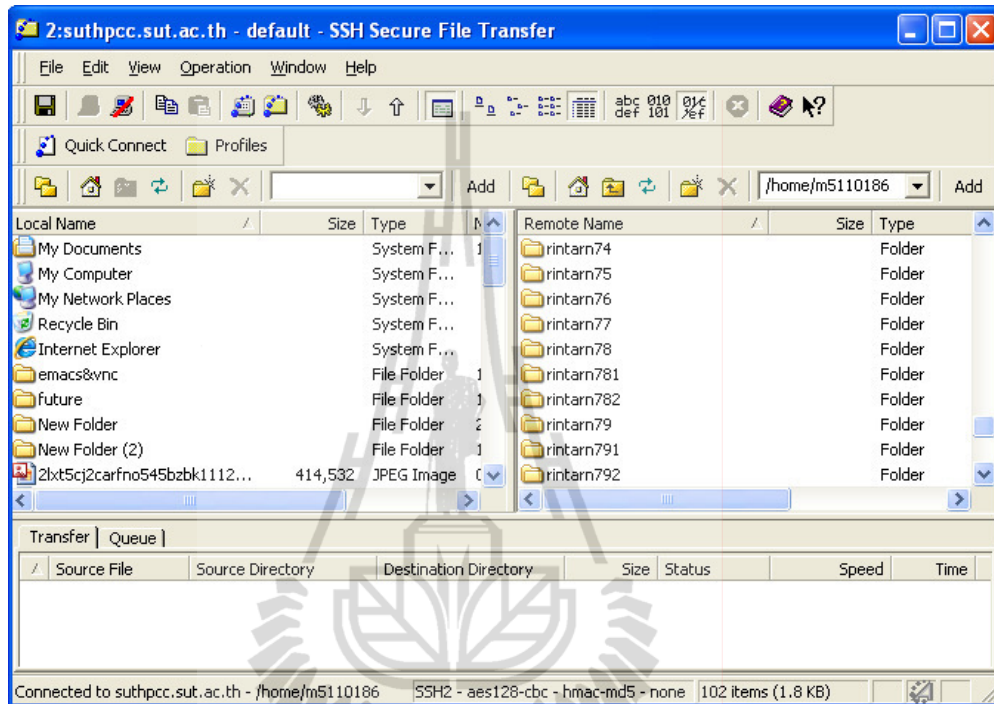


Figure B.5 SSH Secure File Transfer in a window with two panels.

B.2 Using the NAG FORTRAN libraries at SUT-HPCC

B.2.1 FORTRAN Source Codes

In order to use FORTRAN source codes, we need to make a directory, using a command in the Linux “`mkdir <directory name>`”, and then use “`ls`” command to see lists of files and directories. For example (Figure B.6), We create a directory named “`rintarn`”, we can change directory to `rintarn` by using “`cd <directory name>`” command.

Generally, a FORTRAN source file has an extension “.F”. In our work we have five important files (Figure B.7).

The screenshot shows an SSH terminal window titled 'suthpcc.sut.ac.th - HPCC - SSH Secure Shell'. The terminal displays a directory listing of files and subdirectories. The user has executed the command 'mkdir rintarn', which is highlighted with a red box. The directory listing includes files like 'ah_read_write', 'BB', 'BB_keep1', 'BB_keep2', 'Desktop', 'example', 'matrix', 'mbox', 'p_doon', 'p_doon2', 'Q1_keep_BB_Ex', 'rintarn', 'rintarn10', 'rintarn11', 'rintarn12', 'rintarn13', 'rintarn14', 'rintarn15', 'rintarn16', 'rintarn17', 'rintarn18', 'rintarn19', 'rintarn20', 'rintarn21', 'rintarn22', 'rintarn23', 'rintarn24', 'rintarn25', 'rintarn26', 'rintarn27', 'rintarn28', 'rintarn29', 'rintarn2_gsub', 'rintarn3', 'rintarn30', 'rintarn31', 'rintarn32', 'rintarn33', 'rintarn34', 'rintarn35', 'rintarn36', 'rintarn37', 'rintarn38', 'rintarn39', 'rintarn4', 'rintarn41', 'rintarn42', 'rintarn43', 'rintarn44', 'rintarn45', 'rintarn46', 'rintarn47', 'rintarn48', 'rintarn49', 'rintarn5', 'rintarn51', 'rintarn52', 'rintarn53', 'rintarn54', 'rintarn55', 'rintarn56', 'rintarn57', 'rintarn58', 'rintarn59', 'rintarn6', 'rintarn61', 'rintarn62', 'rintarn63', 'rintarn64', 'rintarn65', 'rintarn66', 'rintarn67', 'rintarn68', 'rintarn69', 'rintarn7', 'rintarn71', 'rintarn72', 'rintarn73', 'rintarn74', 'rintarn75', 'rintarn76', 'rintarn77', 'rintarn78', 'rintarn79', 'rintarn8', 'rintarn80', 'rintarn81', 'rintarn82', 'rintarn9', 'test', 'test.nb', and 'YY'. The 'rintarn' directory is circled in red. The terminal prompt is '[m5110186@suthpcc ~]#'. The status bar at the bottom indicates 'Connected to suthpcc.sut.ac.th' and 'SSH2 - aes128-cbc - hmac-md5 - none 95x22'.

Figure B.6 Making a directory to contain source codes.

1. **NAG.sh** is a script file to call NAG library from the server compile all source code and execute the program using qsub.
2. **PARACS.F** is a source code file for configuration important parameters used in MAINS.F, KAONIC.F and KP.F (see Appendix D).
3. **MAINS.F** is a main source code file for our calculation (see Appendix E).
4. **KAONIC.F** and 5. **KP.F** are subroutines code for supporting the main program (see section E.3 in Appendix E).

To create an executable program from source codes, this involves two main steps, first compiling the source files to produce object files, and second linking all the object files to form an executable file.

B.2.2 Compiling Multiple Source Files

The program is composed of several source files. They must be compiled individually to produce object files with the suffix “.o”. These .o files are linked

```

suthpcc.sut.ac.th - HPCC - SSH Secure Shell
File Edit View Window Help
Quick Connect Profiles

matrix      rintarn19      rintarn31      rintarn45      rintarn59      rintarn72      rintarn802
mbox       rintarn1_original  rintarn32      rintarn46      rintarn6       rintarn73      rintarn81
p_doon     rintarn20      rintarn33      rintarn47      rintarn60      rintarn74      rintarn82
p_doon2    rintarn21      rintarn34      rintarn48      rintarn61      rintarn75      rintarn9
Q1_keep_BB_Ex  rintarn22      rintarn35      rintarn49      rintarn62      rintarn76      test
rintarn    rintarn23      rintarn36      rintarn5       rintarn63      rintarn77      test.nb
rintarn10  rintarn24      rintarn37      rintarn50      rintarn64      rintarn78      YY
rintarn11  rintarn25      rintarn38      rintarn51      rintarn65      rintarn781
rintarn12  rintarn26      rintarn39      rintarn52      rintarn66      rintarn782

[m5110186@suthpcc ~]# cd rintarn
[m5110186@suthpcc rintarn]# ls
compilie.sh  file_management.sh  KAONIC.F  KP.F  MAINCS.F  nag.sh  PARACS
[m5110186@suthpcc rintarn]# ls -l
total 52
-rw-r--r--  1 m5110186 m5110186  577 Jan 28 11:28 compilie.sh
-rw-r--r--  1 m5110186 m5110186 1188 Jan 28 10:56 file_management.sh
-rw-r--r--  1 m5110186 m5110186  732 Jan 27 00:07 KAONIC.F
-rw-r--r--  1 m5110186 m5110186  2947 Jan 27 00:08 KP.F
-rw-r--r--  1 m5110186 m5110186 23815 Jan 28 11:01 MAINCS.F
-rw-r--r--  1 m5110186 m5110186  1155 Jan 28 11:03 nag.sh
-rw-r--r--  1 m5110186 m5110186   328 Jan 27 00:08 PARACS
[m5110186@suthpcc rintarn]#

```

Figure B.7 Showing a script file and source code files for NAG FORTRAN Libraries.

together to form “myprog”.

```

suthpcc.sut.ac.th - HPCC - SSH Secure Shell
File Edit View Window Help
Quick Connect Profiles

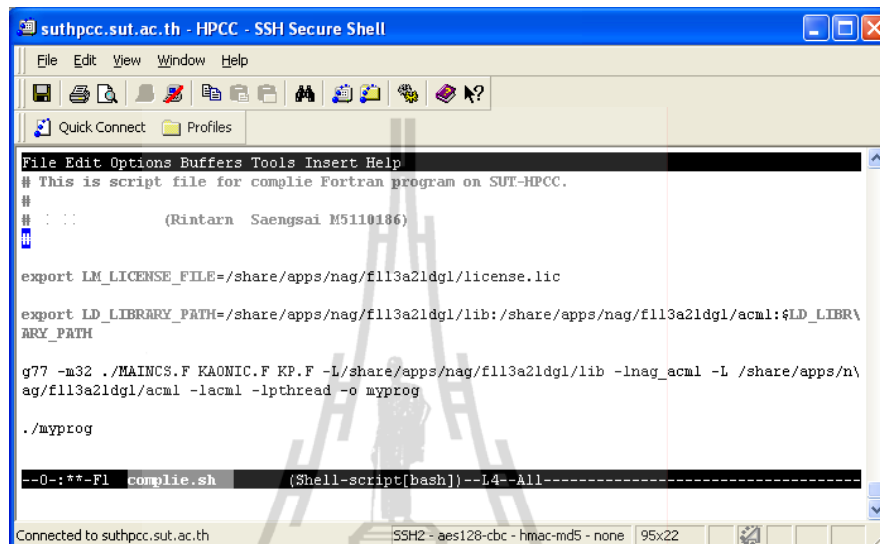
[m5110186@suthpcc rintarn]# ls -l
total 52
-rwxrwxr-x  1 m5110186 m5110186  577 Apr 17 12:37 compilie.sh
-rwxrwxr-x  1 m5110186 m5110186 1188 Apr 17 12:37 file_management.sh
-rw-r--r--  1 m5110186 m5110186  732 Apr 17 12:37 KAONIC.F
-rw-r--r--  1 m5110186 m5110186  2947 Apr 17 12:37 KP.F
-rw-r--r--  1 m5110186 m5110186 23815 Apr 17 12:37 MAINCS.F
-rw-r--r--  1 m5110186 m5110186  1155 Apr 17 12:37 nag.sh
-rw-rw-r--  1 m5110186 m5110186   328 Apr 17 12:37 PARACS
[m5110186@suthpcc rintarn]# ls -l
total 52
-rwxrwxr-x  1 m5110186 m5110186  577 Apr 17 12:37 compilie.sh
-rwxrwxr-x  1 m5110186 m5110186 1188 Apr 17 12:37 file_management.sh
-rw-r--r--  1 m5110186 m5110186  732 Apr 17 12:37 KAONIC.F
-rw-r--r--  1 m5110186 m5110186  2947 Apr 17 12:37 KP.F
-rw-r--r--  1 m5110186 m5110186 23815 Apr 17 12:37 MAINCS.F
-rw-r--r--  1 m5110186 m5110186  1155 Apr 17 12:37 nag.sh
-rw-rw-r--  1 m5110186 m5110186   328 Apr 17 12:37 PARACS
[m5110186@suthpcc rintarn]# emacs compilie.sh

```

Figure B.8 Using Emacs editor to make a script file for compiling our programs.

First, we want to build a program from many input source files. To do this,

we need to put the list of source files in the script file using emacs editor. In Figure B.8 we create the script file in emacs called “`compile.sh`”.



```

File Edit Options Buffers Tools Insert Help
# This is script file for compile Fortran program on SUT-HPCC.
#
# :::: (Rintarn Saengsai M5110186)
#
export LM_LICENSE_FILE=/share/apps/nag/f113a21dgl/license.lic
export LD_LIBRARY_PATH=/share/apps/nag/f113a21dgl/lib:/share/apps/nag/f113a21dgl/acml:$LD_LIBRARY_PATH

g77 -m32 ./MAINCS.F KAONIC.F KP.F -L/share/apps/nag/f113a21dgl/lib -lnag_acml -L /share/apps/nag/f113a21dgl/acml -lacml -lpthread -o myprog

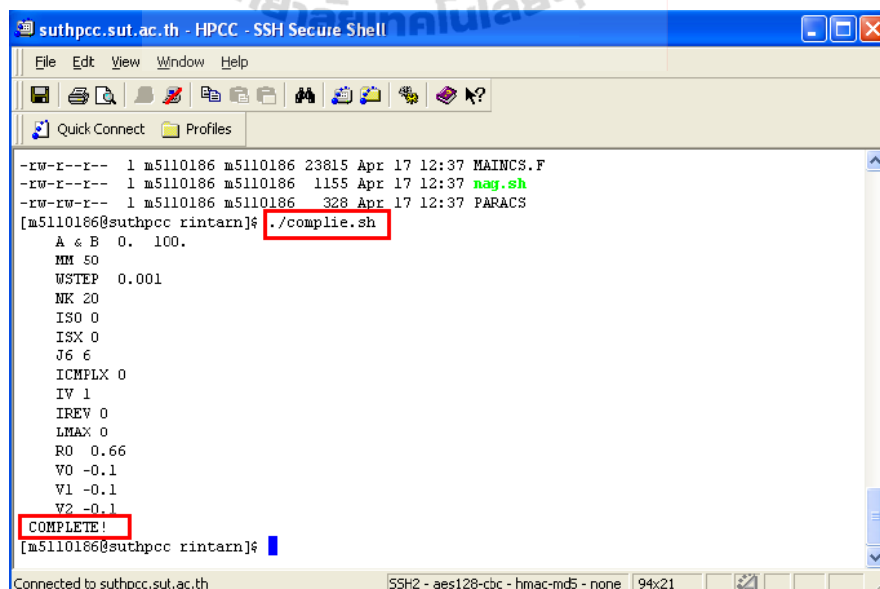
./myprog

--0-:*-F1 compile.sh (Shell-script[bash])--L4--All-----

```

Figure B.9 Showing the script file in Emacs.

The details of the script can be seen in Appendix C. In Figure B.9 is the script for compiling our FORTRAN program in SUT-HPCC.



```

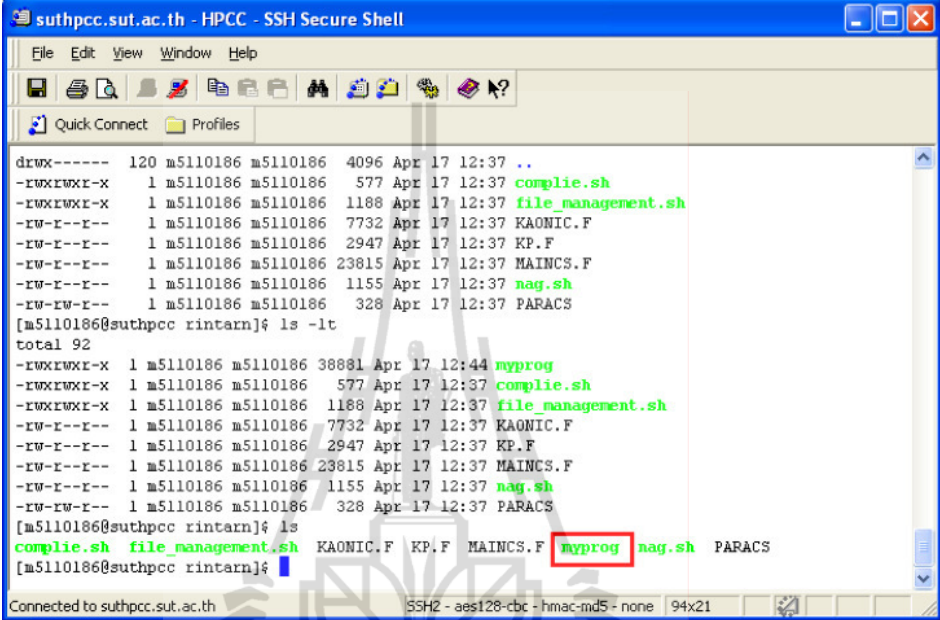
-rw-r--r-- 1 m5110186 m5110186 23815 Apr 17 12:37 MAINCS.F
-rw-r--r-- 1 m5110186 m5110186 1155 Apr 17 12:37 nag.sh
-rw-rw-r-- 1 m5110186 m5110186 328 Apr 17 12:37 PARACS
[m5110186@suthpcc rintarn]$ ./compile.sh
  A & B  0. 100.
  MM 50
  WSTEP 0.001
  NK 20
  ISO 0
  ISX 0
  J6 6
  ICMLX 0
  IV 1
  IREV 0
  LMAX 0
  RO 0.66
  VO -0.1
  V1 -0.1
  V2 -0.1
COMPLETE!
[m5110186@suthpcc rintarn]$

```

Figure B.10 Showing the outputs when we use the `compile.sh` script.

We use “`./compile .sh`” on the command line in SSH window to compile

the multiple source files (MAINS.F, KAONIC.F and KP.F file), and wait until the word “COMPLETE!” occur on the window (Figure B.10).



```

suthpcc.sut.ac.th - HPCC - SSH Secure Shell
File Edit View Window Help
Quick Connect Profiles
drwx----- 120 m5110186 m5110186 4096 Apr 17 12:37 ..
-rwxrwxr-x 1 m5110186 m5110186 577 Apr 17 12:37 complic.sh
-rwxrwxr-x 1 m5110186 m5110186 1188 Apr 17 12:37 file_management.sh
-rw-r--r-- 1 m5110186 m5110186 7732 Apr 17 12:37 KAONIC.F
-rw-r--r-- 1 m5110186 m5110186 2947 Apr 17 12:37 KP.F
-rw-r--r-- 1 m5110186 m5110186 23815 Apr 17 12:37 MAINCS.F
-rw-r--r-- 1 m5110186 m5110186 1155 Apr 17 12:37 nag.sh
-rw-rw-r-- 1 m5110186 m5110186 328 Apr 17 12:37 PARACS
[m5110186@suthpcc rintarn]$ ls -lt
total 92
-rwxrwxr-x 1 m5110186 m5110186 38881 Apr 17 12:44 myprog
-rwxrwxr-x 1 m5110186 m5110186 577 Apr 17 12:37 complic.sh
-rwxrwxr-x 1 m5110186 m5110186 1188 Apr 17 12:37 file_management.sh
-rw-r--r-- 1 m5110186 m5110186 7732 Apr 17 12:37 KAONIC.F
-rw-r--r-- 1 m5110186 m5110186 2947 Apr 17 12:37 KP.F
-rw-r--r-- 1 m5110186 m5110186 23815 Apr 17 12:37 MAINCS.F
-rw-r--r-- 1 m5110186 m5110186 1155 Apr 17 12:37 nag.sh
-rw-rw-r-- 1 m5110186 m5110186 328 Apr 17 12:37 PARACS
[m5110186@suthpcc rintarn]$ ls
complic.sh file_management.sh KAONIC.F KP.F MAINCS.F myprog nag.sh PARACS
[m5110186@suthpcc rintarn]$
Connected to suthpcc.sut.ac.th SSH2 - aes128-ctr - hmac-md5 - none 94x21

```

Figure B.11 Showing the executable files “myprog” after compiling.

Then we use “ls” command to see the lists of files after compiling multiple source files. If the compiling process is succeed, we get the executable files called “myprog” (Figure B.11).

B.3 Using NAG FORTRAN Libraries

The NAG FORTRAN Library is a comprehensive collection of FORTRAN 77 routines for solving numerical and statistical problems. The word routine is used to denote a subroutine or a function. For SUT-HPCC, the NAG FORTRAN library is located in /share/apps/nag. It is a symbolic link into the NAG installation tree. This makes it possible to refer uniformly to the library with the flag -L/share/apps/nag/f113a21dgl/lib -lnag_acml.

In order to use NAG FORTRAN library on the cluster we have to export

the NAG license file across or all compute nodes. This can be done by writing a script named “nag.sh” (Figure B.12).

```

suthpcc.sut.ac.th - HPCC - SSH Secure Shell
File Edit View Window Help
Quick Connect Profiles

drwx----- 120 m5110186 m5110186 4096 Apr 17 12:37 ..
-rwxrwxr-x 1 m5110186 m5110186 577 Apr 17 12:37 compile.sh
-rwxrwxr-x 1 m5110186 m5110186 1188 Apr 17 12:37 file_management.sh
-rw-r--r-- 1 m5110186 m5110186 7732 Apr 17 12:37 KAONIC.F
-rw-r--r-- 1 m5110186 m5110186 2947 Apr 17 12:37 KP.F
-rw-r--r-- 1 m5110186 m5110186 23815 Apr 17 12:37 MAINCS.F
-rw-r--r-- 1 m5110186 m5110186 1155 Apr 17 12:37 nag.sh
-rw-rw-r-- 1 m5110186 m5110186 328 Apr 17 12:37 PARACS

[m5110186@suthpcc rintarn]$ ls -lt
total 92
-rwxrwxr-x 1 m5110186 m5110186 38881 Apr 17 12:44 myprog
-rwxrwxr-x 1 m5110186 m5110186 577 Apr 17 12:37 compile.sh
-rwxrwxr-x 1 m5110186 m5110186 1188 Apr 17 12:37 file_management.sh
-rw-r--r-- 1 m5110186 m5110186 7732 Apr 17 12:37 KAONIC.F
-rw-r--r-- 1 m5110186 m5110186 2947 Apr 17 12:37 KP.F
-rw-r--r-- 1 m5110186 m5110186 23815 Apr 17 12:37 MAINCS.F
-rw-r--r-- 1 m5110186 m5110186 1155 Apr 17 12:37 nag.sh
-rw-rw-r-- 1 m5110186 m5110186 328 Apr 17 12:37 PARACS
[m5110186@suthpcc rintarn]$ ls
compile.sh file_management.sh KAONIC.F KP.F MAINCS.F myprog nag.sh PARACS
[m5110186@suthpcc rintarn]$ emacs nag.sh

```

Figure B.12 Creating nag.sh in Emacs.

```

suthpcc.sut.ac.th - HPCC - SSH Secure Shell
File Edit View Window Help
Quick Connect Profiles

File Edit Options Buffers Tools Insert Help
export MPICH_HOME=/opt/mpich/gnu
export MPICH_APP=/home/m5110186/BB/nag.sh

$MPICH_HOME/bin/mpirun -np $NSLOTS -machinefile $TMPDIR/machines

$MPICH_APP

export LM_LICENSE_FILE=/share/apps/nag/f113a21dgl/license.lic
export LD_LIBRARY_PATH=/share/apps/nag/f113a21dgl/lib:/share/apps/nag/f113a21dgl/acml:$LD_
LIBRARY_PATH

rm CHANNEL*
rm Check*
rm RESULT*

./myprog

--0:---F1 nag.sh (Shell-script[bash])--L32--69%-----

```

Figure B.13 Showing the nag.sh script in Emacs.

In Figure B.13 we show the details for writing NAG FORTRAN script for

the cluster (more detail in Appendix C).

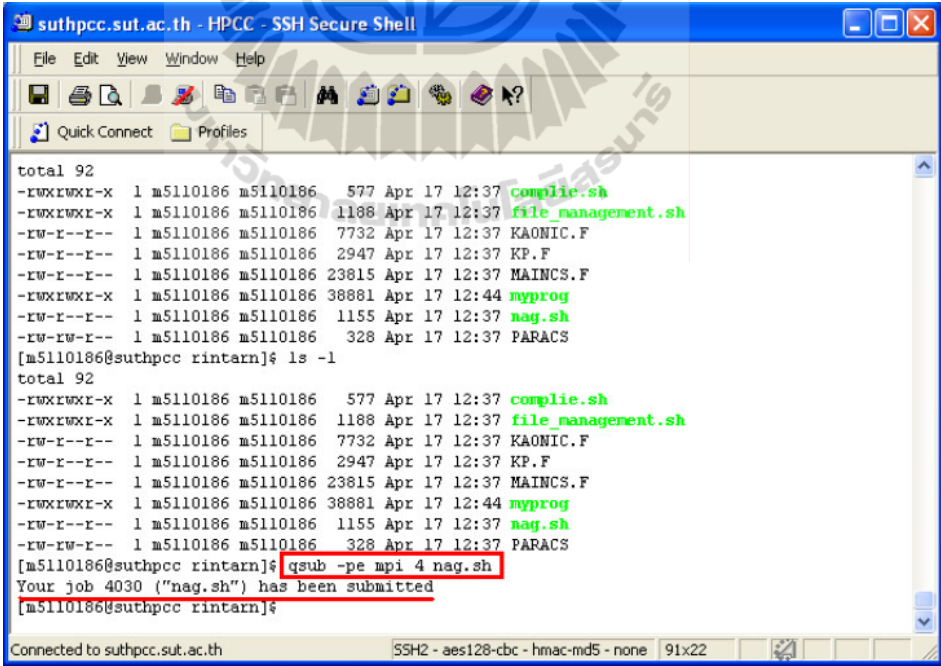
B.4 Job submission by the qsub command

Job submission is accomplished by using the qsub command, which takes a number of command line arguments and integrates such into the specified command file. The command file may be specified as a filename on the qsub command line.

For example :

```
> qsub -pe mpi 4 <script file name>
```

This job needed for executing parallel jobs and requests 4 cpu. the system will randomly select nodes for the submitted job.



```
suthpcc.sut.ac.th - HPCC - SSH Secure Shell
File Edit View Window Help
Quick Connect Profiles
total 92
-rwxrwxr-x 1 m5110186 m5110186 577 Apr 17 12:37 compie.sh
-rwxrwxr-x 1 m5110186 m5110186 1188 Apr 17 12:37 file_management.sh
-rw-r--r-- 1 m5110186 m5110186 7732 Apr 17 12:37 KAONIC.F
-rw-r--r-- 1 m5110186 m5110186 2947 Apr 17 12:37 KP.F
-rw-r--r-- 1 m5110186 m5110186 23815 Apr 17 12:37 MAINCS.F
-rwxrwxr-x 1 m5110186 m5110186 38881 Apr 17 12:44 myprog
-rw-r--r-- 1 m5110186 m5110186 1155 Apr 17 12:37 nag.sh
-rw-rw-r-- 1 m5110186 m5110186 328 Apr 17 12:37 PARACS
[m5110186@suthpcc rintarn]# ls -l
total 92
-rwxrwxr-x 1 m5110186 m5110186 577 Apr 17 12:37 compie.sh
-rwxrwxr-x 1 m5110186 m5110186 1188 Apr 17 12:37 file_management.sh
-rw-r--r-- 1 m5110186 m5110186 7732 Apr 17 12:37 KAONIC.F
-rw-r--r-- 1 m5110186 m5110186 2947 Apr 17 12:37 KP.F
-rw-r--r-- 1 m5110186 m5110186 23815 Apr 17 12:37 MAINCS.F
-rwxrwxr-x 1 m5110186 m5110186 38881 Apr 17 12:44 myprog
-rw-r--r-- 1 m5110186 m5110186 1155 Apr 17 12:37 nag.sh
-rw-rw-r-- 1 m5110186 m5110186 328 Apr 17 12:37 PARACS
[m5110186@suthpcc rintarn]# qsub -pe mpi 4 nag.sh
Your job 4030 ("nag.sh") has been submitted
[m5110186@suthpcc rintarn]#
```

Figure B.14 Showing the qsub command for submitting job on SUT-HPCC.

When we log into the Front end via SSH. We can type

```
> qsub -pe mpi 4 nag.sh
```

If we have jobs running on the cluster the results will print the word like: “Your job 4030 (“nag.sh”) has been submitted” (number 4030 is the job-ID on the cluster SUT-HPCC) as shown in Figure B.14.

```

suthpcc.sut.ac.th - HPCC - SSH Secure Shell
[ms110186@suthpcc rintang]# qstat
job-ID prior name user state submit/start at queue slots ja-task-I
-----
3985 0.60500 CH4_10_10_ B5003884 r 03/07/2011 12:21:09 all.q@compute-0-1.local 4
3988 0.60500 CH4_12_10_ B5003884 r 03/07/2011 12:22:09 all.q@compute-0-1.local 4
3978 0.60500 CH4_7_7_30 B5003884 r 03/07/2011 12:19:22 all.q@compute-0-17.local 4
3979 0.60500 CH4_7_10_3 B5003884 r 03/07/2011 12:19:37 all.q@compute-0-18.local 4
3980 0.60500 CH4_8_4_30 B5003884 r 03/07/2011 12:19:53 all.q@compute-0-19.local 4
3987 0.60500 CH4_12_7_3 B5003884 r 03/07/2011 12:22:09 all.q@compute-0-3.local 4
4023 0.50500 run.jit D4910114 r 04/15/2011 09:51:50 all.q@compute-0-4.local 1
4024 0.50500 run.jit D4910114 r 04/15/2011 09:56:09 all.q@compute-0-4.local 1
4025 0.60500 C02Per16_2 n5240272 r 04/16/2011 00:48:53 all.q@compute-0-4.local 4
3984 0.60500 CH4_10_7_3 B5003884 r 03/07/2011 12:20:54 all.q@compute-0-5.local 4
3986 0.60500 CH4_12_4_3 B5003884 r 03/07/2011 12:21:24 all.q@compute-0-5.local 4
3981 0.60500 CH4_8_7_30 B5003884 r 03/07/2011 12:20:09 all.q@compute-0-6.local 4
4026 0.60500 C02Per17_2 n5240272 r 04/16/2011 01:04:44 all.q@compute-0-6.local 4
4027 0.60500 C02Per18_2 n5240272 qw 04/16/2011 01:06:38 4
4030 0.60500 nag.sh n5110186 qw 04/17/2011 13:23:10 4
[ms110186@suthpcc rintang]#

```

Figure B.15 Checking the status of the job using “qstat” command.

After submitting job we can use command “qstat” to look at the status of our job (see Figure B.15). Under the state column we can see the status of our job. The meaning of each letters are following

- “r” : the job is running,
- “t” : the job is being transferred to a cluster node,
- “qw” : the job is queued (and not running yet),
- “Eqw” : an error occurred with the job.

Another important thing to note is the job-ID for our job. If we need to make changes to our job, for example, to delete the job from the cluster, we can run command

```
> qdel 4030
```

where 4030 is the job-ID getting from running the command “qstat”. The SSH window will show the line “m5110186 has delete job 4030” (see Figure

```

suthpcc.sut.ac.th - HPCC - SSH Secure Shell
File Edit View Window Help
Quick Connect Profiles
3985 0.60500 CH4_10_10_ B5003884 r 03/07/2011 12:21:09 all.q@compute-0-1.local 4
3988 0.60500 CH4_12_10_ B5003884 r 03/07/2011 12:22:09 all.q@compute-0-1.local 4
3978 0.60500 CH4_7_7_30 B5003884 r 03/07/2011 12:19:22 all.q@compute-0-17.local 4
3979 0.60500 CH4_7_10_3 B5003884 r 03/07/2011 12:19:37 all.q@compute-0-18.local 4
3980 0.60500 CH4_8_4_30 B5003884 r 03/07/2011 12:19:53 all.q@compute-0-19.local 4
3987 0.60500 CH4_12_7_3 B5003884 r 03/07/2011 12:22:09 all.q@compute-0-3.local 4
4023 0.50500 run.jit D4910114 r 04/15/2011 09:51:50 all.q@compute-0-4.local 1
4024 0.50500 run.jit D4910114 r 04/15/2011 09:55:09 all.q@compute-0-4.local 1
4025 0.60500 C02Per16_2 m5240272 r 04/16/2011 00:48:53 all.q@compute-0-4.local 4
3984 0.60500 CH4_10_7_3 B5003884 r 03/07/2011 12:20:54 all.q@compute-0-5.local 4
3986 0.60500 CH4_12_4_3 B5003884 r 03/07/2011 12:21:24 all.q@compute-0-5.local 4
3981 0.60500 CH4_8_7_30 B5003884 r 03/07/2011 12:20:09 all.q@compute-0-6.local 4
4026 0.60500 C02Per17_2 m5240272 r 04/16/2011 01:04:44 all.q@compute-0-6.local 4
4027 0.60500 C02Per18_2 m5240272 qv 04/16/2011 01:05:38 4
4030 0.60500 nag.sh m5110186 qv 04/17/2011 13:23:10 4
[m5110186@suthpcc rintarn]# qdel 4030
m5110186 has deleted job 4030
[m5110186@suthpcc rintarn]#
Connected to suthpcc.sut.ac.th SSH2 - aes128-cbc - hmac-md5 - none 103x18

```

Figure B.16 Qdel is a command to delete the job from the cluster.

B.16) to confirm that our job has been deleted from cluster. (The details for writing qsub script can be seen in Appendix C)

```

suthpcc.sut.ac.th - HPCC - SSH Secure Shell
File Edit View Window Help
Quick Connect Profiles
-rw-rw-r-- 1 m5110186 m5110186 0 Apr 17 13:28 Check9
-rwxrwxr-x 1 m5110186 m5110186 577 Apr 17 12:37 complie.sh
-rwxrwxr-x 1 m5110186 m5110186 1188 Apr 17 12:37 file_management.sh
-rw-r--r-- 1 m5110186 m5110186 7732 Apr 17 12:37 KAONIC.F
-rw-r--r-- 1 m5110186 m5110186 2947 Apr 17 12:37 KP.F
-rw-r--r-- 1 m5110186 m5110186 23815 Apr 17 12:37 MAINCS.F
-rwxrwxr-x 1 m5110186 m5110186 38881 Apr 17 13:28 myprog
-rw-r--r-- 1 m5110186 m5110186 1155 Apr 17 12:37 nag.sh
-rw-rw-r-- 1 m5110186 m5110186 328 Apr 17 12:37 PARACS
-rw-rw-r-- 1 m5110186 m5110186 99986 Apr 17 13:28 RESULT1
-rw-rw-r-- 1 m5110186 m5110186 748 Apr 17 13:28 RESULT2
-rw-rw-r-- 1 m5110186 m5110186 787 Apr 17 13:28 RESULT3
-rw-rw-r-- 1 m5110186 m5110186 788 Apr 17 13:28 RESULT4
-rw-rw-r-- 1 m5110186 m5110186 780 Apr 17 13:28 RESULTS
-rw-rw-r-- 1 m5110186 m5110186 787 Apr 17 13:28 RESULT6
[m5110186@suthpcc rintarn]# ls
CHANNEL1 CHANNEL5 Check2 Check6 complie.sh MAINCS.F RESULT1 RESULTS
CHANNEL2 CHANNEL6 Check3 Check7 file_management.sh myprog RESULT2 RESULT6
CHANNEL3 Check1 Check4 Check8 KAONIC.F nag.sh RESULT3
CHANNEL4 Check10 Check5 Check9 KP.F PARACS RESULT4
[m5110186@suthpcc rintarn]#
Connected to suthpcc.sut.ac.th SSH2 - aes128-cbc - hmac-md5 - none 92x21

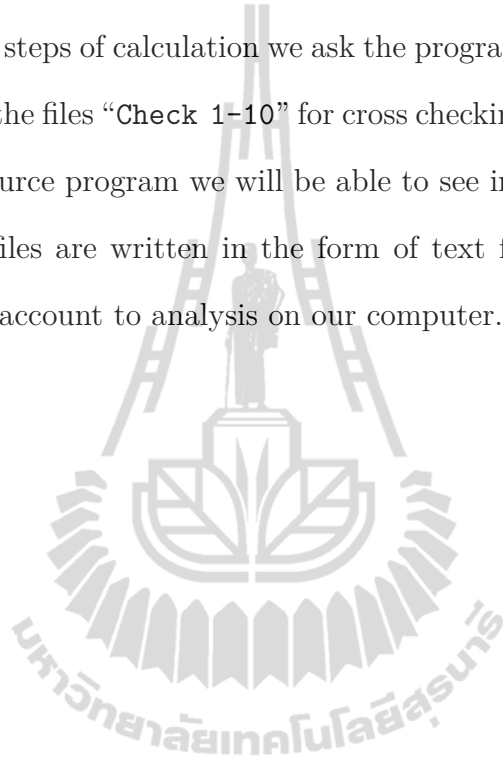
```

Figure B.17 The list of our results.

When our job is finished, we type “ls” to see the list of our results as shown in Figure B.17. The result files are RESULTS1, RESULTS2, RESULTS3, RESULTS4,

RESULTS5, RESULTS6. They contain over all parameters using in the calculation and all numerical results. The number 1 to 6 in the name of the files refer to the channels of the reaction $K^-p \rightarrow K^-p, \bar{K}^0n, \pi^0\Sigma^0, \pi^-\Sigma^+, \pi^+\Sigma^-$ and $\pi^0\Lambda$ respectively. The numerical cross section for each channels are given in CHANNEL files. To check our steps of calculation we ask the program to write some numerical computation into the files “Check 1-10” for cross checking. If something have gone wrong with the source program we will be able to see in these files.

All output files are written in the form of text file which we can transfer from SUT-HPCC account to analysis on our computer.



APPENDIX C

SCRIPT FILES FOR SUT-HPCC

C.1 Script for NAG FORTRAN Libraries

In order to use the NAG library on the SUT-HPCC cluster, we need to write some script file calling libraries. Because the license for the NAG library can only be used on the front end machine of the SUT-HPCC cluster. The following are requirements we need to put in the script file:

1. the environment variables `LM LICENSE FILE` and `LD LIBRARY PATH` are needed to point to the license file and library path using export command

```
export LM LICENSE FILE = /share/apps/nag/f113a21dgl/license.lic
export LD LIBRARY PATH = /share/apps/nag/f113a21dgl/lib:/share/apps
/nag/f113a21dgl/acml: $ \$ LD LIBRARY PATH
```

2. to use only 32-bit executable program, this can be done by using the `-m32` flag.

```
g77 -m32 ./MAINS.F KAONIC.F KP.F
```

GNU FORTRAN, `g77`, is an opensource substitute for `f77` in Linux. It reads our programs, `MAINS.F`, `KAONIC.F` and `KP.F`, written in the FORTRAN. `MAINS.F` file contains source code for calculating the radial part of Lippmann-Schwinger equation for the out scattered wave. We set all dynamical functions of integral equations as a kernel and transform the integral equation into the matrix form. Then we use the Gaussian-Legendre method to perform the iteration process to obtain the eigenvalues and eigenstates. `KAONIC.F` and `KP.F` contain source

code for kaonic potential parameters, subroutine and functions to support the main program.

```
-L /share/apps/nag/f113a21dgl/lib -lnag acml
-L /share/apps/nag/f113a21dgl/acml -lacml -lpthread -o myprog
./myprog
```

These three lines tell the location of the NAG Library and create the executable file called “myprog”.

C.2 qsub script for submitting jobs to the SUT-HPCC cluster

The SUT-HPCC cluster will distribute requested jobs on its compute nodes, depending on the current load of the nodes, the priority of the job and the numbers of jobs a user has already running on the cluster. Direct login onto the nodes and interactive executions of programs are strongly discourage. It can cause incomplete execution of batch jobs. So, for submitting a job, programs require a small shell script, which is a wrapper for the program to be run. Note that the script must be an executable. If the program requires interactive input the input has to be piped in by an external file. In this thesis we write a small shell script called nag.sh (the example script shown in Figure B.13 in Appendix B).

Next we will describe how to write a script for qsub command. There are some syntax that we have to follow. First we tell Linux which interpreter to use

```
#!/$ /bin/bash
```

the “#!/\$ /bin/bash” option tells the operating system to use Bourne-again shell (bash) to run this script.

Then we use the specific command in qsub.

```
#!/$ -cwd
```

The “-cwd” option is an option for changing a directory from the home directory to the directory containing our source program. If it is not specified, qsub will use your home directory as the working directory.

```
#$ -S
```

The “-S” option tells the qsub program to use the bash (Bourne) shell to run the program.

```
#$ -j y
```

The “-j y” option is an option for merging the normal output and any error messages into one file, typically with the name <job-name>.o<job-id>.

The qsub program will redirect standard output from nag.sh (stdout) to a file called nag.sh.oNNNN where NNNN is the UNIX process number, and also redirect standard error messages (stderr) to a file called nag.sh.eNNNN, again where NNNN is the UNIX process number.

```
export MPICH_HOME = /opt/mpich/gnu
```

```
export MPICH_APP = /home/m5110186/rintarn/nag.sh
```

The first line tells the location of mpich home directory. The second line specifies the location of nag.sh. In above example it is located in the directory /home/m5110186/rintarn.

The usage of mpirun requires also some non-standard environmental variables, which is then filled by grid engine at the execution of the script. The formats are

```
$ MPICH_HOME/bin/mpirun -np $ NSLOTS -machinefile $ TMPDIR/  
machines $ MPICH_APP
```

\$ MPICH_HOME/bin/mpirun tells where the location of mpirun is. The option -np \$ NSLOTS -machinefile tells the server how many CPUs needed. The details will be described in the variables NSLOTS and the machinefile. Normally, \$NSLOTS

and \$TMPDIR will be defined by the grid engine.

To check that the script runs correctly, we type “./nag.sh” at the command line. If there is no error, we are ready to submit the job with the qsub command :

```
> qsub -pe mpi N <script file name.sh>
```

qsub is a command for submitting jobs to the queue. It requires a shell scripts, which is wrapped around the program to be run. Options can be either defined as command line arguments or in the script file. The `-pe <parallel environment>` is needed for executing parallel jobs. N is the number of the desired CPU (we can choose between 1-8 for SUT-HPCC machines). The `<script file name.sh>` in this case we use “nag.sh”.

Apart from qsub, there are other common gridengine commands.

```
> qdel NNNN
```

qdel is a command for deleting job. It requires the job-id(NNNN) and not the job name, which can be ambiguous.

```
> qstat
```

qstat is a command to show the status of the queue or of a specific job if it is specified with the `-j <job-id>` option. The status of the job is indicated by one or more characters:

r - running,

t - transferring to a node,

qw - waiting in the queue,

Eqw - an error occurred with the job,

d - marked for deletion,

R - marked for restart.

APPENDIX D

CONFIGURATION PARAMETERS

D.1 Bounds of integrations

Integrations in the LS equation are set bounds by using the parameters LBOUND and UBOUND in PARACS file. The program reads these values to the main program and prints values to A and B with

A = LBOUND as the Lower Bound of R,

B = UBOUND as the Upper Bound of R.

For the integration

$$\int_A^B f(R)R^2 dR, \quad (D.1)$$

A is always zero in our calculation.

D.2 Integration points

Integrations are carried out numerically,

$$\int_A^B f(r)dr = \sum_{i=1}^{MM} w_i g(r_i), \quad (D.2)$$

where MM is the number of integration points or Gaussian points, w_i are the Gaussian weights. ENERGY in the file PARACS is to control the values of the center of mass energy. The program reads the energy values to main program and prints to array WSTEP. NK is the number of energy or momentum points in question.

D.3 Selection of basis, isospin and the number of channel

ISO is a parameter for selecting the working basis. We can choose two parameters, zero and one.

ISO = 1 for isospin basis

If we choose $ISO = 1$, this means we are using the isospin basis. In this case we also have to specify the isospin quantum number of the systems by using the parameter **ISX**. For the total isospin is zero we set $ISX = 0$. If the total isospin is one we set $ISX = 1$.

In case of **ISX = 0** we have to use a parameter **J6** to select the number of channel to be two (**J6 = 2**) which means we use only two channels in our calculation. Those two channels are

$$\bar{K}N \rightarrow \bar{K}N,$$

$$\bar{K}N \rightarrow \pi\Sigma.$$

In case of **ISX = 1** we have to use a parameter **J6** to select the number of channel to be three (**J6 = 3**) which means we use only three channels in our calculation. Those three channels are

$$\bar{K}N \rightarrow \bar{K}N,$$

$$\bar{K}N \rightarrow \pi\Sigma,$$

$$\bar{K}N \rightarrow \pi\Lambda.$$

ISO = 0 for particles basis

If we choose $ISO = 0$, this means we are using the particles basis. In this case we also have to specify the number of channel to be 6 channels (**J6 = 6**). Those six channels are

$$K^-p \rightarrow K^-p,$$

$$K^-p \rightarrow \bar{K}^0n,$$

$$K^-p \rightarrow \pi^+\Sigma^-,$$

$$K^-p \rightarrow \pi^-\Sigma^+,$$

$$K^-p \rightarrow \pi^0\Sigma^0,$$

$$K^-p \rightarrow \pi^0\Lambda.$$

D.4 Input the potential into the program

In this section we want to explain how to select the potential input by using parameter ICMPLX and IV in the PARACS file. The main program reads these values and pass them to the subroutine RMASS, CALLLINEAREQ, POTGUIDE, XXINS1 and PHINT.

The type of Potential (ICMPLX)

We have to specify the type of potential by setting the value of ICMPLX in the PARACS file. For the complex potential or optical potential we set ICMPLX = 1. If the potential are real, we set ICMPLX = 0.

The theoretical potential (IV)

Next we have to choose the theoretical potential from three different models by setting the value of IV in the PARACS file. If we choose IV = 1, this means we are using the Akaishi-Yamazaki potential. If we choose IV = 2, this means we are using the Chiral potential. If we choose IV = 3, this means we are using our potential which can be defined by extra parameters V0, V1 and V2.

D.5 Relativistic and Non-Relativistic calculation (IREV)

We have to specify the details of calculation either relativistic or non-relativistic by setting the value of the parameter IREV in the PARACS file. The

main program reads this value and passes it to the subroutine RMASS. If we choose $IREV = 1$, this means we are considering the problem in relativistic case. If we choose $IREV = 0$, this means we are considering the problem in non-relativistic case. In our work, we can choose both values because our system is a low-energy process, there are not much differences in the results.

D.6 Highest angular momentum in question (LMAX)

We have to specify the highest angular momentum in our calculation by using parameter LMAX in the PARACS file. The program read this value to the main program. In case of $LMAX = 0$, this means we are considering the case of s-wave. In case of $LMAX = 1$, this means we are considering the case of p-wave. In case of $LMAX = 2$, this means we are considering the case of d-wave. But in our work it is only a low-energy process, therefore, we consider only the case of s-wave.

APPENDIX E

FORTRAN SOURCE CODE

E.1 MAINS.F source code

This section we explain some important steps, we use for calculating the numerical cross section of the reaction $\bar{K}N \rightarrow \bar{K}N, \pi\Sigma$ and $\pi\Lambda$ in this thesis.

```
C-----C
C This is FORTRAN source code for calculate the numerical cross C
C section of the reaction  $\bar{K}N \rightarrow \bar{K}N, \pi\Sigma$  and C
C  $\pi\Lambda$  on SUT-HPCC. C
C-----C
C          Modify October, 2009 - December, 2010 C
C by Rintarn Saengsai and Particles Physics Group, SUT, THAILAND C
C For Master Thesis, Physics M.SC. C
C Adviser are Assit.Prof.Chinorat Kobdaj and Prof.Dr.Yupeng Yan C
C-----C
C This input file includes parameters:
C
C      A : LOWER BOUND OF R
C      B : UPPER BOUND OF R
C      MM : NUMBER OF INTEGRATION POINTS
C      WSTEP: CM ENERGY INTERVAL
C      NK : NUMBER OF ENERGY (MOMENTUM) POINTS IN QUESTION
```

```

C      ISO : ISO=1 FOR ISOSPIN BASIS; ISO=0 FOR PARTICLE BASIS
C      J6 : NUMBER OF CHANNELS
C      ICMLPX: ICMLPX = 1 FOR COMPLEX POTENTIAL;
C              ICMLPX = 0 FOR REAL POTENTIAL
C      IV : LEAD THE PROGRAM TO CALL DIFFERENT POTENTIALS
C      IREV : IREV = 1 FOR RELETIVIC CASE;
C              IREV = 0 FOR NON-RELEVATIC CASE
C      LMAX : HIGHEST ANGULAR MOMENTUM IN QUESTION
C-----C

```

Our FORTRAN program consists of a main program (MAINS.F) and two subprograms (KAONIC.F and KP.F) and a parameter program (PARACS).

E.1.1 FORTRAN code in MAINPROGRAM

This is a part of the program name and some declarations.

```

C-----C
PROGRAM MAINPROGRAM
IMPLICIT DOUBLE PRECISION(A-H,O-Z)
DOUBLE COMPLEX PHAS
DIMENSION QLAB(10,100),SIG(10,100),QCM(10,100)
COMMON /PMASS/ AM(10,2),DELTA(10)
COMMON /PARA/ PPI,HB,QE,AMN(10),F2(10),Q2(10)
COMMON /CONTROL/ IV,ICMLPX,ISO,ISX,J6
COMMON /EO/ W,PHAS(10,0:20)
COMMON /POTFACTOR/ R0,V0,V1,V2
C

```

```
HB=0.1973286D0
```

```
HBS=HB**0.5
```

```
QE=7.297D-03
```

```
PPI=4.D0*DATAN(1.D0)
```

C-----C

E.1.2 READ and PRINT parameters

In the PARACS file, we define some parameters (the details for configuration parameters are explained in Appendix D)

C-----C

```
0.0 LBOUND
```

```
100.0 UBOUND
```

```
500 MM
```

```
0.001 ENERGY
```

```
50 NK
```

```
0 ISO
```

```
0 ISX
```

```
6 J6
```

```
0 ICMLX
```

```
1 IV
```

```
0 IREV
```

```
0 LMAX
```

```
0.66 R0
```

```
-0.1 V0
```

```
-0.1 V1
```

```
-0.1 V2
```

C-----C

The FORTRAN program reads the PARACS file using the following code.

C-----C

```
OPEN (9, FILE='PARACS')
```

```
READ (9,*) A
```

```
READ (9,*) B
```

```
READ (9,*) MM
```

```
READ (9,*) WSTEP
```

```
READ (9,*) NK
```

```
READ (9,*) ISO
```

```
READ (9,*) ISX
```

```
READ (9,*) J6
```

```
READ (9,*) ICMLX
```

```
READ (9,*) IV
```

```
READ (9,*) IREV
```

```
READ (9,*) LMAX
```

```
READ (9,*) R0
```

```
READ (9,*) V0
```

```
READ (9,*) V1
```

```
READ (9,*) V2
```

```
REWIND 9
```

C-----C

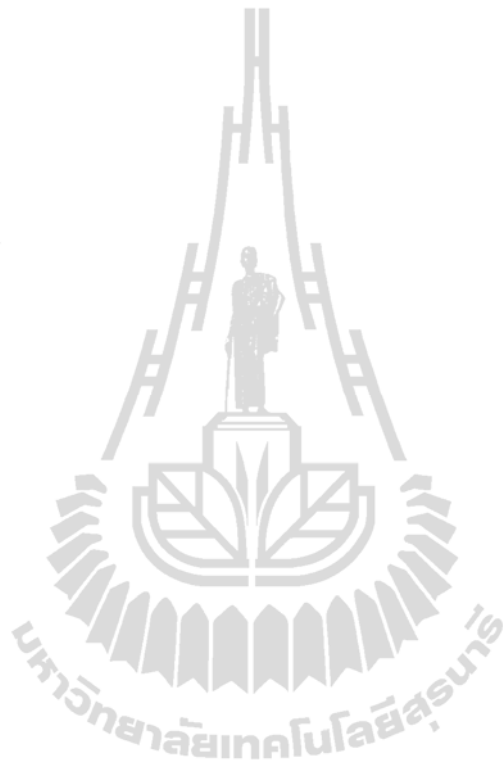
For printing out these parameters we use command “PRINT*, '” to write the following parameters into the output file called “nag.sh.oNNNN”.

C-----C

```

A & B  0.  100.
MM 500
WSTEP  0.001
NK 50
ISO 0
ISX 0
J6 6
ICMPLX 0
IV 1
IREV 0
LMAX 0
R0  0.66
V0 -0.1
V1 -0.1
V2 -0.1

```



C-----C

E.1.3 Open a files for writing the calculation results

Before doing our calculation, we use “OPEN (UNIT=NN, FILE='<file name >', STATUS='NEW')” to open new some files for writing our data and results.

C-----C

```
OPEN(UNIT=60,FILE='Check1',STATUS = 'NEW')
```

```
OPEN(UNIT=61,FILE='Check2',STATUS = 'NEW')
```

.....

.....

```
OPEN(UNIT=70,FILE='RESULT1',STATUS = 'NEW')
```

```
OPEN(UNIT=71,FILE='RESULT2',STATUS='NEW')
```

```
.....
```

```
.....
```

```
OPEN(UNIT=80,FILE='CHANNEL1',STATUS='NEW')
```

```
OPEN(UNIT=81,FILE='CHANNEL2',STATUS='NEW')
```

```
.....
```

```
.....
```

```
C-----C
```

1. open “Check 1-10” for checking input data of the program,
2. open “RESULTS 1-6” for writing all data and all numerical results of six channels,
3. open “CHANNEL 1-6” for writing theoretical cross sections calculated from six channels of the reactions $K^-p \rightarrow K^-p$, \bar{K}^0n , $\pi^0\Sigma^0$, $\pi^+\Sigma^-$, $\pi^-\Sigma^+$ and $\pi^0\Lambda$.

E.1.4 Starting numerical calculation

The MAINPROGRAM reads parameters from the PARACS file. In case of “ISO = 0”, that is, we select the particles basis for our calculation and the program chooses all amplitudes (AM) below.

```
>>> ISO = 0
```

```
C-----C
```

```
IF (ISO.EQ.0) THEN
```

```
AM(1,1)=0.938272D0
```

```
AM(1,2)=0.493677D0
```

```
AM(2,1)=0.939565D0
```

```
AM(2,2)=0.497672D0
```

```
C
```

```

AM(3,1)=1.192642D0
AM(3,2)=0.134977D0
AM(4,1)=1.18937D0
AM(4,2)=0.139570D0
AM(5,1)=1.197449D0
AM(5,2)=0.139570D0
C
AM(6,1)=1.115683D0
AM(6,2)=0.134977D0
C
ELSE IF (ISO.EQ.1) THEN
.....
.....
END IF .
C-----C

```

To calculate the equation “ $W=WSTEP*DFLOAT(I)+AM(1,1)+AM(1,2)$ ”, the program will need “NK” to define the momentum points. “WSTEP” read the parameter “ENERGY” from the PARACS file to define the center of mass energy interval.

```

C-----C
DO I=1,NK
W=WSTEP*DFLOAT(I)+AM(1,1)+AM(1,2)
WRITE (61,*) I,W
C
CALL RMASS(IREV)
C-----C

```

The command “CALL” is used for calling subroutines or functions in the main file. The above example we call the “SUBROUTINE RMASS(IREV)” (section E.4.1).

```
C-----C
      DO LX=0,LMAX
          CALL CALLLINEAREQ(A,B,MM,LX)
      ENDDO
```

```
C-----C
```

In this thesis we consider only the case of low-energy, so we call “SUBROUTINE CALLLINEAREQ(A,B,MM,LX)” (section E.4.2). In case of s-wave, with the highest angular momentum “LMAX = 0”, the program reads the value LMAX from the PARACS file.

```
C-----C
      DO JX=1,J6
          QLAB(JX,I)=Q2(JX)*W/AM(JX,1)
          QCM(JX,I)=Q2(JX)
          XT=0.DO
          DO LX=0,LMAX
              XT=XT+(2*LX+1)*ABS(PHAS(JX,LX))**2
              SIG(JX,I)=4.DO*PPI*(Q2(JX)/Q2(1))*XT*10.DO
          ENDDO
      ENDDO
  ENDDO
```

```
C-----C
```

The parameter “JX” tell the number of possible channels. If we select “ISO = 0” (in particles basis) the number of possible channels are 6 channel (J6 = 6),

then the program will start to calculate “QLAB”, “QCM” and “SIG” for $K^-p \rightarrow K^-p$, $K^-p \rightarrow \bar{K}^0n$, $K^-p \rightarrow \pi^0\Sigma^0$, $K^-p \rightarrow \pi^-\Sigma^+$, $K^-p \rightarrow \pi^+\Sigma^-$, $K^-p \rightarrow \pi^0\Lambda$.

```

C-----C
C      DO JX=1,J6
          DO I=1,NK
C          WRITE(6,*) JX,QCM(JX,I),QLAB(JX,I),SIG(JX,I)
          WRITE (70,*) I,QCM(1,I)*1000,QLAB(1,I)*1000,SIG(1,I)
          .....
          .....
          WRITE (80,*) QLAB(1,I)*1000,SIG(1,I)
          .....
          .....
          ENDDO
          WRITE(6,*) 'COMPLETE!'
C      ENDDO
C
          STOP
          END
C-----C

```

The last step in our main program is to write the value of cross section, SIG(JX,I), in laboratory momentum, QLAB(JX,I), corresponding to the number of energy or momentum points used and the center of mass energy interval. Finally, when the calculation are finished and all results are written to the output files, the word 'COMPLETE!' will printed in the file "nag.sh.oNNNN".

E.2 Source code for numerical functions

FORTRAN functions in this program are mathematical functions, they take a set of input parameters and return a value in a single result. There are some functions which are written into FORTRAN and can be used by calling from the main program.

To write our functions at the end of the main program, first, we declare the function name in the first line. Next, we declare variables and arguments in the variables declaration section after the first line. Then, we write down the code for calculation for which its values will be passed back to the main program. Finally, we exit finish the function with RETURN and END statements.

The FORTRAN functions we have been using in our main program are CK1, CK2, FJ, FN, FJD and FND (shown in sections E.2.1 - E.2.6).

E.2.1 Function CK1(X,S,L)

```
C-----C
      IMPLICIT DOUBLE PRECISION(A-H,O-Z)
      DOUBLE COMPLEX CK1
      CK1=FJ(S,L)*FN(X,L)-DCMPLX(0.DO,1.DO)*FJ(S,L)*FJ(X,L)
      RETURN
      END
```

E.2.2 Function CK2(X,S,L)

```
C-----C
      IMPLICIT DOUBLE PRECISION(A-H,O-Z)
```

```
DOUBLE COMPLEX CK2
```

```
C
```

```
CK2=FJ(X,L)*FN(S,L)-DCMPLX(0.D0,1.D0)*FJ(X,L)*FJ(S,L)
```

```
RETURN
```

```
END
```

```
C-----C
```

E.2.3 Function FJ(X,L)

```
C-----C
```

```
IMPLICIT DOUBLE PRECISION(A-H,O-Z)
```

```
C
```

```
IF (L.EQ.0) THEN
```

```
    FJ=DSIN(X)/X
```

```
ELSE IF (L.EQ.1) THEN
```

```
    FJ=DSIN(X)/X/X-DCOS(X)/X
```

```
ELSE IF (L.EQ.2) THEN
```

```
    FJ=DSIN(X)*(3.D0/X**3-1.D0/X)-3.D0*DCOS(X)/X/X
```

```
END IF
```

```
C
```

```
RETURN
```

```
END
```

```
C-----C
```

E.2.4 Function FN(X,L)

```
C-----C
```

```
IMPLICIT DOUBLE PRECISION(A-H,O-Z)
```

C

```

IF (L.EQ.0) THEN
    FN=-DCOS(X)/X
ELSE IF (L.EQ.1) THEN
    FN=-DSIN(X)/X-DCOS(X)/X/X
ELSE IF (L.EQ.2) THEN
    FN=-DCOS(X)*(3.DO/X**3-1.DO/X)-3.DO*DSIN(X)/X/X
END IF

```

C

```

RETURN
END

```

C

E.2.5 Function FJD(X,L)

C

```

IMPLICIT DOUBLE PRECISION(A-H,O-Z)

```

C

```

IF (L.EQ.0) THEN
    FJD=DCOS(X)/X-DSIN(X)/(X*X)
ELSE IF (L.EQ.1) THEN
    FJD=2.DO*DCOS(X)/X/X-2.DO*DSIN(X)/(X*X*X)+DSIN(X)/X
ELSE IF (L.EQ.2) THEN
    FJD=(6*Cos(x))/x**3 + ((3 - x**2)*Cos(x))/x**3 + Sin(x)/x**2 -
    & (3*(3 - x**2)*Sin(x))/x**4
END IF

```

C

```
RETURN
```

```
END
```

```
C-----C
```

E.2.6 Function FND(X,L)

```
C-----C
```

```
IMPLICIT DOUBLE PRECISION(A-H,O-Z)
```

```
C
```

```
IF (L.EQ.0) THEN
```

```
    FND=DCOS(X)/(X*X)+DSIN(X)/X
```

```
ELSE IF (L.EQ.1) THEN
```

```
    FND=(2*Cos(x))/x**3 - Cos(x)/x + (2*Sin(x))/x**2
```

```
ELSE IF (L.EQ.2) THEN
```

```
    FND=-((-9/x**4 + x**(-2))*Cos(x)) - (3*Cos(x))/x**2 +
& (3/x**3 - 1/x)*Sin(x) + (6*Sin(x))/x**3
```

```
END IF
```

```
C
```

```
RETURN
```

```
END
```

```
C-----C
```

```
C-----C
```

```
C                                END OF PROGRAMS                                C
```

```
C                                2010                                C
```

```
C-----C
```

E.3 List of Subroutines

A FORTRAN function can essentially only return one value. To return two or more values or none we need to use the subroutines. Our subroutines can be found in MAINS.F, KAONIC.F and KP.F. The list of all subroutines are shown in sections E.3.1, E.3.2, E.3.3 and E.3.4.

E.3.1 Subroutine in MAINS file

1. SUBROUTINE CALLINEAREQ(AA, BB, MM, LX)
2. SUBROUTINE PRINT(B, N, LX)
3. SUBROUTINE XXINS1(N, LX)
4. SUBROUTINE XXINS2(N, LX)
5. SUBROUTINE POTGUIDE(M, LL)
6. SUBROUTINE RMASS(IREV)
7. SUBROUTINE POINTOUT(N, AA, BB)
8. SUBROUTINE GAUSSPP(N, E, W)

E.3.2 Subroutine in KAONIC file

1. SUBROUTINE POTKAONICAY6(N)
2. SUBROUTINE POTKAONICAY2(N)
3. SUBROUTINE POTKAONICHNJH2(N, IP)

E.3.3 Subroutine in KP file

1. SUBROUTINE POTK(N)

E.3.4 External Subroutine

1. SUBROUTINE FO7ANF(JJ, NRHS, A, LDA, IPIV, B, LDB, INFO)

E.4 Subroutine for calculate cross section

This section we show details of all subroutine in MAINS.F, KAONIC.F and KP.F. These subroutines are used for calculating some parameters of the interaction terms inside the integral equation given in Chapter II.

E.4.1 Subroutine RMASS(IREV)

```

C-----C
      IMPLICIT DOUBLE PRECISION(A-H,O-Z)
      DOUBLE COMPLEX PHAS
      COMMON /PMASS/ AM(10,2),DELTA(10)
      COMMON /PARA/ PPI,HB,QE,AMN(10),F2(10),Q2(10)
      COMMON /CONTROL/ IV,ICMPLX,ISO,ISX,J6
      COMMON /EO/ W,PHAS(10,0:20)

C
      DO I=1,J6

      AMX=AM(I,1)*AM(I,2)/(AM(I,1)+AM(I,2))

      AMN(I)=2.DO*AMX

      DELTA(I)=(AM(I,1)+AM(I,2))-(AM(1,1)+AM(1,2))

      ENDDO

C
      DO I=1,J6

      AP2=(AM(I,1)+AM(I,2))**2

```

```
AM2=(AM(I,1)-AM(I,2))**2
```

```
C
```

```
Q1=(W*W-AM2)*(W*W-AP2)/(4.DO*W*W)
```

```
IF (Q1.LE.0.DO) THEN
```

```
Q2(I)=-DSQRT(-Q1)
```

```
ELSE
```

```
Q2(I)=DSQRT(Q1)
```

```
END IF
```

```
IF (IREV.EQ.0) THEN
```

```
F2(I)=AMN(I)
```

```
ELSE IF (IREV.EQ.1) THEN
```

```
.....
```

```
END IF
```

```
ENDDO
```

```
RETURN
```

```
END
```

```
C-----C
```

E.4.2 Subroutine CALLLINEAREQ(A,B,MM,LX)

```
C-----C
```

```
IMPLICIT DOUBLE PRECISION(A-H,O-Z)
```

```
DOUBLE COMPLEX A,B,PHAS
```

```
PARAMETER (NPX=10000)
```

```
DIMENSION IPIV(NPX)
```

```
EXTERNAL F07ANF
```

```

COMMON /PMASS/ AM(10,2),DELTA(10)
COMMON /PARA/ PPI,HB,QE,AMN(10),F2(10),Q2(10)
COMMON /CONTROL/ IV,ICMPLX,ISO,ISX,J6
COMMON /EO/ W,PHAS(10,0:20)
COMMON /QAQB/ BBX(NPX),BBW(NPX)
COMMON /FINAL/ A(NPX,NPX),B(NPX)
COMMON /POTCBL/ TSS(NPX,6,6),TDD(NPX,6,6)
COMMON /POTFACTOR/ RO,V0,V1,V2
C
CALL POINTOUT(MM,AA,BB)
CALL POTGUIDE(MM,LL)
C
IF (ICMPLX.EQ.0) THEN
    CALL XXINS1(MM,LX)
ELSE IF (ICMPLX.EQ.1) THEN
    .....
    .....
END IF
C
CALL F07ANF(JJ,NRHS,A,LDA,IPIV,B,LDB,INFO)
CALL PHINT(B,MM,LX)
999 FORMAT (E20.8,4E15.5)
RETURN
END
C-----C

```

E.4.3 Subroutine POINTOUT(MM,AA,BB)

```

C-----C
      IMPLICIT DOUBLE PRECISION(A-H,O-Z)
      PARAMETER (NPX=10000)
      DIMENSION BX(NPX),BW(NPX)
      COMMON /QAQB/ BBX(NPX),BBW(NPX)
C
      HB=0.1973286D0
      PPI=4.D0*DATAN(1.D0)
C
      CALL GAUSSPP (N,BX,BW)
      DO I=1,N
          BBX(I)=(BB+AA)/2.D0+(BB-AA)*BX(I)/2.D0
          BBW(I)=(BB-AA)*BW(I)/2.D0
      ENDDO
      RETURN
      END
C-----C

```

E.4.4 Subroutine POTGUIDE(MM,LL)

```

C-----C
      IMPLICIT DOUBLE PRECISION(A-H,O-Z)
      PARAMETER (NPX=10000)
      COMMON /POTCBL/ TSS(NPX,6,6),TDD(NPX,6,6)

```

```
COMMON /CONTROL/ IV,ICMPLX,ISO,ISX,J6
```

```
COMMON /POTFACTOR/ R0,V0,V1,V2
```

C

```
IF (IV.EQ.1) THEN
```

```
IF (ICMPLX.EQ.0) THEN
```

```
CALL POTKAONICAY6(M)
```

```
ELSE IF (ICMPLX.EQ.1) THEN
```

```
.....
```

```
END IF
```

```
ELSE IF (IV.EQ.2) THEN
```

```
.....
```

```
END IF
```

```
RETURN
```

```
END
```

C-----C

E.4.5 Subroutine XXINS1(MM,LX)

C-----C

```
IMPLICIT DOUBLE PRECISION(A-H,O-Z)
```

```
DOUBLE COMPLEX CK1,CK2,SS
```

```
DOUBLE COMPLEX GK,GF
```

```
PARAMETER (NPX=10000)
```

```
COMMON /FINAL/ GK(NPX,NPX),GF(NPX)
```

```
COMMON /QAQB/ BBX(NPX),BBW(NPX)
```

```
COMMON /PARA/ PPI,HB,QE,AMN(10),F2(10),Q2(10)
```

```
COMMON /POTCBL/ TSS(NPX,6,6),TDD(NPX,6,6)
```

```
COMMON /CONTROL/ IV,ICMPLX,ISO,ISX,J6
```

C

```
DO I=1,N
  XI=BBX(I)
  DO JX=1,J6
X=Q2(JX)*XI
    IF (JX.EQ.1) THEN
      GF(J6*(I-1)+JX)=FJ(X,LX)
    ELSE
      GF(J6*(I-1)+JX)=0.DO
    END IF
  ENDDO
ENDDO
```

C

```
DO I=1,N
  XI=BBX(I)
  DO J=1,N
    WT=BBW(J)
    SI=BBX(J)
    DO JX=1,J6
      X=Q2(JX)*XI
      S=Q2(JX)*SI
      DO JY=1,J6
        VR=TSS(J,JX,JY)*F2(JX)
      IF (I.GT.J) THEN
```

```

SS=WT*Q2(JX)*CK1(X,S,LX)*VR*BBX(J)*BBX(J)
ELSE
SS=WT*Q2(JX)*CK2(X,S,LX)*VR*BBX(J)*BBX(J)
END IF
IF (I.EQ.J.AND.JX.EQ.JY) THEN
GK(J6*(I-1)+JX,J6*(J-1)+JY)=1.DO-SS
ELSE
GK(J6*(I-1)+JX,J6*(J-1)+JY)=-SS
END IF
ENDDO
ENDDO
ENDDO
ENDDO
C
RETURN
END
C-----C

```

E.4.6 Subroutine PHINT(B,MM,LX)

```

C-----C
IMPLICIT DOUBLE PRECISION(A-H,O-Z)
DOUBLE COMPLEX B,DD,DT,D1,D2,FTHETA,FTH,PHAS
PARAMETER (NPX=10000)
COMMON /QAQB/ BBX(NPX),BBW(NPX)
DIMENSION B(NPX),DT(6)

```

```
COMMON /PARA/ PPI,HB,QE,AMN(10),F2(10),Q2(10)
```

```
COMMON /POTCBL/ TSS(NPX,6,6),TDD(NPX,6,6)
```

```
COMMON /CONTROL/ IV,ICMPLX,ISO,ISX,J6
```

```
COMMON /PMASS/ AM(10,2),DELTA(10)
```

```
COMMON /EO/ W,PHAS(10,0:20)
```

```
.....
```

```
.....
```

```
DO JX=1,J6
```

```
  IF (Q2(JX).GE.0.DO) THEN
```

```
    X=BBX(J)*Q2(JX)
```

```
    DD=(B(J6*(J2-1)+JX)-B(J6*(J1-1)+JX))/(X2-X1)
```

```
    DD=DD/B(J6*(J-1)+JX)
```

```
    D1=Q2(JX)*FJD(X,LX)-DD*FJ(X,LX)
```

```
    D2=Q2(JX)*FND(X,LX)-DD*FN(X,LX)
```

```
    DT(JX)=D1/D2
```

```
  END IF
```

```
ENDDO
```

C

```
DO JX=1,J6
```

```
  IF (Q2(JX).GE.0.DO) THEN
```

```
    IF (JX.EQ.1) THEN
```

```
      FTHETA=Q2(JX)/DT(JX)-Q2(JX)*DCMPLX(0,1.DO)
```

```
      FTH=HB/FTHETA
```

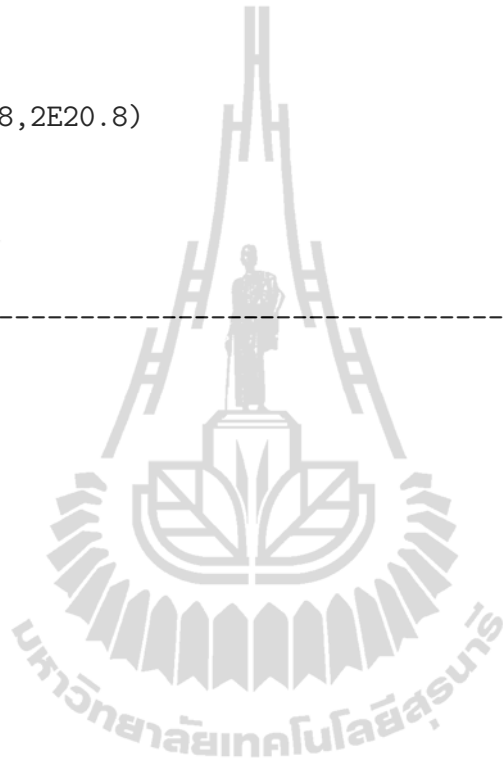
```
    ELSE
```

```
      FTHETA=B(J6*(J-1)+JX)*EXP(Q2(JX)*BBX(J)*DCMPLX(0,-1.DO))
```

```
      FTH=HB*BBX(J)*FTHETA*(DCMPLX(0,1.DO))**LX
```

```
END IF  
PHAS(JX,LX)=FTH  
END IF  
ENDDO  
C  
999 FORMAT (I8,2E20.8)  
RETURN  
END
```

C-----C



APPENDIX F

GLE (Graphics Layout Engine)

F.1 The example GLE source code for drawing graphs

```
!-----!  
! This sequence of graphs illustrates the six main channel      !  
! to obtain the theoretical cross section of the reaction      !  
!  $\bar{K}N \rightarrow \bar{K}N$  compared with the experimental data.  !  
!                                                              !  
! Author: Rintarn Saengsai                                     !  
! Date: December, 2010                                       !  
! Project: Master thesis                                       !  
!                                                              !  
! set page size A4 = 21 cm * 29.7 cm                          !  
! set graph size 20 30                                        !  
!-----!  
  
size 20 30  
  
a = 0; b = 0; c = 0; d = 0; r = 0  
  
set texlabels 1 titlescale 1 boxwidth = 0.4  
  
%include "graphutil.gle"  
  
amove 1 19 ! CH1 -----  
amove 10 19 ! CH2 -----  
  
begin graph  
  
size 10 10
```

```

!-----Set graph title-----!
xtitle "$p_L (MeV/c)$"
yttitle "$\sigma(mb)$"
    title "$Channel 2:K^-p \rightarrow \bar{K}^0 n$"
!-----Input data-----!
data "Ex1-2.CSV"
data "Ex1-2_2.CSV"
data "Ex1-2_3.CSV"
data "Ex1-2_4.CSV"
data "Ex1-2_5.CSV"
data "Ex1-2_6.CSV"
data "CH2"
!-----Set minimum and maximum of graph-----!
xaxis min 90 max 355
yaxis min 0 max 50
!-----Set plot line for input data-----!

d1 marker fdiamond color blue msize .5*boxwidth
key "Mast \em{et} al (1976)"

d8 marker ftriangle color darkred msize .5*boxwidth
key "Armenteros \em{et} al (1970)"

d15 marker circle color red msize .5*boxwidth
key "Evans \em{et} al (1983)"

d22 marker square color green msize .5*boxwidth
key "Humphrey \em{et} al (1962)"

d29 marker diamond color magenta msize .5*boxwidth
key "Kittel \em{et} al (1966)"

```

```

d36 marker ftriangle color red msize .5*boxwidth
key "Abrams \em{et} al (1965)"

d43 line smooth color black key "Theoretical result"
end graph

!-----Draw Error bar-----!

draw_box_plot 1
draw_box_plot 8
draw_box_plot 15
draw_box_plot 22
draw_box_plot 29
draw_box_plot 36

!-----!

amove 1 10 ! CH3 -----
amove 10 10 ! CH4 -----
amove 1 1 ! CH5 -----
amove 10 1 ! CH6 -----

!-----Set graph caption-----!

set just bc amove pagewidth()/2 0.5

begin text width 17.2

\setstretch{.1} Figure 1. Theoretical cross section of the reaction
 $K^-p \rightarrow K^-p, K^0n, \pi^0\Sigma^0, \pi^+\Sigma^-, \pi^-\Sigma^+$ 
and  $\pi^0\Lambda$ , compared with the experimental data.

end text

!-----Subroutines for drawing graphs-----!

sub draw_box_plot ds0

set cap round

```

```

for i = 1 to ndata("d"+num$(ds0))
  local x = dataxvalue("d"+num$(ds0), i)
  ! avg min Q.25 Q.5 Q.75 max
  ! 0 1 2 3 4 5
  local meanv = datayvalue("d"+num$(ds0), i)
  local minv = datayvalue("d"+num$(ds0+1), i)
  local q25 = datayvalue("d"+num$(ds0+2), i)
  local q50 = datayvalue("d"+num$(ds0+3), i)
  local q75 = datayvalue("d"+num$(ds0+4), i)
  local maxv = datayvalue("d"+num$(ds0+5), i)
  amove xg(x)-boxwidth/2 yg(minv)
  aline xg(x)+boxwidth/2 yg(minv)
  amove xg(x) yg(minv)
  aline xg(x) yg(q25)
  amove xg(x)-boxwidth/2 yg(q25)
  box boxwidth yg(q75)-yg(q25)
  amove xg(x)-boxwidth/2 yg(q50)
  aline xg(x)+boxwidth/2 yg(q50)
  amove xg(x) yg(q75)
  aline xg(x) yg(maxv)
  amove xg(x)-boxwidth/2 yg(maxv)
  aline xg(x)+boxwidth/2 yg(maxv)
  amove xg(x) yg(meanv)

  next i
end sub

```

!-----!

F.2 The GLE graph plots six channels in one product page

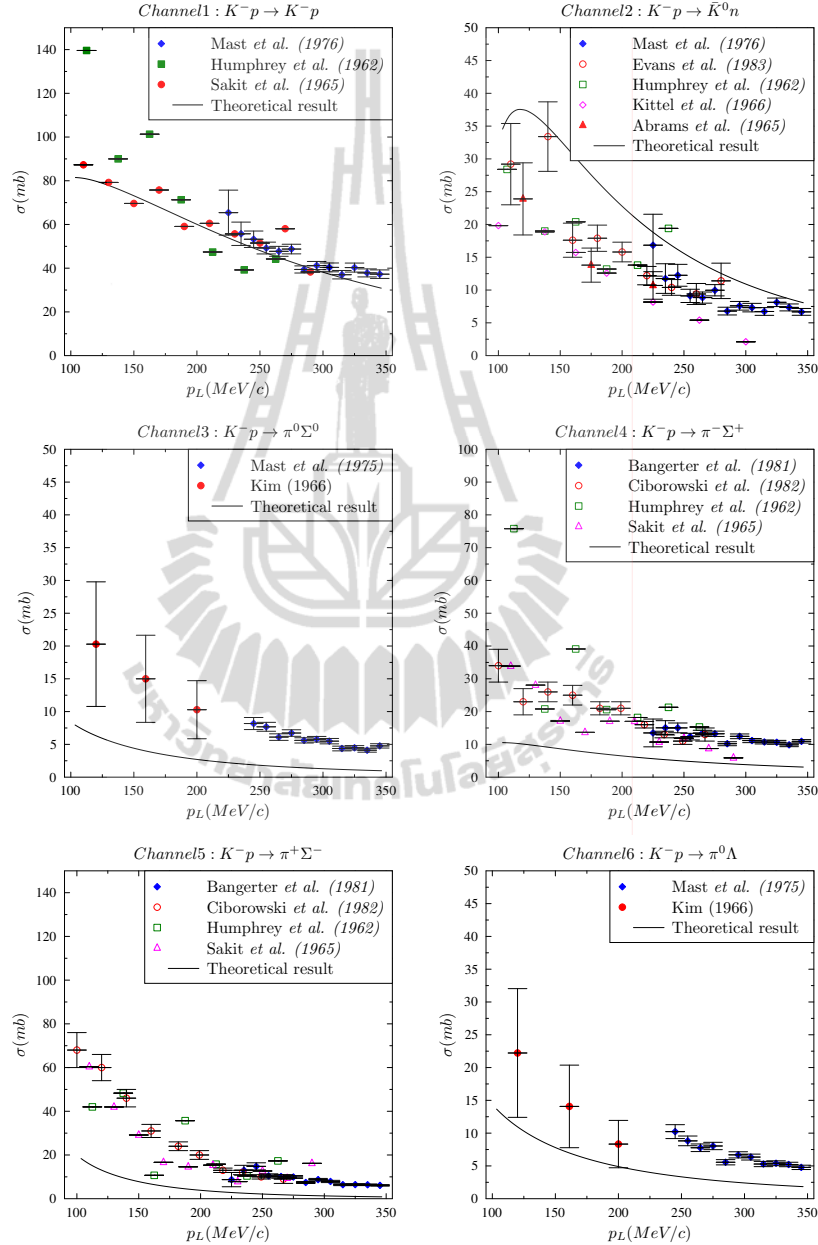


Figure F.1 The example of GLE plots (theoretical cross section of the reaction $K^-p \rightarrow K^-p$, \bar{K}^0n , $\pi^0\Sigma^0$, $\pi^+\Sigma^-$, $\pi^-\Sigma^+$ and $\pi^0\Lambda$, compared with the experimental data).

APPENDIX G

USING TightVNC ON THE SUT-HPCC

In order to use TightVNC to access a Linux cluster on the SUT-HPCC, we need to forward the connection through SSH Secure Shell. In Appendix B we have already explained how to set up SSH and connecting to the SUT-HPCC.

G.1 The installation of TightVNC Client

TightVNC is a free remote control software package, giving we full remote access to our Linux system on SUT-HPCC. The steps for installing TightVNC software are :

1. download the TightVNC file from
“<http://www.TightVNC.com/download.php>”,
2. install TightVNC for windows, double click on the package and choose option “Setup” in the dialog box,
3. install TightVNC for Linux, use the command “`rpm -ivh tightvnc-server-x.x.x-x.i386.rpm`” at the command line (x.x.x-x. is a version number of TightVNC).

G.2 Getting started with TightVNC Client

1. We use SSH secure shell to login to the SUT-HPCC. If an user starts a program TightVNC for the first time he/she needs to set the TightVNC password on the linux host.

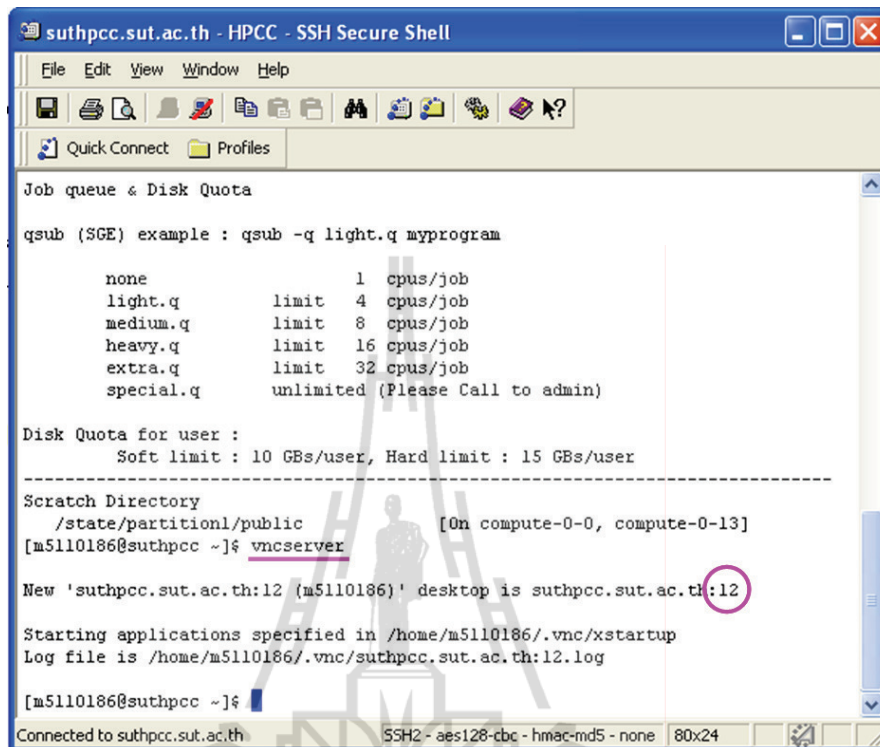


Figure G.1 Connecting to the SUT-HPCC using the SSH Secure Shell and showing how to start vncserver.

2. The vncserver program must be running on the linux host in order for you to establish a connection using TightVNC. To do this, simply type “vncserver” at the SSH window. Note that we need to put a display number after “suthpcc.sut.ac.th:” in order to connect from TightVNC client to the server (see Figure G.1).

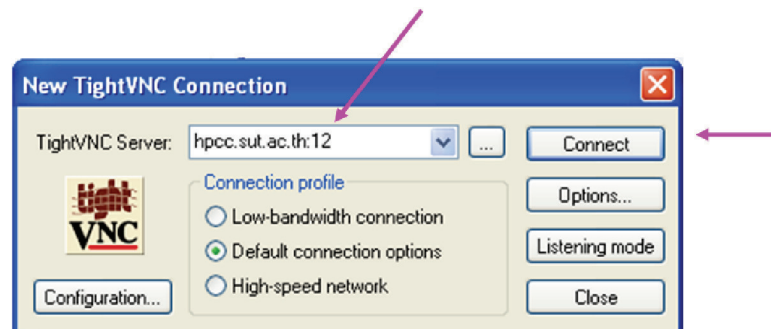


Figure G.2 Inserting server name or IP address and the display number.

3. Run the TightVNC client on your PC (windows) by going to start manu > AllPrograms > TightVNC > TightVNC Viewer. Inserting a server name or IP address and display number, in the “TightVNC server” field, in our case it is `suthpcc.sut.ac.th:12`. Then click on “Connect” (see Figure G.2). The display number can be different each time we start vncserver depending on how many people are using vncserver at the same time.
4. After, entering the TightVNC password we click on “OK” (see Figure G.3).



Figure G.3 Entering the TightVNC password at the password box.

5. A TightVNC window will appear on the desktop screen. It also opens a terminal which can be used for typing Linux commands. TightVNC can run application program on the server in graphic mode. For example in Figure G.4 we show how to run Mathematica 7.0 by typing command “`/share/apps/Wolfram/Mathematica/7.0/Executables`”.

The Mathematica window will appear on TightVNC screen(see Figure G.5).

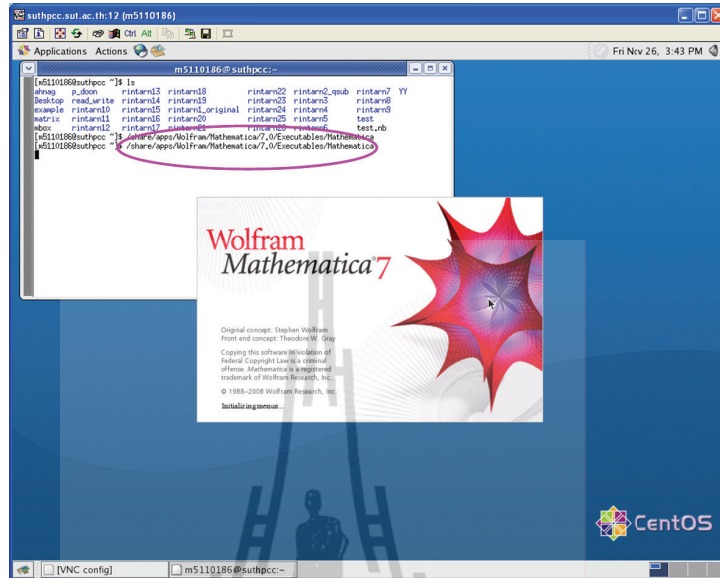


Figure G.4 Showing how to run Mathematica 7.0 via TightVNC.

Now we can use Mathematica like it is installed on our computer.

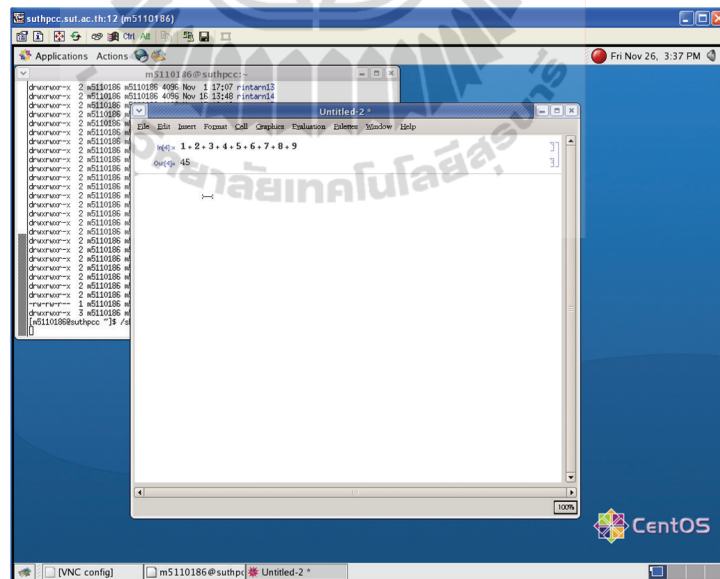


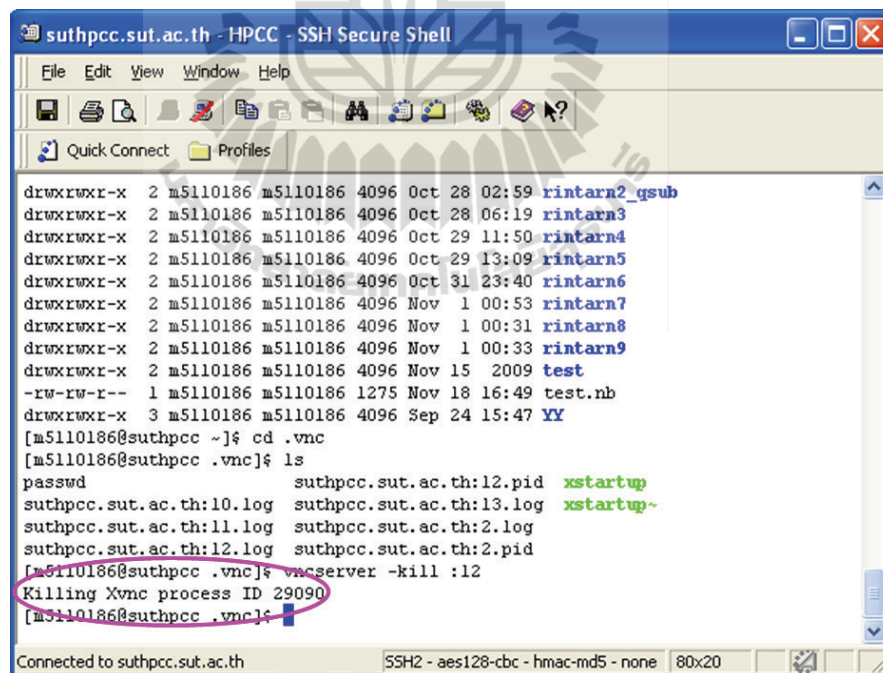
Figure G.5 Showing the Mathematica window on TightVNC screen.

G.3 How to stop the vncserver process

After finishing our work on the server we need to stop the vncserver process.

Here we describe how to stop the vncserver process:

1. save and exit application program on TightVNC
2. go to the terminal windows close TightVNC desktop and then, go back to command line in SSH secure shell.
3. we have to explicitly kill a particular process by type “`vncserver -kill :[display number]`” at the command line to stop the vncserver process. Replacing [display number] with the number of the TightVNC that you created earlier. In our case we type “`vncserver -kill :12`” (see Figure G.6).



```

suthpcc.sut.ac.th - HPCC - SSH Secure Shell
File Edit View Window Help
Quick Connect Profiles
drwxrwxr-x 2 m5110186 m5110186 4096 Oct 28 02:59 rintarn2_qsub
drwxrwxr-x 2 m5110186 m5110186 4096 Oct 28 06:19 rintarn3
drwxrwxr-x 2 m5110186 m5110186 4096 Oct 29 11:50 rintarn4
drwxrwxr-x 2 m5110186 m5110186 4096 Oct 29 13:09 rintarn5
drwxrwxr-x 2 m5110186 m5110186 4096 Oct 31 23:40 rintarn6
drwxrwxr-x 2 m5110186 m5110186 4096 Nov 1 00:53 rintarn7
drwxrwxr-x 2 m5110186 m5110186 4096 Nov 1 00:31 rintarn8
drwxrwxr-x 2 m5110186 m5110186 4096 Nov 1 00:33 rintarn9
drwxrwxr-x 2 m5110186 m5110186 4096 Nov 15 2009 test
-rw-rw-r-- 1 m5110186 m5110186 1275 Nov 18 16:49 test.nb
drwxrwxr-x 3 m5110186 m5110186 4096 Sep 24 15:47 YY
[m5110186@suthpcc ~]# cd .vnc
[m5110186@suthpcc .vnc]# ls
passwd suthpcc.sut.ac.th:12.pid xstartup
suthpcc.sut.ac.th:10.log suthpcc.sut.ac.th:13.log xstartup~
suthpcc.sut.ac.th:11.log suthpcc.sut.ac.th:2.log
suthpcc.sut.ac.th:12.log suthpcc.sut.ac.th:2.pid
[m5110186@suthpcc .vnc]# vncserver -kill :12
Killing Xvnc process ID 29090
[m5110186@suthpcc .vnc]#

```

Figure G.6 Showing how to stop the vncserver process in SSH secure shell.

If the killing process is succeed, we should see “Killing Xvnc process ID 29090” appear on SSH screen. This means that the vncserver process 12 has been stopped.

APPENDIX H

PUBLICATIONS

H.1 Conference proceeding

1. R. Saengsai, C. Kobdaj, K. Khosonthongkee, W. Poonsawat and Y. Yan. (2010). “Study of $\bar{K}N$ interaction based on chiral SU(3) symmetry”, Thai Physics Journal series 6.

Proceeding in Thai Physics Journal series 6 shown in Figures H.1, H.2, H.3, H.4.

H.2 Presentation in conference

1. Numerical Calculation of $\bar{K}N$ interaction based on chiral SU(3) symmetry., The 3rd SUT Graduate Conference 2010, Nakhon Ratchasima Thailand, November 21-23, 2010.

Abstract for oral presentation in The 3rd SUT Graduate Conference 2010 shown in Figures H.5, H.6.

2. Cross Section of $\bar{K}N$ potential based on chiral SU(3) symmetry., Theoretical Physics Conference 2010, Nakhon Ratchasima Thailand, September 12-15, 2010.

3. Study of $\bar{K}N$ interaction based on chiral SU(3) symmetry., TP-01, Siam Physics Congress 2010, Khanchanaburi Thailand, March 25-27, 2010.



STUDY OF $\bar{K}N$ INTERACTION BASED ON CHIRAL $SU(3)$ SYMMETRY

R. Saengsai^{*}, C. Kobdaj, K. Kosonthongkee, W. Poonsawat, and Y. Yan

*School of Physics, Institute of Science, Suranaree University of Technology, Nakhon Ratchasima 30000, Thailand
(Dated: March 26, 2010)*

The work is part of a project which is proposed to derive a potential in coordinate space for the coupled $\bar{K}N - \pi\Sigma - \pi\Lambda$ system. The potential is expected to reproduce the low-energy scattering data of the reactions $K^-p \rightarrow K^-p$, \bar{K}^0n , $\pi^0\Sigma^0$, $\pi^+\Sigma^-$, $\pi^-\Sigma^+$ and $\pi^0\Lambda$, the properties of the $\Lambda(1405)$ resonance, kaonic hydrogen atom data, and transition amplitudes predicted by other theoretical approaches. In this work we derive the dynamical equations for the coupled-channel $\bar{K}N$ system and evaluate the cross sections of the reactions $K^-p \rightarrow \pi^0\Sigma^0$, $\pi^+\Sigma^-$ and $\pi^-\Sigma^+$ with a phenomenological potential for the coupled $\bar{K}N$ system.

Keywords: $\bar{K}N$ potentials, coupled-channel, $\Lambda(1405)$ resonance, Lippmann-Schwinger (LS), cross sections.

1. INTRODUCTION

The \bar{K} -nuclear systems have drawn considerable attentions recently. Experimentally, the K^-p collisions provides information of interactions of the coupled $\bar{K}N - \pi\Sigma - \pi\Lambda$ system above the $\bar{K}N$ threshold. However, the interaction below the $\bar{K}N$ threshold, which is dominated by the $\Lambda(1405)$ resonance, is not well understood. It is, therefore, essential to study the extrapolation of the $\bar{K}N$ interaction below the threshold, by properly treating the $\Lambda(1405)$ [1, 2]. Historically, the $\Lambda(1405)$ which is the lowest-energy negative-parity baryon with nonzero strangeness, has been studied for some time. In recent works [3, 4, 5, 6], the $\Lambda(1405)$ has been reexamined as a baryon-meson resonance. It is found that the $\Lambda(1405)$ may not an elementary particle, but the bound state of $\bar{K}N$ that becomes a resonance when there is a coupling between the $\bar{K}N$ and $\pi\Sigma$ [7, 8].

The $\bar{K}N$ interaction has been studied in the vector-meson exchange model. The basic ingredient of this method is the single meson exchange, which provides the driving force (potential). The scattering equation is usually the relativistic form of the Lippmann-Schwinger(LS) equation or the Blankenbecler-Sugar (BbS) equation. The original idea was that, in the absence of any well-defined low-mass scalar mesons, the potential should be due to the

exchange of vector mesons. In [9, 10, 11], the $\Lambda(1405)$ has been successfully described in the coupled channel approach with vector-meson exchange potential [2].

Recently, a large number of works on $\bar{K}N$ interactions has been done in the chiral coupled channel approach [7, 12, 13, 14, 15, 16, 17], where the interaction Lagrangian is determined by chiral $SU(3) \times SU(3)$ symmetry of Quantum chromodynamics (QCD). The idea of chiral perturbation theory is to realize that at low energies the dynamics should be controlled by the symmetry of QCD and the lightest particles such as pions or nucleon.

The $\bar{K}N$ interactions derived in the above approaches are in momentum space and energy dependent. It is inconvenient to apply such interactions to multiparticle systems, for example, the \bar{K} -nuclear states. There have been attempts to construct $\bar{K}N$ potentials in r-space phenomenologically [3] or by reproducing transition amplitudes derived in the chiral coupled channel approach [2]. However, these potentials are capable of understanding only parts of experimental data. We have been constructing a potential in coordinate space for the coupled $\bar{K}N - \pi\Sigma - \pi\Lambda$ system, which is expected to reproduce the low-energy scattering data of the reactions $K^-p \rightarrow K^-p$, \bar{K}^0n , $\pi^0\Sigma^0$, $\pi^+\Sigma^-$, $\pi^-\Sigma^+$ and $\pi^0\Lambda$, the properties of the $\Lambda(1405)$ resonance, kaonic hydrogen atom data, and transition amplitudes predicted by other theoretical approaches. In this work we derive the dynamical equations for the coupled-channel $\bar{K}N$ system and evaluate the cross sections of the reactions $K^-p \rightarrow$

^{*}Corresponding author.
Tel: + 668 1748 4817 ; E-mail: m5110186@g.sut.ac.th

R. Saengsai *et al.*

$\pi^0\Sigma^0$, $\pi^+\Sigma^-$ and $\pi^-\Sigma^+$ with the phenomenological potential for the coupled $\bar{K}N$ system introduced in the work [3].

2. DYNAMICAL EQUATIONS FOR COUPLED $\bar{K}N$ SYSTEMS

We start from the Lippmann-Schwinger equation

$$|\psi_\alpha\rangle = |\phi_\alpha\rangle + \frac{1}{E - H_0 + i\varepsilon} V_{\alpha\beta} |\psi_\beta\rangle, \quad (1)$$

where $V_{\alpha\beta}$ is the interaction between the α and β channels (sum over repeated β), and $|\phi_\alpha\rangle$ satisfied the homogeneous equation

$$(E - H_0)|\phi_\alpha\rangle = 0. \quad (2)$$

In equation (2), H_0 is a hamiltonian of free particles. The formal solution of the Lippmann-Schwinger equation for outgoing scattered waves takes the form

$$\psi_\alpha(\vec{r}) = \phi_\alpha(\vec{r}) + \int d^3\vec{r}' G(\vec{r}, \vec{r}') V_{\alpha\beta}(\vec{r}') \psi_\beta(\vec{r}'), \quad (3)$$

where $G(\vec{r}, \vec{r}')$ is the Green's function, satisfying the equation,

$$(\nabla^2 + k^2)G(\vec{r}, \vec{r}') = \delta^3(\vec{r} - \vec{r}'). \quad (4)$$

In the $|JMLS\rangle$ basis the radial part of the outgoing wave $\psi_\alpha(\vec{r})$ is derived as

$$R_{L'S',LS}^{\alpha,J}(k_\alpha, r) = j_L(k_\alpha, r) \delta_{\alpha\alpha_0} \delta_{LL'} \delta_{SS'} + \sum_{L''S''} \int_0^\infty r'^2 dr' g_L(k_\alpha, r, r') V_{L''S'',L'S'}^{\alpha\beta,J}(r') R_{L''S'',LS}^{\beta,J}(k_\beta, r') \quad (5)$$

Where L, L' are the total orbital angular momentum of initial and final states, S, S' are the spin of initial and final states, J is the total angular momentum, k_α, k_β are the momenta of channels α and β , respectively. g_L is the radial component of the Green's function $G(\vec{r}, \vec{r}')$ and $V_{L''S'',L'S'}^{\alpha\beta,J}(r')$ is the radial part of the interaction from the channel β to α [18].

3. INTERACTION WITH CHIRAL SYMMETRY

Considering in the framework of SU(3) flavor symmetry where the strong interaction is invariant under the unitary transformation of u, d and s quarks, the interactions among the channels $\bar{K}N, \pi\Sigma$ and $\pi\Lambda$ are related with each other. The relative coupling strengths C_{ij} may be expressed in the isospin basis with the following matrices,

$$C_{ij}^{I=0} = \begin{pmatrix} 3 & -\sqrt{\frac{3}{2}} \\ -\sqrt{\frac{3}{2}} & 4 \end{pmatrix} \text{ (for isospin } I=0 \text{)} \quad (6)$$

where $i = 1, 2$ refers to the $\pi\Sigma$ and $\bar{K}N$ channels, and

$$C_{ij}^{I=1} = \begin{pmatrix} 1 & -1 & -\sqrt{\frac{3}{2}} \\ -1 & 2 & 0 \\ -\sqrt{\frac{3}{2}} & 0 & 0 \end{pmatrix} \text{ (for isospin } I=1 \text{)} \quad (7)$$

where $i = 1, 2, 3$ refers to the $\pi\Sigma, \pi\Lambda$ and $\bar{K}N$ channels, respectively.

The interactions in the particle basis can be expressed in terms of interactions in the isospin space, for example, for the processes $K^-p \rightarrow \pi^0\Sigma^0, \pi^+\Sigma^-$ and $\pi^-\Sigma^+$,

$$\langle K^-p | V | \pi^-\Sigma^+ \rangle = -\frac{1}{\sqrt{6}} C_{12}^{I=0} V^0(r) - \frac{1}{2} C_{12}^{I=1} V^1(r) \quad (8)$$

$$\langle K^-p | V | \pi^+\Sigma^- \rangle = -\frac{1}{\sqrt{6}} C_{12}^{I=0} V^0(r) + \frac{1}{2} C_{12}^{I=1} V^1(r) \quad (9)$$

$$\langle K^-p | V | \pi^0\Sigma^0 \rangle = \frac{1}{\sqrt{6}} C_{12}^{I=1} V^1(r) \quad (10)$$

where $V^0(r)$ and $V^1(r)$ are the isospin-based $I=0$ and $I=1$ potentials, respectively. The determination of the $V^0(r)$ and $V^1(r)$ is the final goal of the research project. We expect that the potentials reproduce the low-energy scattering data of the reactions $K^-p \rightarrow K^-p, \bar{K}^0n, \pi^0\Sigma^0, \pi^+\Sigma^-, \pi^-\Sigma^+$ and $\pi^0\Lambda^0$, the properties of the $\Lambda(1405)$ resonance, kaonic hydrogen atom data, and transition amplitudes predicted by other theoretical approaches.

Figure H.2 Proceeding in Thai Physics Journal series 6 page 2.

4. CROSS SECTIONS OF $\bar{K}N$ COLLISION

Mainly for checking our numerical program, we apply the Lippmann-Schwinger equation (5) to evaluate the cross sections of the reactions $K^- p \rightarrow \pi^0 \Sigma^0$, $\pi^+ \Sigma^-$ and $\pi^- \Sigma^+$ with the potential constructed phenomenologically in the works [3, 6]. The employed potential takes the form

$$V_{\alpha\beta}^I(r) = V_{\alpha,\beta}^I \exp\left[-\left(\frac{r}{b}\right)^2\right] \quad (11)$$

where the range parameter $b = 0.66$ fm and $V_{\alpha,\beta}^I$ are as follows:

$$\begin{aligned} V_{\bar{K}N,\bar{K}N}^{I=0} &= -436 \text{ MeV}, & V_{\bar{K}N,\bar{K}N}^{I=1} &= -62 \text{ MeV} \\ V_{\bar{K}N,\pi\Sigma}^{I=0} &= -412 \text{ MeV}, & V_{\bar{K}N,\pi\Sigma}^{I=1} &= -285 \text{ MeV} \\ V_{\bar{K}N,\pi\Lambda}^{I=0} &= 0 \text{ MeV}, & V_{\bar{K}N,\pi\Lambda}^{I=1} &= -285 \text{ MeV} \end{aligned} \quad (12)$$

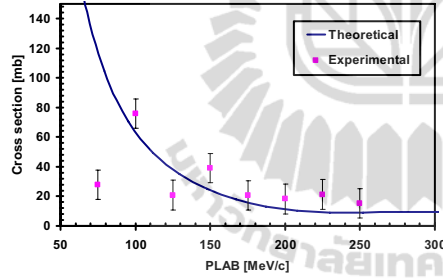


FIGURE 1. Theoretical cross section of the reaction $K^- p \rightarrow \pi^- \Sigma^+$ compared with the experimental data from [19].

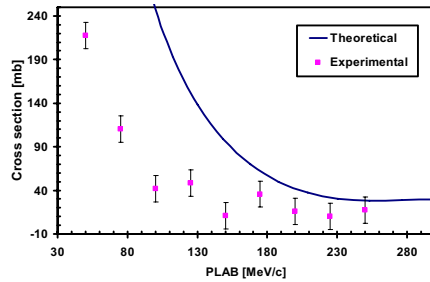


FIGURE 2. Theoretical cross section of the reaction $K^- p \rightarrow \pi^+ \Sigma^-$ compared with the experimental data from [19].

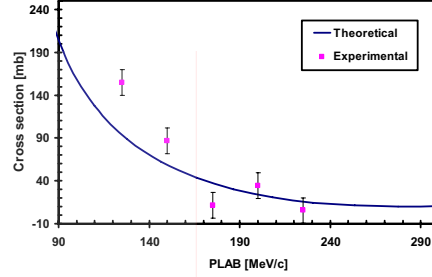


FIGURE 3. Theoretical cross section of the reaction $K^- p \rightarrow \pi^0 \Sigma^0$ compared with the experimental data from [19].

Shown in Figs.1., 2., 3., are the theoretical results on the cross section of the reactions $K^- p \rightarrow \pi^- \Sigma^+$, $K^- p \rightarrow \pi^+ \Sigma^-$ and $K^- p \rightarrow \pi^0 \Sigma^0$, respectively.

5. REMARKS

In this work we have worked out the Lippmann-Schwinger equation for the coupled $\bar{K}N$ system and the relations for interactions among various channels for the coupled $\bar{K}N$ channels in the framework of the flavor SU(3) symmetry. The cross sections of the reactions $K^- p \rightarrow \pi^- \Sigma^+$, $K^- p \rightarrow \pi^+ \Sigma^-$ and $K^- p \rightarrow \pi^0 \Sigma^0$ are evaluated with the phenomenological potentials [3, 6].

ACKNOWLEDGMENTS

This work is supported by the Commission on Higher Education, CHE-RG-Theoretical Physics and Thailand Center of Excellence in Physics (ThEP).

1. Dot e' , A., Hyodo, T. and Weise, W., Variational calculation of $K^- pp$ with chiral SU(3)-based $\bar{K}N$ interaction, Nucl. Phys. A Vol. 827, pp. 315c-317c, 2009
2. Hyodo, T. and Weise, W., Effective $\bar{K}N$ interaction based on chiral SU(3) dynamics, Phys.Rev. C, Vol. 77, pp. 035204, 2008
3. Akaishi, Y. and Yamazaki, T., Nuclear \bar{K} bound states in light nuclei, Phys. Rev. C, Vol. 65, pp. 044005, 2002
4. Kaiser, N., Siegel, P. B. and Weise, W., Chiral dynamics and the $S_{11}(1535)$ nucleon resonance*, Phys. Lett. B, Vol. 362, pp. 23-28, 1995
5. Takeuchi, S. and Shimizu, K., $\Lambda(1405)$ resonance in baryon-meson scattering with a bound state embedded in the continuum, Phys. Rev. C, Vol. 79, pp. 045204, 2009

R. Saengsai *et al.*

6. Yamazaki, T. and Akaishi, Y., (K^-, π^-) production of nuclear \bar{K} bound states in proton-rich system via Λ^* doorways, Phys. Lett. B, Vol. 535, pp. 70-76, 2002
7. Nacher, J. C., Parreno, A., Oset, E., Ramos, A., Hosaka, A. and Oka, M., Chiral unitary approach to the $\pi N^* N^*$, $\eta N^* N^*$ couplings for the $N^*(1535)$ resonance, Nucl. Phys. A, Vol. 678, pp. 187-211, 2000
8. Hyodo, T., Jido, D. and Hosaka, A., Origin of resonances in the chiral unitary approach, Phys. Rev. C, Vol. 78, pp. 025203, 2008
9. Durso, J. W., Meson exchange model of meson-meson interactions*, Acta. Phys. Pol. B, Vol. 29, pp. 9, 1998
10. Siegel, P. B. and Weise, W., Low-energy K^- - nucleon potentials and the nature of the $\Lambda(1405)$, Phys. Rev. C, Vol. 38, pp. 5, 1988
11. Landau, R. H., $K^- p$ bound states with coupling to hyperons channels, Phys. Rev. C, Vol. 28, pp. 3, 1983
12. Hyodo, T. and Weise, W., Effective $\bar{K}N$ interaction and role of chiral symmetry, arXiv:0903.4972v1 [nucl-th] 28 Mar 2009
13. Kaiser, N., Siegel, P. B. and Weise, W., Chiral dynamics and the low-energy kaon-nucleon interaction, Nucl. Phys. A, Vol. 594, pp. 325-345, 1995
14. Dot e' , A., Hyodo, T. and Weise, W., Variational calculation of the ppK^- system base on chiral SU(3) dynamics, Phys. Rev. C, Vol. 79, pp. 014003, 2009
15. Entem, D. R., Fernandez, F. and Valcarce, A., Chiral quark model of the NN system within a Lippmann-Schwinger resonating group method, Phys. Rev. C, Vol. 62, pp. 034002, 2000
16. Bianco, S., et al., KAON-NUCLEON INTERACTION STUDIED BY KAONIC X RAY WITH DEAR AT DA $\pi N E^*$, Acta. Phys. Pol. B, Vol. 20, pp. 9, 1998
17. Waas, T. and Weise, W., S-wave interactions of \bar{K} and η mesons in nuclear matter*, Nucl. Phys. A, Vol. 625, pp. 287-306, 1997
18. Landau, R. H. and P a' ez, M. J., Computational Physics Problem Solving with Computers, John Wiley and Sons Lnc, USA, 1997
19. William, E. H. and Ronald, R. R., Low-Energy Interactions of K^- Mesons in Hydrogen, Phys. Rev., Vol. 127, pp. 1305, 1962



Figure H.4 Proceeding in Thai Physics Journal series 6 page 4.



Numerical calculation of $\bar{K}N$ interaction based on chiral SU(3) symmetry

R. Saengsai¹, C. Kobdaj¹, K. Kosonthongkøe¹, W. Poonsawat², and Y. Yan¹

¹School of Physics, Institute of Science, Suranaree University of Technology,
Nakhon Ratchasima 30000, Thailand

²Department of Applied Physics, Faculty of Sciences and Liberal Arts,
Rajamangala University of Technology Isan, Nakhon Ratchasima 30000, Thailand

E-Mail: m5110186@g.sut.ac.th

Abstract

Finding that the $\Lambda(1405)$ consist of $\bar{K}N$ bound state with only small admixture of elementary three-quark state suggests a reasonable model is possible with the $\bar{K}N$ Σ and π as elementary particles interacting via potentials or meson-exchange. In this work we have derived the dynamical equations for the coupled-channel $\bar{K}N$ system. The cross section of the reaction $\bar{K}N \rightarrow \bar{K}N$ is evaluated with one of the famous phenomenological $\bar{K}N$ potentials and the theoretical results indicate that it is necessary to develop better versions of $\bar{K}N$ potentials. We use a method of coupled-channel Lippmann Schwinger equations, which allows us to evaluate the $l=0$ amplitudes and obtain a good description of the $K^- p \rightarrow K^- p, K^0 n, \pi^+ \Sigma^0, \pi^+ \Sigma^-, \pi^0 \Sigma^+, \pi^0 \Lambda^0$ cross sections at low energies plus the properties of the $\Lambda(1405)$ resonance. By changing only the potential in the LS equations, we get better versions of $\bar{K}N$ potentials and obtain the cross sections consistent with experimental data.

Keywords: $\bar{K}N$ potentials, coupled-channel, $\Lambda(1405)$ resonance, Lippmann-Schwinger (LS), cross sections.



การคำนวณเชิงตัวเลขของอินตริกิริยาปฏิอนุภาคเคออน - นิวคลีออน บนพื้นฐานของสมมาตรโคเลอเรลแบบ SU(3)

ถนธรา แสงไสย์¹ ชินรัตน์ กอบเดช¹ ชรรค์ชัย โกศลทองกี¹ วันเฉลิม พูนสวัสดิ์² และยูเบียง แยน¹
¹สาขาวิชาฟิสิกส์ สำนักวิทยาศาสตร์ มหาวิทยาลัยเทคโนโลยีสุรนารี

นครราชสีมา 30000 ประเทศไทย

²ภาควิชาฟิสิกส์ประยุกต์ คณะวิทยาศาสตร์และศิลปศาสตร์ มหาวิทยาลัยเทคโนโลยีราชมงคลธัญบุรี

วิทยาเขตนครราชสีมา นครราชสีมา 30000 ประเทศไทย

E-Mail: m5110186@g.sut.ac.th

บทคัดย่อ

ผลของการศึกษาอนุภาค Λ (1405) ที่เกิดเป็นสภาพกักกันของ $\bar{K}N$ ซึ่งเป็นการผสมกันเพียงชั่วขณะของอนุภาคมูลฐานในสถานะสาม-ควาร์ก ได้ชี้ให้เห็นถึงแบบจำลองที่สมเหตุสมผลและเป็นไปได้ว่า อนุภาคมูลฐาน $\bar{K}N$ Σ และ π สามารถมีอันตรกิริยาต่อกันได้โดยผ่านทางศักดิ์หรือการแลกเปลี่ยนอนุภาคเมซอน ในงานวิจัยนี้เราจะเริ่มต้นจากสมการเชิงพลวัตของระบบ $\bar{K}N$ ซึ่งค่าภาคตัดขวางของอันตรกิริยา $\bar{K}N \rightarrow \bar{K}N$ เป็นสิ่งที่ทำได้โดยใช้ศักดิ์ ซึ่งผลลัพธ์ในเชิงทฤษฎีมีความจำเป็นที่จะต้องได้รับการพัฒนาเพื่อให้ได้ค่าของศักดิ์ $\bar{K}N$ ที่แม่นยำกว่าในปัจจุบันในส่วนของวิธีการศึกษาเราจะใช้สมการลิปมานท์-ชวิงค์เกอร์คำนวณหาค่าแอมพลิจูดที่ $l = 0$ และบรรจุค่าภาคตัดขวางของอันตรกิริยา $K^+p \rightarrow K^+p, K^+n, \pi^+\Sigma^+, \pi^+\Sigma^0, \pi^+\Lambda^0$ ที่พลังงานต่ำรวมกับสมบัติการเกิดขึ้นเพียงชั่วขณะของ Λ (1405) จากนั้นทดลองเปลี่ยนค่าศักดิ์ในสมการลิปมานท์-ชวิงค์เกอร์ จนกระทั่งได้ค่าที่ดีที่สุดที่เมื่อนำไปคำนวณค่าภาคตัดขวางแล้วให้ค่าที่สอดคล้องกับผลที่ได้จากการทดลอง

คำสำคัญ: ศักย์ปฏิเคออน-นิวคลีออน ช่องคู่ควบ Λ (1405) เรโซแนนท์ สมการลิปมานท์-ชวิงค์เกอร์ ค่าภาคตัดขวาง

CURRICULUM VITAE

FIRST NAME: MISS RINTARN

LAST NAME: SAENGSAI

EDUCATIONS:

- Bachelor of Science in Physics, 2007, Prince of Songkla University (PSU), Pattani, Thailand.

EXPERIENCE:

- Intern in Thailand Institute of Nuclear Technology, April to May 2007.
- Teaching Assistant in Laboratory physics for Bachelor students (Engineering) in Suranaree University of Technology, September to December 2008.

SCHOLARSHIPS:

- Assistantship from Thailand Center of Excellence in Physics (2009-2011).
- Scholarship for graduate students to research projects funded from outside capital sources, from Suranaree University of Technology (2008-2009).
- Research Scholar for Bachelor student, Academic year 2008 from Prince of Songkla University (2008).

HORNORS AND AWARDS:

- Advanced Technology Certificate of Presentation From Thailand Institute of Nuclear Technology (TINT), Bangkok Thailand (2007).
- Advanced Technology Certificate of Diligence From Thailand Institute of Nuclear Technology (TINT), Bangkok Thailand (2007).